INUNDATION RISK ANALYSIS OF THE STORM SURGE AND FLOOD FOR THE ARIAKE SEA COASTAL DISASTER MANAGEMENT

September 2016

Department of Science and Advanced Technology
Graduate School of Science and Engineering
Saga University

JAPAN

ARTHUR HARRIS THAMBAS

INUNDATION RISK ANALYSIS OF THE STORM SURGE AND FLOOD FOR THE ARIAKE SEA COASTAL DISASTER MANAGEMENT

by

ARTHUR HARRIS THAMBAS

A dissertation submitted in partial fulfillment of the requirements
for the degree of Doctor of Engineering

Department of Science and Advanced Technology
Graduate School of Science and Engineering
Saga University

JAPAN

September 2016

THESIS EXAMINATION COMMITTEE

Professor Koichiro OHGUSHI
Department of Civil Engineering and Architecture
Graduate School of Science and Engineering
Saga University
JAPAN

Professor Hiroyuki ARAKI
Institute of Lowland and Marine Research
Saga University
JAPAN

Associate Professor Hideo OSHIKAWA
Department of Civil Engineering and Architecture
Graduate School of Science and Engineering
Saga University
JAPAN

Associate Professor Narumol VONGTHANASUNTHORN
Graduate School of Science and Engineering
Department of Civil Engineering and Architecture
Saga University
JAPAN

ABSTRACT

The storm surge and flood occurred on Kyushu island in the past such as Typhoon Pat 1985 and river flooding by torrential rain caused inundation in the coastal area of the Ariake Sea. The Ariake Sea has the largest tidal range in Japan, i.e., 6 m at the bay head. This sea area is about 1,700 km^2 wide with about 96 km long of the bay axis, 18 km of the average width, 20 m of the mean depth. It faces on four prefectures, i.e., Nagasaki, Saga, Fukuoka, and Kumamoto. Most of the plains in Saga Prefecture are adjacent to the Ariake Sea. It is mainly lowland area with an unusually small slope, so once the sea water enters into these areas, it will immediately create largely inundated area despite the fact that these areas are being used for agricultural, offices, residential, industrial, airport, etc.

In this dissertation, the storm surge by the past main typhoon and flood are studied to analyze in the case that two disasters simultaneously occur and to know the conditions of the water level causing the inundation in the coastal area of the Ariake Sea and Saga lowland. This study also considers the inundation risk in the coastal area, in particular on the buildings or houses and public facilities by evaluating of future disaster management.

1-D Hydrodynamic model is used to analyze of water level in the Chikugo River and branches when the high discharge by torrential rain occurs in the Chikugo River. 2-D Hydrodynamic model is used to analyze of water level or tide in the Ariake Sea when the storm surge by typhoon Pat occurs in the Ariake Sea. A coupled model of hydrodynamic model of 1-D and 2-D are used to analyze of water level when the storm surge and high discharge take place in the same time in the coastal area of the Ariake Sea and Saga lowland.

This research makes assumption that two disasters simultaneously occurred at the same time, storm surge by the typhoon in the Ariake Sea and high discharge or river flood by torrential rain in the Chikugo River that empty in the Ariake Sea. The simulation results of 1-D and 2-D model analysis separately gives, no water level exceeded the existing coastal dyke when the storm surge by typhoon Pat occurred in the Ariake Sea on August to September 1985 by 2-D analysis. In the coupled model simulation result, in which storm surge and river flood simultaneously occurred at the same time, the coastal area of the Ariake Sea and Saga lowland were inundated.

The GIS model analysis indicates a high risk of inundation in the Ariake Sea coastal area and Saga lowland, i.e. more than 96,000 buildings or houses and 245 public facilities are inundated. For the disaster management of flood and storm surge in the coastal area of Ariake Sea and Saga lowland, it is recommended to implement the disaster management system based on flood disaster management cycle by mitigation, awareness/preparedness, response, and recovery.

Keywords: inundation simulation, storm surge, river flood, Ariake sea, Chikugo river

ACKNOWLEDGEMENTS

Only with love and grace of God so that this dissertation can be completed. Thank you Lord Jesus Christ has given me the ability and strength during taking and completing this study.

The highest appreciation I would like to express to my supervisor Professor Koichiro Ohgushi. Thanks for the guidance, encouragement, and support both mentally and academically made finish this dissertation. Also, I want to thank him for the constant monitoring, sustainable development, help the criticisms, suggestions and encouragement along the way research. Deep gratitude is expressed to the members of the examination committee of this dissertation; Professor Hiroyuki Araki, Institute of Lowland and Marine Research, Saga University, Associate Professor Hideo Oshikawa, Department of Civil Engineering and Architecture, Graduate School of Environmental Science and Engineering, Saga University and Associate Professor Narumol Vongthanasunthorn, Department of Civil Engineering and Architecture, Graduate School of Environmental Science and Engineering, Saga University, for their kind encouragements and critical suggestions for improving this research.

In this opportunity, I would like to give special thanks to Sam Ratulangi University and the Indonesian Government for supporting me to continue doctoral study program at Saga University. Thanks to Mr. Takeshi Noguchi, for his valuable support in setting and analyzing, Mr. Francois Salesse and Mr. Takahiro Kazama from DHI-Japan, for supporting in MIKE software and give me some lectures. Special thanks are also to all of my laboratory mates in Professor Ohgushi Laboratory since 2012, for their kindness and friendliness during my study. Thanks to Dr. Morita,

Terao and Koga for our discussion about MIKE. Also, thanks to all Indonesian friends, who live in Saga in the period of 2012 to 2016 for supporting me.

I would like to thanks to my beloved father, H. M. Thambas and my mother in law N. Moray for their support. Special thanks to the people whom I love and have loved and no longer with me because now they were in heaven, for my beloved mother Beatrix Juliana Donsu and Ma' Ina. Thanks also for my beloved sisters Jane S. Thambas, Joice M. Thambas and Hellen C. Thambas for their support to me.

Of course, this acknowledgements not be completed without thanking to my family; my wife Dr. Pingkan Peggy Egam, my lovely daughters Anastasia Talita Thambas, Gabriela Tabita Thambas, and Beatrix Tesalonika Thambas for their true support and always give me endless inspiration and provide invaluable happiness. Because of them I struggle and hard effort to complete this dissertation.

TABLE OF CONTENTS

LIST OF FIGURES

LIST OF TABLES

Chapter 1

INTRODUCTION

1.1. BACKGROUND

Japan has suffered many storm surges and other disasters such as high discharge by torrential rain in the past. As Japan is located in the region of the high tropical cyclone, it often experiences storm surge disaster caused mainly by typhoons. On September 26, 1959, super Typhoon Vera, also known as Isewan Typhoon in Japan, made landfall in the area of the southern coast of Japan, striking the Kushimoto region in the Wakayama Prefecture. The storm was the most destructive typhoon to impact the country in recent history, causing more than US$260 million worth of damage of buildings (RMS Special Report, 2009). The Japan Meteorological Agency (JMA) named the storm "Isewan" Typhoon. By the strength and extent of the storm's wind field and storm surge, most of the country sustained damaging winds, and more than 310 km^2 of land inundated. Also, it caused destroying thousands of homes, leaving more than 5,000 people dead and injuring more than 39,000 individuals. Super Typhoon Vera made a large storm area; the strong wind rocked almost the whole of Japan. The maximum wind speed recorded was 45.4 m/s and maximum instantaneous wind speed: 55.3 m/s in Arako, Aichi Prefecture. In Nagoya, the maximum wind speed recorded was 37.0 m/s while the maximum instantaneous wind speed was 45.7 m/s. More than 20 m/s of wind speed and over 30 m/s of the maximum instantaneous wind speed recorded in almost every part of Japan from Kyushu to Hokkaido. An extraordinarily high surge of up to 3.45 m overthrow dykes along the coast and at river mouths. The flooding sea water rushed inland, washing away many people who had no time to escape. Typhoon Isewan caused the worst damage by the

typhoon in the history of Japan, including 5,092 persons dead or missing and 38,921 people injured. In 2005, super typhoon Nabi occurred to the far southeast of Japan. Powerful typhoon Nabi has pummeled southwestern Japan with torrential rain and high winds, causing floods and landslides, crippling transport and prompting officials to tell more than 100,000 people to flee their homes. According to press reports, 32 people were killed and 140 people were injured. At least 270,000 households were without electricity, and around 10,000 buildings damaged (source: Monthly Global Tropical Cyclone Summary, 2005).

Besides storm surge, flood by heavy rain or torrential rain is also a frequent disaster in the region of Japan. Every year in this region torrential rains occur with the small and big scale. Torrential rains fed by the warm ocean waters surrounding Japan can cause significant flooding and mudslides on the islands. In June 1953, a flood hit Northern Kyushu, Japan (Fukuoka Prefecture, Saga Prefecture, Kumamoto Prefecture and Oita Prefecture). More than 1,000 mm precipitation on Aso and Hikosan mountains, produced the great flood into many rivers such as Chikugo River when the torrential rain occur on the rainy season. More than 1,000 people dead and missing, 450,000 houses were flooded, and 1,000,000 people suffered from the flood (Takezawa, 2014). In July 2012, heavy rains fell on the Kyushu island, causing floods and landslides, especially in northern regions. Some towns were temporally isolated. Hundreds of thousands of victims had to leave their homes, more than 25 people lost their lives.

1.2. OBJECTIVES

The aim of this study is analyzed the storm surge by the past main typhoon and river flooding occurrs in this study area. With a scenario two disaster

simultaneously occurred in the same time, the conditions of the water level will be presented, which causes the inundation in the coastal area of the Ariake Sea and Saga lowland. In this research, estimate the inundation risk due to storm surge and flood will be conducted. A map of inundation risk area is also created for coastal disaster management.

1.3. LIMITATIONS AND ASSUMPTIONS

Limitations and assumptions of the problem of research in this dissertation are as follows:

1. The software used to analyze the water level in the river is a MIKE 11 developed by Danish Hydraulic Institute (DHI).
2. The software used to analyze the water level at the sea and inundation is a MIKE 21 FM (hydrodynamic module) developed by Danish Hydraulic Institute (DHI).
3. A typhoon was selected based on the previous research in this study area, especially the mouth of the Ariake Sea. Typhoon Pat that occurred in this study area was selected as a reference.
4. A flood or high discharge was selected based on the torrential rain that took place in this study area in July 2012.
5. The Chikugo River was selected for analyzing the water level based on the high discharge or river flood when the torrential rain occurred in this study area and based on previous research.
6. The selection of data from the stations to be used is done based on the computational mesh employed in hydrodynamic simulations.

7. In the simulations we assumed that two disasters, the storm surge by Typhoon Pat and high discharge by torrential rain simultaneously occur at the same time in July 2012.
8. In the hydrodynamic simulations, we assumed that there was no structural failure of the dyke.
9. Evaluation sites in the Saga Plain are the area in front of the Shiroishi City, Rokkaku River Estuary, Kase River Estuary, Higashiyoka, Saga Airport, Chikugo River Estuary and Ohamma.

1.4. OUTLINE OF DISSERTATION

This dissertation consists of eight chapters. Chapter 1 contains an introduction, background, and aims of this dissertation.

Chapter 2 contains several references review. In this chapter, the theory and references that used in this study and also the previous research related to this research as a reference will be presented.

Chapter 3, discusses about the Ariake Sea coastal area and Saga lowland. In this chapter, the history and disaster occurred in this area also the problem in this area are explained.

Chapter 4, a 2-D simulation model is presented for modeling of storm surges in the Ariake Sea. In this chapter, the software MIKE 21 numerical model hydraulic developed by DHI is used for analysis of storm surge.

Chapter 5, 1-D hydrodynamic modeling of flooding in the Chikugo River will be presented. In this chapter, MIKE 11 numerical model hydraulic is used for analysis of river flooding or high discharge.

Chapter 6, model coupled analysis of inundation in the coastal area of the Ariake Sea due to storm surge and flood is done. In this chapter, the coupling of 1D and 2D numerical model hydraulic is conducted using MIKE FLOOD.

Chapter 7, disaster management in the coastal area of the Ariake Sea and saga lowland is presented. In this chapter, inundation risk analysis using GIS is conducted and planning for flood disaster management in the coastal area of the Ariake sea and Saga lowland is done based on the simulation result of inundation in this area.

Chapter 8, the overall findings of the previous chapters and the recommendation for further research are summarized and discusses in this chapter.

Chapter 2

LITERATURE REVIEW

This chapter consists of seven parts. The first part focuses on related researches, the second part focuses on storm surge, third part focuses on the typhoon, fourth part focuses on river flooding, fifth part discusses the numerical model, and seven part is about conclusions.

2.1 RELATED RESEARCHES

In recent year, the research about the influence of the storm surge by the typhoon to inundation in the saga lowland and the surrounding has been conducted by Dundu et al. (2012). They analyzed, the storm surges by the past main typhoons, such as Typhoon Songda (T200418), Typhoon Nabi (T200514), Typhoon Wilda (T196420), Typhoon Pat (T198513) are analyzed under several scenarios with the high wind speed, to obtain the effect of tide levels to the storm surge and to know the conditions that the water level exceeds the height of coastal dyke, which causes the inundation in the Saga Plain. The performance of the old coastal dykes is calculated and also coastal flood hazard management in this area is conducted. The result of this research, typhoon Sonda, typhoon Nabi, typhoon Wilda and typhoon Pat do not bring about water level to exceed the existing coastal dyke 7.5 m. The scenario using of wind speed maximum 80 m/s and wind direction 180^0 are constant occurred can cause the water level exceed the existing coastal dyke in the several area.

According to Yoong et al. (2013), using a numerical finite-volume coastal ocean model, a storm surge was simulated to investigate the inundation

characteristics for the coastal area at Masan, Yeosu and Busan cities on the southern coast of Korea. In the model, a moving boundary condition (wet-dry treatment) was applied to examine inundation propagation by the storm surge. Simulated inundation range and depth were compared with the inundation map made from field measurements after the typhoon event. The results of inundation simulations in this study show good correspondence with not only the observed inundation area but also inundation depth.

From the research of Prashant and Dhrubajyoti (2012), with title "Flood inundation simulation in Ajoy River using MIKE-FLOOD", the simulated values for the validation period were having good agreement with observed values. Manning's roughness coefficient, n, was the only calibrating parameter. The bathymetry of the study area for the MIKE-21 hydrodynamic setup was the only significant input for 2-D MIKE-21 cells with lateral links. The simulation by MIKE-FLOOD was carried out for two monsoon months of the year 2000 as flooding was severe for this year. In their study, the flow in the main river channel was simulated using the 1D equations. For the water spilling over the banks of the overflowing river onto the flood plain, the 2D equations were solved using numerical schemes. Mass conversion equation usually does the link between the two kinds of flow.

Yamashiro et al. (2014), on their research, to understand the characteristic of storm surge along the coast of innermost in the Ariake Sea. The observational results of this research show that the storm surge amplifies remarkably in the innermost area of the Ariake Sea in particular. The numerical simulation results that there is the risk of severe storm surge disaster in the Ariake Sea under event the present climate condition.

Hashimoto et al. (2015), on their research, comparing the values is used to discussed a bias correction method of typhoon strength. Also, they evaluated a maximum storm surge anomaly on the Ariake Sea coast by correcting bias of the typhoons with the proposed method. The results of their research indicated the possibility of storm surge anomaly of 2.8 m, exceeding the current design storm surge anomaly of 2.36 m at the innermost of the Ariake Sea.

2.2 STORM SURGE

A storm surge is an abnormally high sea level produced by severe atmospheric conditions, lasting for a period ranging from a few minutes to a few days (Hardword, 2012). Famous storm surges include the 1953 North Sea Flood, the 1970 Bangladesh floods, Hurricane Katrina in New Orleans in 2005 and Hurricane Sandy in 2013.

Storm surge is simply a behavior of water that is pushed toward the shore by the force of the winds swirling around the storm. This advancing surge combines with the normal tides to create the hurricane storm tide, which can increase the mean water level 4.5 m or more. Also, wind waves are superimposed on the storm tide. This rise in water level can cause severe flooding in coastal areas, particularly when the storm tide coincides with the normal high tides.

The water level produced by a storm surge is the result of a complex set of interactions between the storm surge, local tidal characteristics, the wind and swell waves, currents and local water flow. However, the main factor is the state of the tide at the time that the storm hits the shore. When a storm hits a low-lying shore at the same time as a high tide, water levels can rise considerably above their normal level, resulting in severe flooding.

The storm surge is created by the wind, waves, and low pressure. Three mechanisms contribute to the storm surge (wheather underground, https://www.wunderground.com/prepare/storm-surge):

1. The action of the winds piling up water (typically more than 85% of the surge).
2. Waves pushing water inland faster than it can drain off. This is called wave set-up. Wave set-up is typically 5 - 10% of the surge.
3. The low pressure of a hurricane sucking water higher into the air near the eye (typically 5 - 10% of the surge).

Storm surge is caused primarily by the strong winds in a hurricane or typhoon. The wind circulation around the eye of a hurricane or typhoon blows on the ocean surface and produces a vertical circulation in the ocean. In deep water, there is nothing to disturb this circulation and there is very little indication of storm surge.

Once the hurricane or typhoon reaches shallower waters near the coast, the vertical circulation in the ocean becomes disrupted by the ocean bottom. The water can no longer go down, so it has nowhere else to go but up and inland. In general, storm surge occurs where winds are blowing onshore. The highest surge tends to occur near the “radius of maximum winds,” or where the strongest winds of the hurricane or typhoon occur.

2.3 TYPHOON

The definition of the typhoon is different between the Japanese standard and the international standard. A tropical storm with the wind speed of more than 34 knots is called a "typhoon" in Japan, while in the international standard, that with the wind speed of more than 64 knots is called a "typhoon". Different names call of tropical cyclones in the world in each basin, such as a "typhoon" and a "hurricane", but the

standard to be called by such names is the same: more than 64 knots of wind. A typhoon with maximum sustained surface winds greater than or equal to 130 knots (approximately Category 5) is called a "super typhoon," and a hurricane of Category 3 and above is known as a "major hurricane." A tropical cyclone weaker than Category 1 is not a "typhoon" in the international standard, but may be classified as a "typhoon" in the Japanese standard. In mainland China and Hong Kong, a typhoon with maximum sustained surface winds greater than or equal to 100 knots are called Super Typhoon. However, maximum sustained winds are measured differently in mainland China, and Hong Kong, where the former uses 2-min mean, and the latter uses 10-min mean. For other regions than Japan and the United States, please refer to the classification of tropical cyclones in the world. (http://agora.ex.nii.ac.jp/digital-typhoon/help/unit.html.en).

Typhoons, hurricanes, and cyclones may have different names according to the region they hit, but typhoons, hurricanes, and cyclones are all violent tropical storms that can generate ten times as much energy as the Hiroshima atomic bomb. The typhoon that devastated the Philippines, wiping out entire towns with a death toll that could soar well over 10,000, is the Asian term for a low-pressure system that is called a hurricane in the Atlantic and northeast Pacific and a cyclone in the South Pacific and the Indian Ocean. However, meteorologists use the term "tropical cyclone" when talking about these immensely powerful natural phenomena, which are divided into five categories according to the maximum sustained wind force and the scale of the potential damage they can inflict. (http://tuoitrenews.vn/international/14985/cyclone-hurricane-typhoon-different-names-same-phenomenon)

2.4 RIVER FLOOD

River flood or flash flood is the high discharge that occurs on the river which is caused by heavy or excessive rainfall in a short period, generally less than 6 hours. River floods are usually characterized by raging torrents after heavy rains that rip through river beds, urban streets, or mountain canyons sweeping everything before them. They can occur within minutes or a few hours of excessive rainfall.

A river flood is one of the most common forms of natural disaster. It occurs when a river fills with water beyond its capacity. The surplus water overflows the banks and runs into adjoining low-lying lands. River floods are responsible for the loss of human life and the damage to property. Each year, the number of deaths from flooding of rivers is more than any other natural disaster. (Debashree, http://www.ehow.com/about_6310709_river-flood_.html).

River floods have serious repercussions. The floodwater drowns human beings and animals. It damages buildings, roads, bridges and crops. A serious aftermath of river flooding is pollution of the water supply. Flood water also damages sewage systems, gas lines, and power lines.

In the reseant year, the river flooding is one of the natural disaster that occurs in the rainy season and typhoon which cause damage and loss of property and lives in Japan. On July, 2012 the Shirakawa River is flooded in Kumamoto, Japan, which cause 19 people confirmed dead and 7 others are still missing in Kumamoto and Oita perfectures (source: record-setting rainfall hit Kyushu-getty images). Also, in September 2015, the Kinugawa River is flooded in Joso, Japan. The flooding has forced more than 100,000 people from their homes, at least 17 people were injured and two people were missing (Aljazeera News, 2015).

2.5 HYDRODYNAMIC MODEL

2.5.1 1-D Numerical Model

The most widely used approach to modeling fluvial hydraulics has been 1-D finite difference solutions of the Saint-Venant Equations (Bates and De Roo, 2000). 1-D solutions of the Saint-Venant Equations are derived based on several assumptions: the flow is one-dimensional, the water level across the section is horizontal, the streamline curvature is small and vertical accelerations are negligible, the effects of boundary friction and turbulence can be accounted for using resistance laws analogous to those for steady flow conditions, and the average channel bed slope is small so the cosine of the angle can be replaced by unity (Cunge, Holly and Verwey, 1980). Widely available, the software MIKE11 uses the general form of the section-averaged Navier-Stokes equations. The basic forms of the equations used in MIKE11 are shown in Equations 2.1 and 2.2.

$$\frac{\partial Q}{\partial x} + \frac{\partial A}{\partial t} = q \tag{2.1}$$

$$\frac{\partial Q}{\partial t} + \frac{\partial\left(\alpha \frac{Q^2}{A}\right)}{\partial x} + gA\frac{\partial h}{\partial x} + \frac{gQ|Q|}{C^2 AR} = 0 \tag{2.2}$$

where Q is discharge, x is longitudinal channel distance, A is a cross-sectional area, q is lateral inflow, t is time, h is flow depth, C is the Chézy coefficient and R is the hydraulic radius.

An inherent assumption of 1-D finite difference river modeling is that flow velocities are perpendicular to cross-sections. Additionally, water surface elevations are assumed constant for entire cross-sections. For river reaches containing backwater areas or naturally occurring diversion channels, these assumptions are frequently violated. For out-of-bank flow, interaction with the floodplain results in highly complex fluid movement with at least two-dimensional properties. Flow at the channel-floodplain transition has been shown to develop a three-dimensional flow field due to intense shear layers (Bates and De Roo, 2000).

Development of a one-dimensional hydraulic model requires user discretion in defining the model geometry. Bates and De Roo (2000) found that subjectivity of cross-section placement is a significant contributor to the overall accuracy of a 1-D hydraulic model. In addition to directly determining overbank reach lengths, placement of cross-sections must be executed so that changes in conveyance due to expansions or contractions are accurately captured.

2.5.2 2-D Numerical Model

The complex interaction of channel and floodplain flow fields makes two-dimensional simulation codes more desirable than one-dimensional codes in many modeling situations (Horritt and Bates, 2002). Continual improvements in computational resources and affordability have also increased implementation of two-dimensional modeling.

The governing equations of 2-D plane storm surge numerical model (LI Daming et al., 2011) are,

$$\frac{\partial \xi}{\partial t} + \frac{\partial}{\partial x}\left[(\xi + h)u\right] + \frac{\partial}{\partial y}\left[(\xi + h)v\right] = 0 \tag{2.3}$$

$$\frac{\partial u}{\partial t} + u\frac{\partial u}{\partial x} + v\frac{\partial u}{\partial y} - fv + g\frac{\partial \xi}{\partial x} + \frac{gu\sqrt{u^2 + v^2}}{(\xi + h)C^2} - \frac{1}{\rho H}\tau_{x,s} = 0 \tag{2.4}$$

$$\frac{\partial v}{\partial t} + u\frac{\partial v}{\partial x} + v\frac{\partial v}{\partial y} + fu + g\frac{\partial \xi}{\partial y} + \frac{gv\sqrt{u^2 + v^2}}{(\xi + h)C^2} - \frac{1}{\rho H}\tau_{y,s} = 0 \tag{2.5}$$

where ξ is tidal level setup; h static water depth; H total water depth, $H = h + \xi$; f Coriolis coefficient; g gravity acceleration; $\tau_{x,s}$ and $\tau_{y,s}$ wind stress in *x* and *y*-direction: *C* Chézy coefficient, $C = \frac{1}{n}\bar{h}^{1/6}$, $\bar{h}$ the average value of water depth; n Manning roughness coefficient; *u* and *v* depth average velocity in *x* and *y*-direction.

2.5.3 Coupling 1-D and 2-D models

The coupled model of 1-D and 2-D can be applied to the simulation of inundation in a floodplain area. One-dimensional numerical models are unable to resolve complex flood plain flow fields and require post-processing to produce realistic flood extents. Two-dimensional numerical models fail to model structural elements that may produce supercritical or pressurized flow conditions. Consequently, recent urban flood modeling efforts have been focused on dynamically coupling one-dimensional and two-dimensional models to avoid these limitations. A one-dimensional numerical model of the river channel complimented by a two-dimensional model of the floodplain provides improvements in hydraulic modeling

accuracy and computational efficiency. If an entire river reach is modeled using a one-dimensional model, then computational nodes within that portion of the two-dimensional mesh will not become active, improving computational efficiency.

2.6 INTEGRATED HYDRODYNAMICAL MODEL

2.6.1 MIKE 11- A modeling system for river and channel hydraulics

MIKE 11 is a software package for simulating flow and water level, water quality and sediment transport in rivers, floodplains, irrigation canals, reservoirs and other inland water bodies. MIKE 11 is a one-dimensional river model. It was developed by DHI Water & Environment Denmark. MIKE11 has long been known as a software tool with advanced interface facilities.

2.6.1.1 Modules

The computational core of MIKE 11 is hydrodynamic simulation engine, and this is complemented by a wide range of additional modules and extensions covering almost all conceivable aspects of river modeling.

2.6.1.2 Development of Model

The processing of the data for the simulation in the MIKE 11 hydrodynamic module involves; preparation of the network (can assume a straight stream channel),

cross section, hydrodynamic and boundary parameters. The data hourly rainfall, water levels, and flows are created incompatible MIKE 11 time series in a separate file as the input for the parameter editors.

a. The River Network file

The River Network file allows the modeler to:

- define the river network and reference cross-sections and control structures to the network, and
- graphically obtain an overview of the model of information in the current simulation.

b. The Cross-Section File

The Cross-Section file contains streambed cross-sections as specified locations along a river network. The geometry of cross-sections is usually obtained from field-surveyed data.

c. The Boundary Files

The Boundary file consists of boundary conditions in a time-series format for the river network's boundaries. The water-level boundary must be applied to either the upstream or downstream boundary condition in the model. The discharge boundary can be applied to either the upstream or downstream boundary condition and can also be applied to a side Tributary flow (lateral inflow).

d. The Hydrodynamic Parameter File

The Hydrodynamic Parameter File bed and floodplain resistance requires the data for the river network. The differentiation between the streambed and floodplain along the river network is accomplished at each cross-section in the cross-section file.

2.6.1.3 Applications

MIKE11 has been used in hundreds of application around the world. Its main application areas are flood analysis and alleviation design, real-time flood forecasting, dam break analysis, optimization of reservoir and canal gate/structure operations, ecological and water quality assessments in rivers and wetlands, sediment transport and river morphology studies, salinity intrusion in rivers and estuaries. Presentation of results from MIKE 11 is carried out with MIKE View. MIKE View is a Windows-based result presentation and reporting tool for MIKE 11.

2.6.2 MIKE 21 - An applications of hydraulic phenomena in lakes, estuaries, bays, coastal areas and seas.

MIKE 21 is a computer program that simulates flows, waves, sediments and ecology in rivers, lakes, estuaries, bays, coastal areas and seas in two dimensions. MIKE 21 was developed by DHI. It applies to the simulation of hydraulic flow in rivers and estuaries in two dimensions. It can be used for design data assessment for coastal and offshore structure, inland flooding and overland flood modeling. Using a

Finite Difference Method (FDM), MIKE 21 model has integrated hydraulic structures in 2-D grids and can be applied for urban and coastal flood mapping.

2.6.2.1 Hydrodynamic Module

The hydrodynamic module is based on the numerical solution of 2-D shallow water equations: the depth integrated incompressible Reynolds-averaged Navier-Stokes equation subject to Boussinesq assumption and the presence of hydrostatic pressure (DHI, 2006).

2.6.2.1.1 Flood and Dry

a. General Description

The approach for the treatment of the moving boundaries (flooding and drying fronts) problem is based on the work by Zhao et al. (1994) and Sleigh et al. (1998). When the depths are small, the problem is reformulated and only when depths are slight the elements/cells are removed from the calculation. The reformulation is made by setting the momentum fluxes to zero and only taking the mass fluxes into consideration.

b. Recommended value

The default values are: drying depth h_{dry} = 0.005 m, flooding depth h_{flood} = 0.05 m and wetting depth h_{wet} =0.1 m. The wetting depth, h_{wet}, must be larger than the drying depth, h_{dry}, and flooding depth, h_{flood}, must satisfy.

In this research based on the previous research by Dundu (2012), the values of flood and dry is used as follows: h_{dry} = 0.1 m, flooding depth h_{flood} = 0.7 m and wetting depth h_{wet} =0.7 m.

2.6.2.1.2 Eddy Viscosity

In many applications, a constant eddy viscosity can be used for the horizontal stress terms. Alternatively, Smagorinsky (1963) proposed to express sub-grid scale transports by an effective eddy viscosity related to a characteristic length scale. The Smagorinsky coefficient, C_s, should be chosen in the interval of 0.25 to 1.0. In Eddy Parameters, if using Smagorinsky formula or coefficient the value of eddy viscosity must specify a minimum and maximum value. The format of the eddy viscosity coefficient (in m^2/s), or Smagorinsky coefficient, can be specified as constant (in domain) and varying in domain. Ueno (1989), in the Abualtayeb et al. (2008, 2007), suggests Eddy viscosity in the interval of 0.1to 1.0. In this research based on the previous research by Dundu (2012), Eddy Viscosity using Smargorinsky coefficient, C_s is 0.1 constant in domain.

2.6.2.1.3 Bed Resistance

The bed resistance can be specified in three different ways:

- No bed resistance
- Chézy number
- Manning number

The format of Chézy number, C ($m^{1/2}/s$), and the Manning number, m ($m^{1/3}/s$), can be specified in two ways constant (in domain) and varying in domain.

The bottom stress, $\overline{\tau_b}$, is determined by a quadratic friction law,

$$\frac{\overline{\tau_b}}{\rho_0} = c_f \overline{u_b}\left|\overline{u_b}\right| \tag{2.6}$$

Where c_f is the drag coefficient, $\overline{u_b}$ is the flow velocity above the bottom and ρ_0 is the density of the water. For two-dimensional calculations $\overline{u_b}$ is the depth average velocity and the drag coefficient can be determined from the Chézy number, *C*, or Manning number, *n*

$$c_f = \frac{g}{C^2} \tag{2.7}$$

$$c_f = \frac{g}{\left(nh^{1/6}\right)^2} \tag{2.8}$$

Where h is the total water depth and g is the gravitational acceleration. The unit of Chézy numbers and Manning numbers are ($m^{1/2}/s$) and ($m^{1/3}/s$), respectively.

The value of Manning number in the range 20-40 $m^{1/3}/s$ is typically used with a suggested value of 32 $m^{1/3}/s$ if no other information is available. The value of Chézy number in the range 30-50 $m^{1/2}/s$ is common for the coastal and marine application (in the MIKE 21 DHI tutorial). The other value of Chézy number has been applied by some researchers at the Ariake Seas be varied. Abualtayeb et al. (2007), used the value of Chézy coefficient, 10 $m^{1/2}/s$ and 50 $m^{1/2}/s$. Kanayama and Dan (2006), used the value 61.4 $m^{1/2}/s$ for Chézy coefficient. The Chézy coefficient is determined as

50 $m^{1/2}/s$ tuning by Yano et al. (2010), on their research. In this research the Chézy coefficient is determined as 32 $m^{1/2}/s$, constant in domain.

2.6.2.1.4 Coriolis Forcing

A Coriolis parameter is defined as,

$$f_c = 2 \cdot \Omega \cdot \sin(\phi) \qquad \ldots\ldots\ldots\ldots\ldots\ldots \quad (2.9)$$

where $2 \cdot \Omega = 1.458 \times 10^{-4} s^{-1}$ and ϕ is latitude. This parameter is constant at any fixed location.

The effect of the Coriolis force can be included in three different ways (DHI, 2011),

- No Coriolis force
- Constant in domain
- Varying in domain

If the constant in domain option is selected the Coriolis force will be calculated using a constant specified reference latitude (in Degree)

If the varying in domain option is selected, the Coriolis force will be calculated based on the geographical information given in the mesh file. In this research the Coriolis force varying in domain is selected.

2.6.2.1.5 Wind Forcing

It is possible to take into account the effect of the wind on the flow field. The format of the wind data can be specified as,

- *Constant.* The wind is blowing from the same direction and with the same magnitude for the whole simulation period and over the entire model area.
- *Varying in time and constant in domain.* The magnitude and direction vary during the simulation period but is the same over the entire model area.
- *Varying in time and domain.* The magnitude and direction vary during the simulation period and over the model area.

The effect of wind blowing over the model area following way :

The surface stress, $\overline{\tau_s}$, is determined by the wind speed above the water. The empirical relation of stress is given by the following,

$$\overline{\tau_s} = \rho_a c_d |u_w| \overline{u_w} \quad \text{..... (2.10)}$$

where ρ_a is the density of air, c_d is the empirical drag coefficient of air, and $\overline{u_w} = (u_w, v_w)$ is the wind speed 10 m above the sea surface.

Definition of wind direction that had been given in degrees blowing from relative to true north can be seen in Figure 2.1.

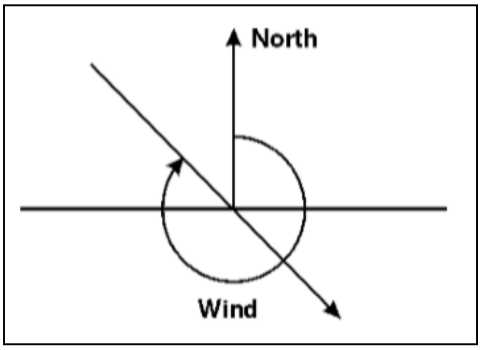

Figure 2.1: Definition of Wind Direction

The drag coefficient can either be a constant value or depend on the wind speed. The empirical formula proposed by Wu (1980, 1994) is used for the parametrization on the drag coefficient as follow:

$$c_d = c_a + \frac{c_b - c_a}{w_b - w_a}.(w_{10} - w_a) \quad \text{if} \quad w_{10} < w_a \qquad \text{..... (2.11a)}$$

$$c_d = c_a + \frac{c_b - c_a}{w_b - w_a}.(w_{10} - w_a) \quad \text{if} \quad w_a \le w_{10} \le w_b \qquad \text{..... (2.11b)}$$

$$c_d = c_b + \frac{c_b - c_a}{w_b - w_a}.(w_{10} - w_a) \quad \text{if} \quad w_{10} > w_b \qquad \text{..... (2.11c)}$$

where c_a , c_b , w_a and w_b are empirical factors and w_{10} is the wind speed 10 m above the sea surface. The default values for the empirical factors are $c_a = 1.255 \cdot 10^{-3}$, $c_b = 2.425 \cdot 10^{-3}$, $w_a = 7 m/s$, $w_b = 25 m/s$. The value gives generally good result for open sea applications. Field measurements of the drag coefficient collected over lakes indicate that the drag coefficient is larger than open ocean data (Geenaert and Plant, 1990).

In this research wind forcing (speed and direction) is the format of wind data varying in time and constant in domain.

2.6.2.1.6 Wind Friction

The wind friction can be specified either as a constant or varying with the wind speed. In the latter case, the friction is linearly interpolated between two values based on the wind speed, and if the wind speed is below the lower limit or above the upper limit, the friction is given the value corresponding to that limit (DHI, 2011).

The wind friction in this research is a constant and the value be used is 0.001255 based on the previous research by Dundu (2012).

2.6.2.2 Basic Parameter

2.6.2.2.1 Domain

The MIKE 21 Flow Model FM is based on flexible mesh approach. Setting up the mesh includes a selection of the appropriate area to be modeled, adequate resolution of the bathymetry, wave wind and flow fields under consideration and definition of codes for open and closed boundaries.

a. Mesh and Bathymetry

The mesh file is ASCII file including information of the geographical position and bathymetry for each node point in the mesh. The file also includes information on the node connectivity in the mesh.

b. Boundary Names

Figure 2.2 shows the definition of codes in a simple application. In this case, three open boundaries have been detected from the mesh file specified in the domain parameters; code 2, code 3 and code 4. In the main boundary name dialog, the name of code values can be re-name to more appropriate names, such as shown in Figure 2.3

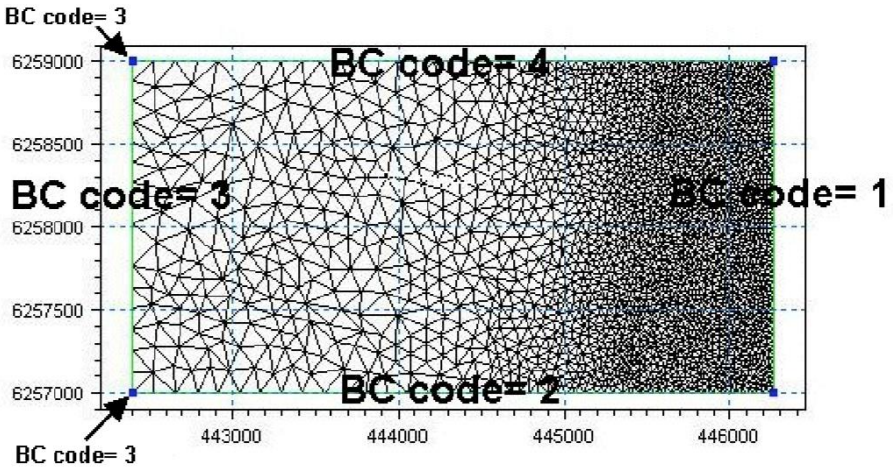

Figure 2.2: The definition of boundary codes in the mesh is made in the Mesh Generator (DHI, MIKE 21 user guide, 2011)

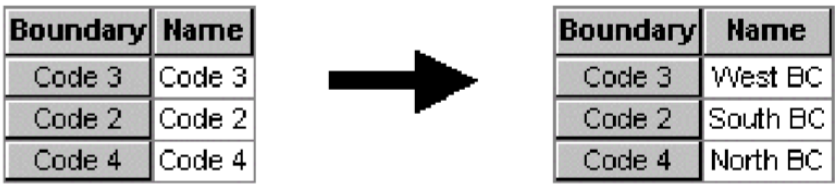

Figure 2.3: Change of default code names to more appropriate names (DHI, MIKE 21 user guide, 2011)

2.6.2.2.2 Time

The period to be covered by the simulation is specified such as specify the simulation start date, the overall number of time steps and the overall time step interval (in seconds). The simulation always starts which the time step number 0 and the simulation start date is the historical data and time corresponding to time step 0. The simulation end date is presented for reference.

The various modules in MIKE 21 Flow Model FM each use an internal time step, see in Figure 2.4.

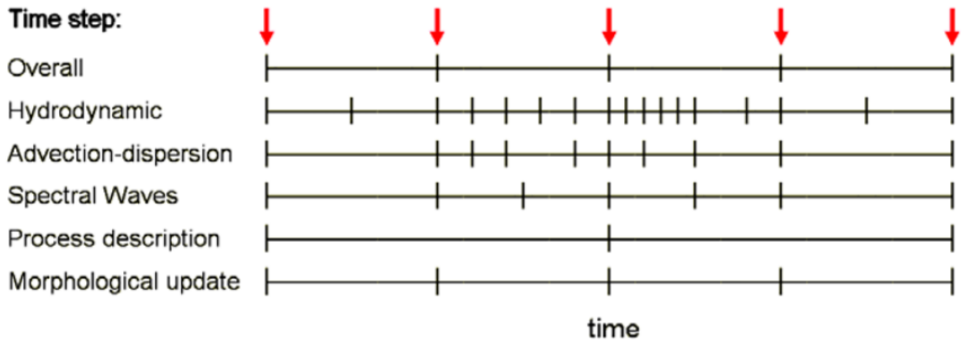

Figure 2.4: Overall time step related to internal time step
(DHI, MIKE 21 user guide, 2011)

The time step for the hydrodynamic calculations, the advection-dispersion calculations, and the spectral waves calculations are dynamic and each determined to satisfy stability criteria. All time steps within the simulation for the various modules are synchronized at the overall discrete time step. The time step for the hydrodynamic calculations is the synchronized at the time step for the advection/dispersion calculation.

2.6.3 MIKE FLOOD

MIKE FLOOD is a tool that integrates the one-dimensional model MIKE 11 and the two-dimensional model MIKE 21 into a single, dynamically coupled modeling system. There are many advantages to using MIKE FLOOD, and many model applications can be improved through its use, including:

- Floodplain application
- Storm surge studies
- Urban drainage
- Dam break
- Hydraulic design of structures
- Broad-scale estuarine applications

By combining the two modelers MIKE 21 and MIKE 11 we can choose that the best features of both and make the best model with these functions. At present, there are six different types of MIKE FLOOD linkage available:

a. Standard link

"MIKE FLOOD user manual (2007) say as follows: This type of link is useful for connecting a detailed MIKE 21 grid into a broader MIKE 11 network, or to connect an internal structure or feature inside a MIKE 21 grid. The application of standard link can be seen in Figure 2.5."

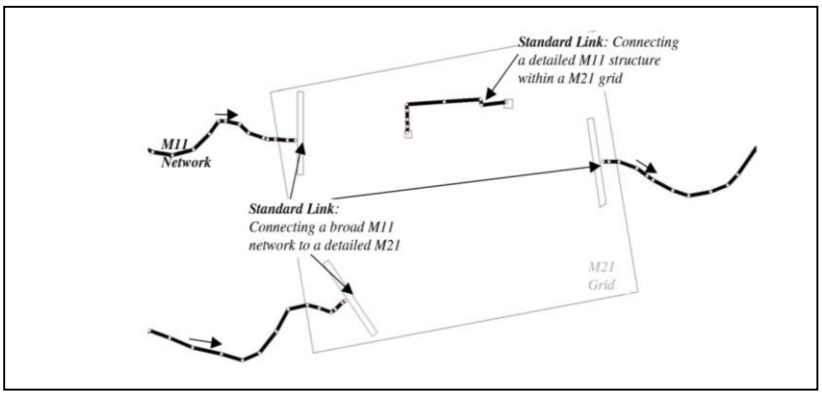

Figure 2.5: Application of Standard Links
(DHI, MIKE FLOOD user manual, 2007)

b. Lateral link

"MIKE FLOOD user manual (2007) say as follows: A lateral link allows a string of MIKE 21 cells to be laterally linked to a given reach in MIKE 11, either a section of a branch. Flow through the lateral link is calculated using a structure equation or QH table. This type of link is particularly useful for simulating overflow from a river channel onto a floodplain, where flow over the river levee is calculated using a weir equation. The application of the lateral link can be seen in Figure 2.6."

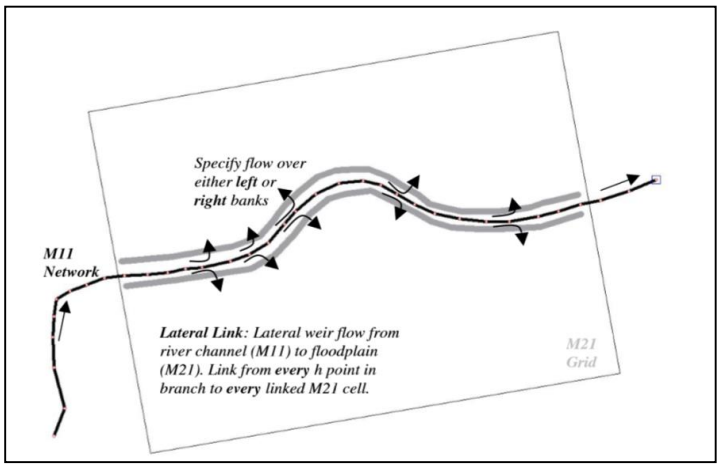

Figure 2.6: Application of Lateral Links
(DHI, MIKE FLOOD user manual, 2007)

c. Structure Link (Implicit)

"MIKE FLOOD user manual (2007) say as follows: The structure link is the first of a series of new developments planned for MIKE FLOOD. The structure link takes the flow terms from a structure in MIKE 11 and inserts them directly into the momentum equations of MIKE 21. This is fully implicit, so should not affect time step considerations in MIKE 21.

The structure link is useful for simulating structures within a MIKE 21 model. The link consists of 3 points MIKE 11 branch (upstream cross-section, structure, downstream cross-section), the flow terms of which are applied to the right or top of a MIKE 21 cell or group of cells. The application of the structure link can be seen in Figure 2.7."

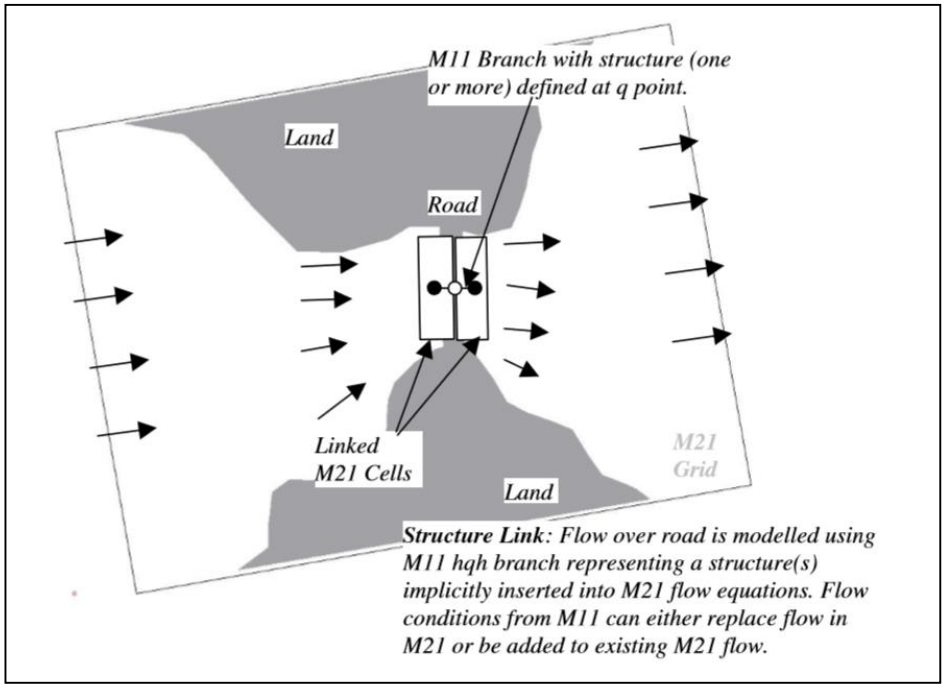

Figure 2.7: Application of Structure Links
(DHI, MIKE FLOOD user manual, 2007)

d. Zero Flow Link (X and Y)

"MIKE FLOOD user manual (2007) say as follows: A MIKE 21 cell specified as a zero flow link in the x direction will have zero flow passing across the right side of the cell. Similarly, a zero flow link in the y direction will have zero flow passing across the top of the cell. The zero flow link were developed to complement the lateral flow links. To ensure that floodplain flow in MIKE 21 does not travel directly across

a river to the opposite side of the floodplain without passing through MIKE 11, zero flow links are inserted to block MIKE 21 flows. An alternative to using the zero-flow links is to apply land cells which, depending upon grid resolution, may not be appropriate. Another useful application of zero flow links is to represent narrow blockages on a floodplain, such as roads and levees. Rather than using a string of land cells, a string of zero flow cells can be utilized."

e. Standard Link (QH Extrapolation)

The standard link uses a predictor term that modifies flow from MIKE 11. This is required to establish a value in MIKE 21 that it is consistent with the time centering differences in the MIKE 11 and MIKE 21 solutions. The extrapolation factor controls this predictor. An alternative method to this is QH extrapolation standard link. This link uses the implicit terms from MIKE 11 to produce a QH relationship through the link. In this way, the predictor from MIKE 11 is, in fact, the slope of the QH curve. In practice, there appears to be little difference between the two standard link methods. It is possible that the QH extrapolation is marginally more stable. However, tests show that while results using this approach remain stable at higher time steps, the accuracy of the solution at these great time steps rapidly deteriorates.

2.7 CONCLUSIONS

Many researches about flood and storm surge are conducted in recently years using numerical model analysis either using 1-D, 2-D, and 3-D hydrodynamic numerical models. Most of the researches were to analyze individually regarding

flood and storm surges. The related researchers used 1-D and 2-D hydrodynamic numerical models is conducted by Kadam and Dhrubajyoti, (2012). They also used coupled of 1-D and 2-D hydrodynamic numerical models but only for analyses of flow in the river.

Some parameters that will be utilized in this research have varying values, both of suggestion value by DHI and which has been used by other researchers in the Ariake Sea in their researches.

Chapter 3

THE ARIAKE SEA COASTAL AREA AND SAGA LOWLAND

3.1 INTRODUCTION

The Ariake Sea is located in Kyushu Island, west part of Japan. The sea opens to the East China Sea such as shown in Figure 3.1. The area and the average depth of the sea are approximately 1,700 km^2 and 20 m respectively. The sea has vast tidal flats in the innermost area. The maximum tidal range during the spring tide reaches 6m at the innermost area. Seawater, therefore, flows to the upstream section of the rivers at high tide. The hinterland is a low flatland that is 0-3 m above sea level since the tidal mudflats have been converted to land or reclaimed by people. As a result, it's hard to use the river water.

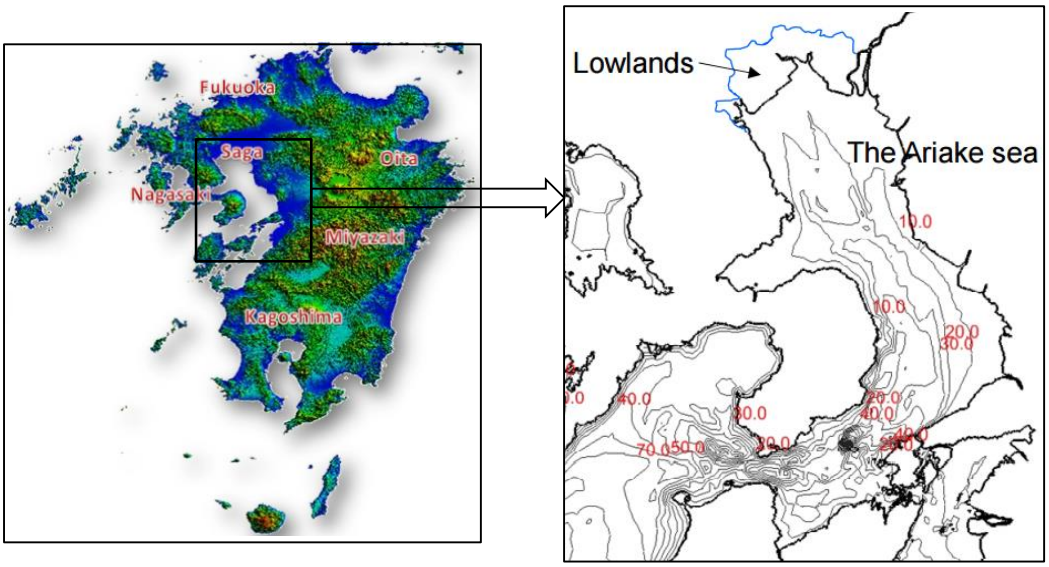

Figure 3.1: The Ariake Sea
(source: Yamashiro, 2014)

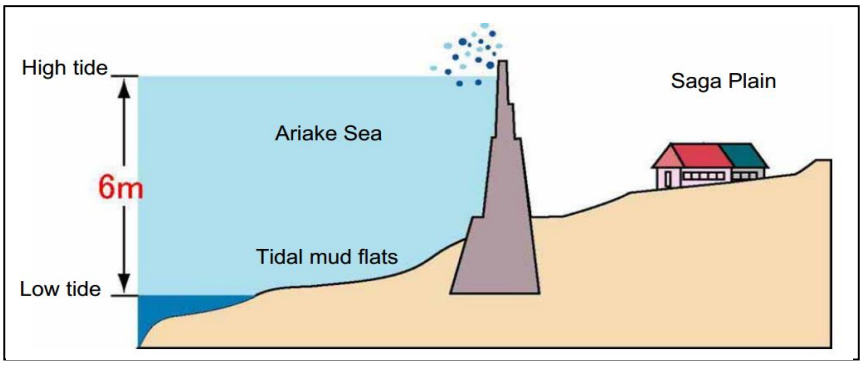

Figure 3.2: Tidal range condition in Ariake Sea
(Source: MLIT Takeo office, 2011)

The Ariake Sea is known as one of the sea areas that have a high risk of the storm surge in Japan because the sea area had been damaged by the storm surges caused by typhoons in the past (Hiyajo et al. 2011).

Many rivers flow into the Ariake Sea, such as the Chikugo, Kase, Rokkaku, Shiota, Kikuchi, Yabe, Midori, and Shira. The annual volume of freshwater inflow is about 8×10^9 m^3 (Tabata et. Al. 2010). The Chikugo River is the largest river flowing into the Ariake Sea, and its inflow amount accounts for 50% of the overall freshwater inflow and makes potential inundation in the coastal area when the high tide condition in the Ariake Sea.

(a) (b)

Figure 3.3: River condition when high tide (a) and low tide (b)
(Source: MLIT Takeo office, 2011)

Ariake Sea coastal area is known to have highest productivity of nori (Rhodophyta algae, Porphyra spp.) in Japan, so the nori production in its cultivation is developed as one of the specialties in Saga Prefecture. However, the harvest amount of nori in the growing in this area has been unstable in recent year, possibly due to the sudden change for worse in the fishery environment. Therefore, the recovery of the fishery environment has become the urgent problem to be settled in Ariake Sea and its coastal area.

In Saga Prefecture, nori is produced about 20 percent of the whole production in Japan (about 18 billion yen), and the nori sheet is commercialized as a brand of 'Saga Nori' produced from Ariake Sea around Saga Prefecture. In recent years, the decrease in the quality by the disease and the discolorment of the thalli of nori had become a serious problem. Therefore, it led uneasy elements in the income for the aquacultural labor of nori (Kato, 2007).

3.2 HISTORY OF ARIAKE SEA COASTAL AREA AND SAGA LOWLAND

The history of the Ariake Sea coastal area and Saga lowland has undergone a major change by reclamation works from the Ariake Sea in Nothern Kyushu, Japan. Reclamation works with very small slope have some problems such as flood prone area, so once the sea water enters these area immediately inundation occurs. Figure 3.4 shown the history of the changes the coastline of the Saga plain from beginning of the alluvial period until present coastline.

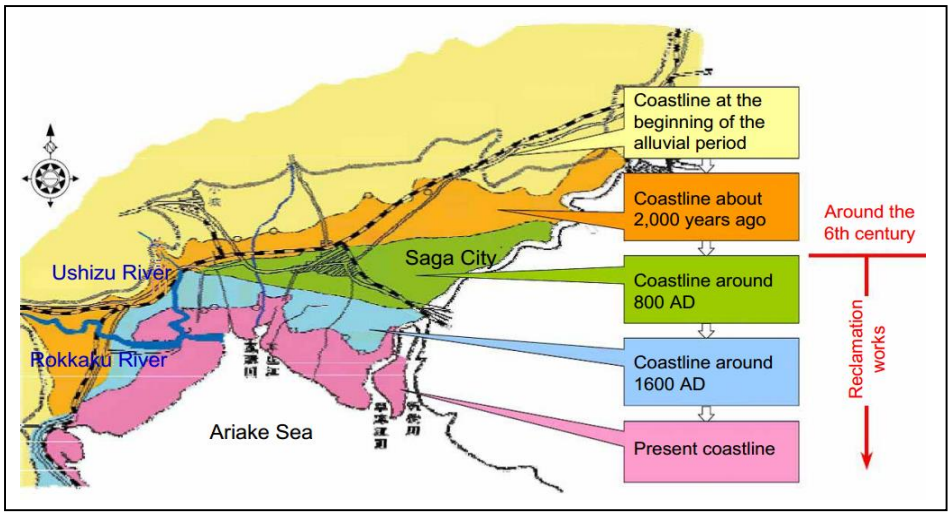

Figure 3.4. : Changes in the coastline of the Saga Plain
(Source: MLIT Takeo office, 2011)

3.3 NATURAL DISASTER OCCURRED IN THE COASTAL AREA OF ARIAKE SEA AND SAGA LOWLAND

As lowland areas with a very small slope, Saga plain and the Ariake Sea coastal area are flood-prone areas. Therefore, when the natural disaster such as torrential rain causing a flood or high discharge and the typhoon causing storm surge occurred in this field once the water enters these areas it will immediately create largely inundated area despite the fact that these areas are used for agricultural, offices, residential, airport, etc.

From 1952 to 2011, 72 typhoon passed through Saga within a radius of 150 km where the typhoon Ruth (1951), Wilda (1964), Pat (1985), Songda (2004), Chaba (2004), Nabi (2005), and several other typhoons resulted damage and casualties (Dundu, 2012). Storm surge by Typhoon Pat, causes damage to fish port by wave overtopping in the Ariake coast, Ashikari cho, Saga Prefecture as shown in Figure 3.5.

Figure 3.5: Storm surge damage during Typhoon Pat 1985
(Source: Kyushu Regional Planning Association, 2009)

The torrential rain causing inundation in the coastal area of Ariake Sea and Saga lowland is the one of the frequent natural disasters in this area. Figure 3.6 to Figure 3.8 show inundation by torrential rains in the Saga lowland area.

Figure 3.6: Inundation by torrential rains in Asahi Town, Takeo, July 1990
(Source: MLIT Takeo office, 2011)

Figure 3.7: Inundation by torrential rains in Asahi Town, Takeo, July 2009
(Source: MLIT Takeo office, 2011)

Figure 3.8: Inundation by torrential rains in Saga City, July 2012
(Source: IALT, 2012)

3.4 PRESENT STATE

Based on the typhoon Vera also known as Isewan typhoon in 1959, the Government has built the dyke along the coastline in the Ariake Sea with maximum

elevation 7.5 m high as shown in Figure 3.9. Modification of rivers, embankments and river channels has been conducted and modified weirs installed to improve the flow-down capability. The government also built the dam construction and drainage pump station. When constructing embankments, the ultra-soft ground has been enhanced using slow banking work. Figure 3.10 show the Kyuragi dam is situated on the Kyuragi River, a tributary of the Matsuura River, Karatsu, Saga, Japan.

Figure 3.9: Coastal dyke along Ariake Sea

Figure 3.10: Kyuragi dam
(Source: MLIT Takeo office, 2011)

3.5 CONCLUSIONS

The Coastal area of the Ariake Sea and Saga lowland has undergone a major change by reclamation works. These areas are flood-prone area caused by torrential rain and typhoon. To mitigate the impact of storm surge by the typhoon and torrential rains in the coastal area of Ariake sea and Saga lowland, the government has built a dyke along the coastline and rivers with a maximum level high 7.5 m. Also, the government has built a variety of dam such as Kyuragi dam for flood control and water use.

This research is necessary to evaluation of the existing dyke along the coastline and river in the coastal area of the Ariake Sea and Saga lowland if the two disaster storm surge and river flood simultaneously occurs in the same time.

Chapter 4

2-D SIMULATION MODEL OF STORM SURGE ANALYSIS IN THE ARIAKE SEA

4.1 INTRODUCTION

Typhoons have caused catastrophic damage by flooding due to storm surges in Japanese history (Torii, 2003). Table 4.1 shows storm surge disaster in Japan. The large scale of storm surge disasters have frequently occurred until 1961. For example, about five thousands of people were dead with storm surge by a typhoon in 1959, which was called Isewan typhoon. After 1970's, catastrophic flood disaster due to storm surges has decreased.

Table 4.1: Storm surge disaster in Japan

Date	Major damaged area	Human casualties			Damage to houses			Typhoon
		Dead	Injured	Missing	Completely destroyed	Partially destroyed	Washed away	
1 Oct. 1917	Tokyo Bay	1,127	2,022	197	34,459	21,274	2,442	
13 Sep. 1934	Ariake Sea	373	181	66	1,420		791	
21 Sep. 1934	Osaka Bay	2,702	14,994	334	38,771	49,275	4,277	Muroto
27 Aug. 1942	Suo Sea	891	1,438	267	33,283	66,486	2,605	
17 Sep. 1945	Southern Kyushu	2,076	2,329	1,046	58,432	55,006	2,546	Makurazaki
3 Sep. 1950	Osaka Bay	393	26,062	141	17,062	101,792	2,069	Jane
14 Oct. 1951	Southern Kyushu	572	2,644	371	21,527	47,948	1,178	Ruth
7 Sep. 1959	Ise Bay	4,697	38,921	401	38,921	113,052	4,703	Isewan
16 Sep. 1961	Osaka Bay	185	3,897	15	13,292	40,954	536	Second Muroto
21 Aug. 1970	Tosa Bay	12	352	1	811	3,628	40	No. 10
30 Aug. 1985	Ariake Sea	3	16	0	0	589	0	Pat

(Source: Torii, 2003)

Every year Japan territory is crossed by typhoon with a variety of categories, ranging from wind speed categories from the smallest to the largest. According to data in Table 4.1, three typhoons gave high damages and causing many casualties. First is typhoon Muroto (1934), that caused high damages to the buildings, largely inundated area for about 927.4 km^2 and 2,702 human casualties. The second one is typhoon Makurazaki (1945) that damaged some buildings, resulted to significantly inundated area for about 898 km^2 and 1,229 people also lost their lives during this typhoon. The last one is Typhoon Isewan (1959) which also gave the same impacts as the first two typhoons mentioned. The Typhoon Isewan created largely inundates on about 8340 km^2 area and 5,098 people killed (Dundu, 2012).

The Ariake Sea located in Kyushu Island is one of the sea areas that have a high risk of severe storm surges caused by typhoons in Japan. The total area of the sea is about 1,700 km^2 with l00 km gulf axial length, 16 km in average width, and 20 m of average water depth (Araki, et al., 2001). The sea has vast tidal flats in the innermost area. The maximum tidal range during the spring tide reaches 6m at the innermost area. The Ariake Sea is located in the region of 4 prefectures i.e. Nagasaki, Saga, Fukuoka, and Kumamoto. Most of the field in Saga Prefecture is adjacent to the Ariake Sea mainly lowland areas with a very small slope, so once the sea water enters these areas, it will immediately create largely inundated area despite the fact that these areas are being used for agricultural, offices, residential, airport, etc. However, the Japanese government has built a coastal dyke along the shorelines and river within this areas with the maximum height of 7.5m.

4.2 STUDY AREA AND DISASTER

4.2.1 Study area

Study areas are coastal area of Ariake Sea and Saga lowland, such as shown in Figure 4.1

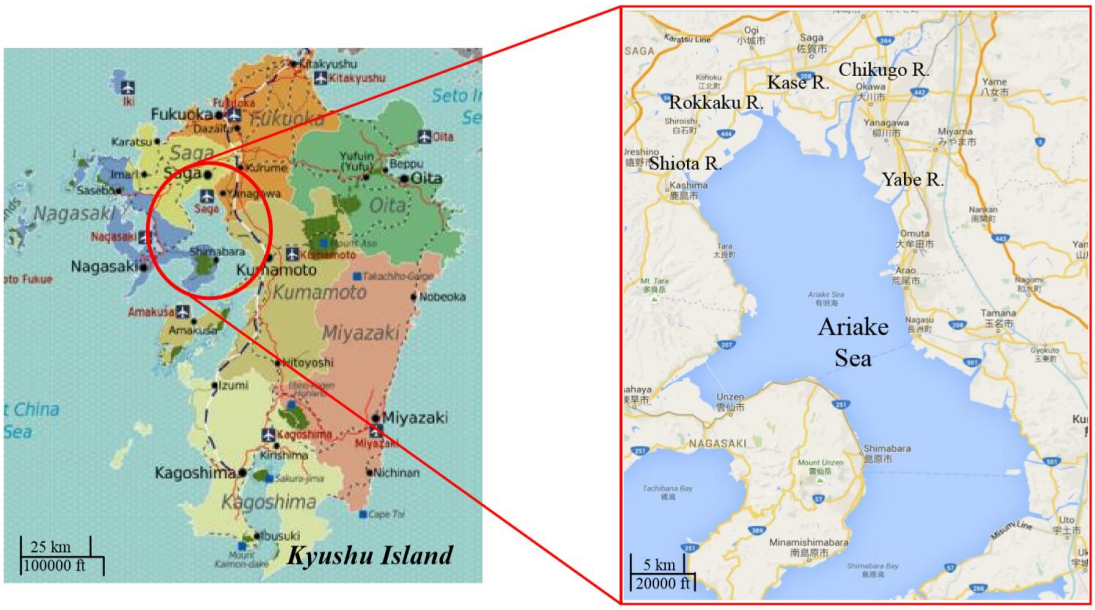

Figure 4.1: Study Area

4.2.1 Studied disaster

Studied disaster is Storm Surge by Typhoon Pat that occurred in the study area on August to September 1985. Three people died due to Typhoon Pat and 16 people were injured. Furthermore, 589 houses were damaged with category partially destroyed.

4.3 METHODOLOGY

This study utilizes a two-dimensional hydrodynamic model, MIKE 21 FM developed by DHI (Danish Hydraulic Institute). MIKE 21 FM is a computer program that simulates flows, waves, sediments and ecologi in rivers, likes, estuaries, bays, coastal areas and seas in two dimensions. This software is used to create a simulation of several typhoons that ever crossed Ariake Sea. In this study, based on the simulation results of the previous research by Dundu (2012) and Thambas (2015), seven measurement lines shown in Figure 4.2 are considered as transects to investigate the inundation in the coastal area, as follow:

1. Shiroishi (S)
2. Higashioka (H)
3. Rokkaku Estuary (RE)
4. Kase Estuary (KE)
5. Chikugo Estuary (CE)
6. Saga Airport (SA)
7. Ohamma (O)

Figure 4.2 : Measurement lines

4.3.1 Data

In the numerical simulations, the following data are taken as input data; bathymetrical data, topographical data, wind data (speed and direction), some of the water level at stations, and a time step of the simulation. Bathymetric data are obtained from the Ariake Project of Saga University in the form of water depth in the Ariake Sea and other areas in the southern of Kyushu Island, from longitude 128^{o} - 131^{o} and latitude 30^{o} - 34^{o}. Topographic data are obtained from 50 m DEM of Japan supplied by Geospatial Information Authority of Japan. The elevation is taken up 20 m considering the number of points will determine the processing time on the computer and the assumption that the boundary conditions for groundwater are 10 m. Figure 4.3 shown bathymetry and topography on grid file.

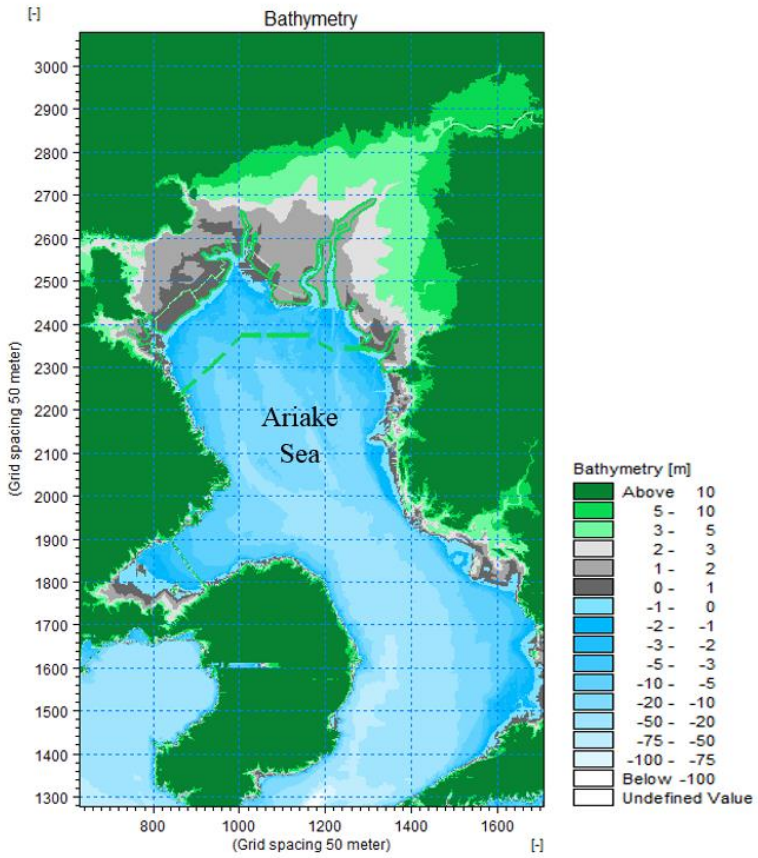

Figure 4.3: Bathymetry and topography in grid file

Wind data in the form of wind speed and wind direction shown in Figure 4.4 were provided by Meteorological Agency. Water level and tide data shown in Figure 4.5 were provided by Meteorological Agency took at the same time with wind data from August 31 to September 1, 1985 in Misumi Station. The simulation was taken from August 31, 1985, 00:00 to September 1, 1985, 00:00 when the Typhoon Pat passed through the Ariake Sea area.

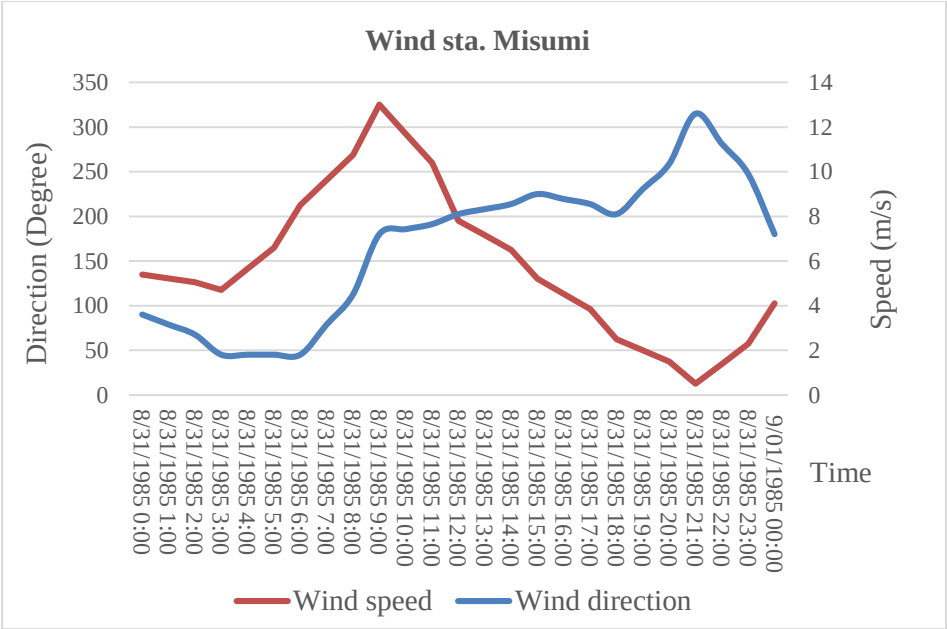

Figure 4.4: Wind data at Misumi Station

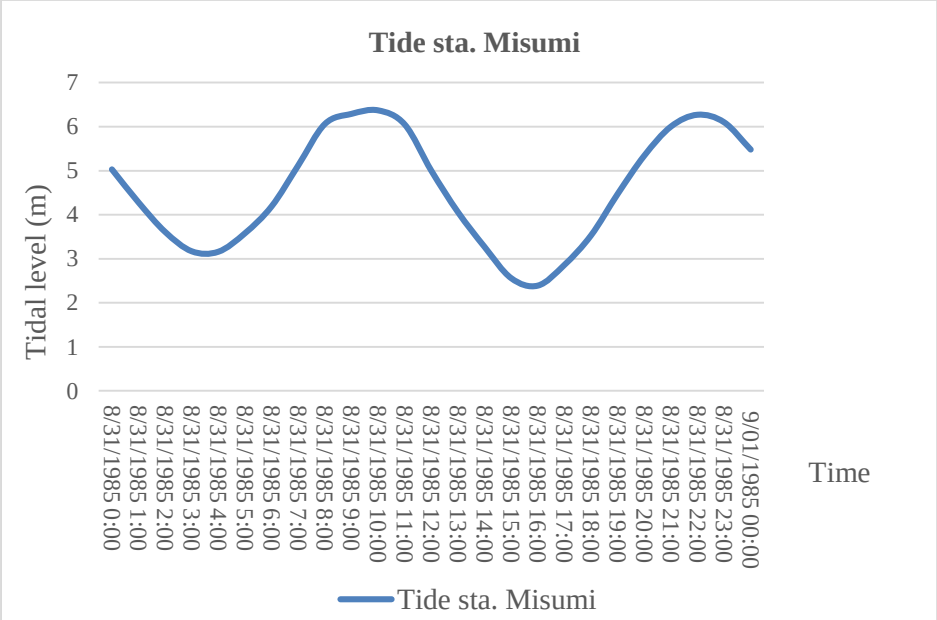

Figure 4.5 : Tide data at Misumi station

Figure 4.6 show observation station of tide data and Figure 4.7 show location of Misumi station.

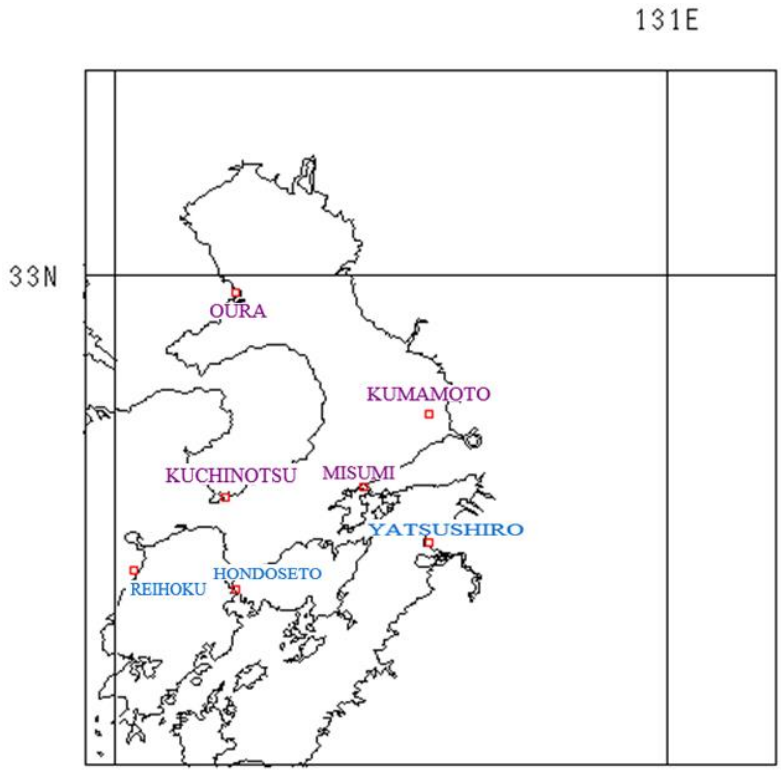

Figure 4.6: Station observation of tide data
(source: Japan Oceanographic Data Center, 2016)

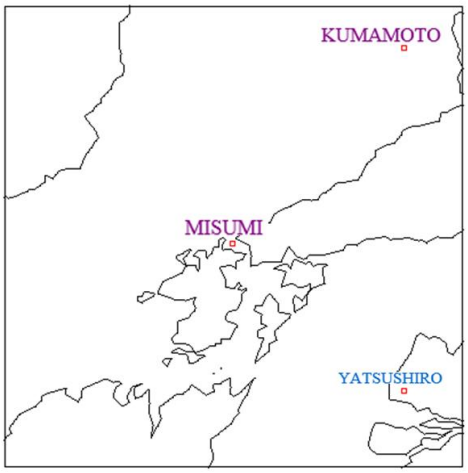

Figure 4.7: Location of Misumi Station

4.3.2 Computational Mesh and Boundary

The calculation model was established by the computational mesh such as shown in Table 4.2 and the Figure 4.8.

Table 4.2 Information of computational mesh

Item	Amount
Number of elements	139072
Number of faces	209562
Number of nodes	70491
Number of sections	2
Min x-coordinate (m)	594392
Max x-coordinate (m)	655838
Min y-coordinate (m)	3609481
Max y-coordinate (m)	3695657
Min z-coordinate (m)	-109.79
Max z-coordinate (m)	9.98

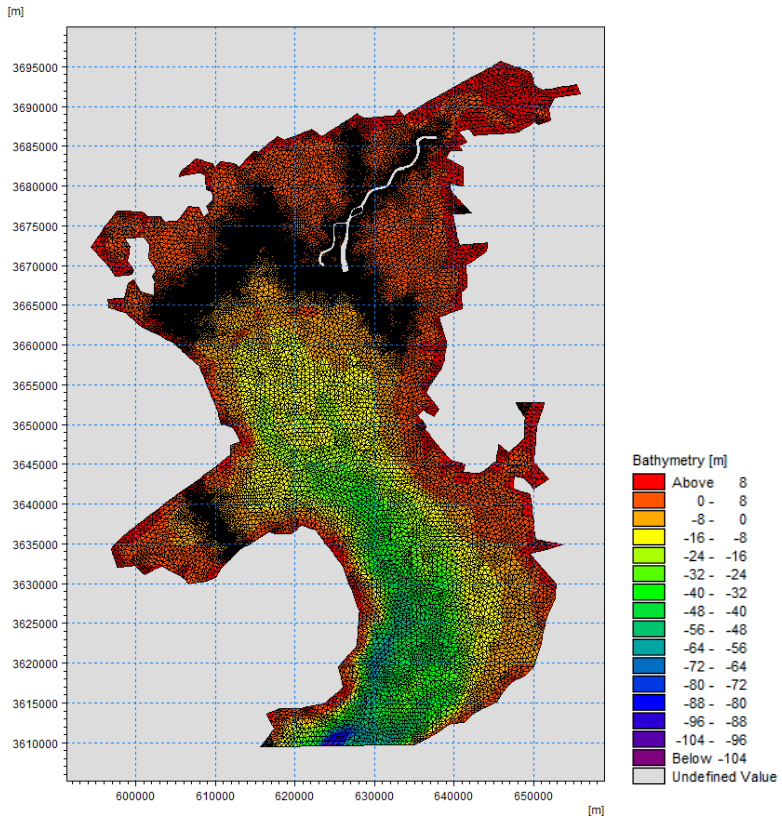

Figure 4.8: Computational mesh

The computational boundary with an open boundary to input time series data of tide can be seen in the Figure 4.9.

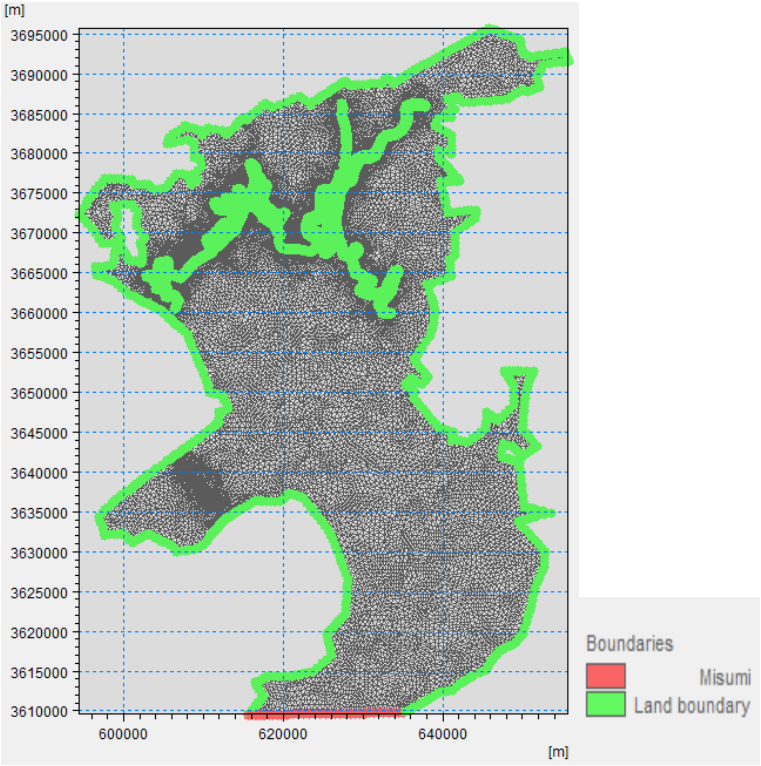

Figure 4.9: Computational boundary

4.4 RESULTS AND DISCUSSIONS

4.4.1 Model Calibration

Model calibration of water level or tide at the Misumi station from August 31 to September 1, 1985 is shown in Figure 4.10. Calibration is also carried out at Oura station as shown in Figure 4.11.

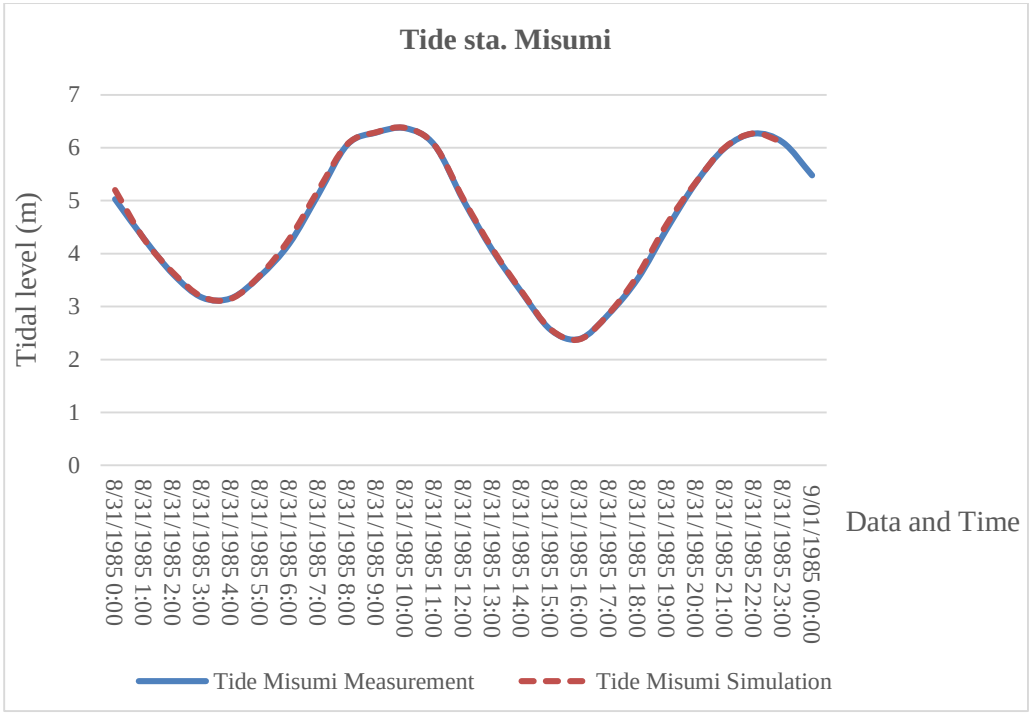

Figure 4.10: Calibration of tide at Misumi station

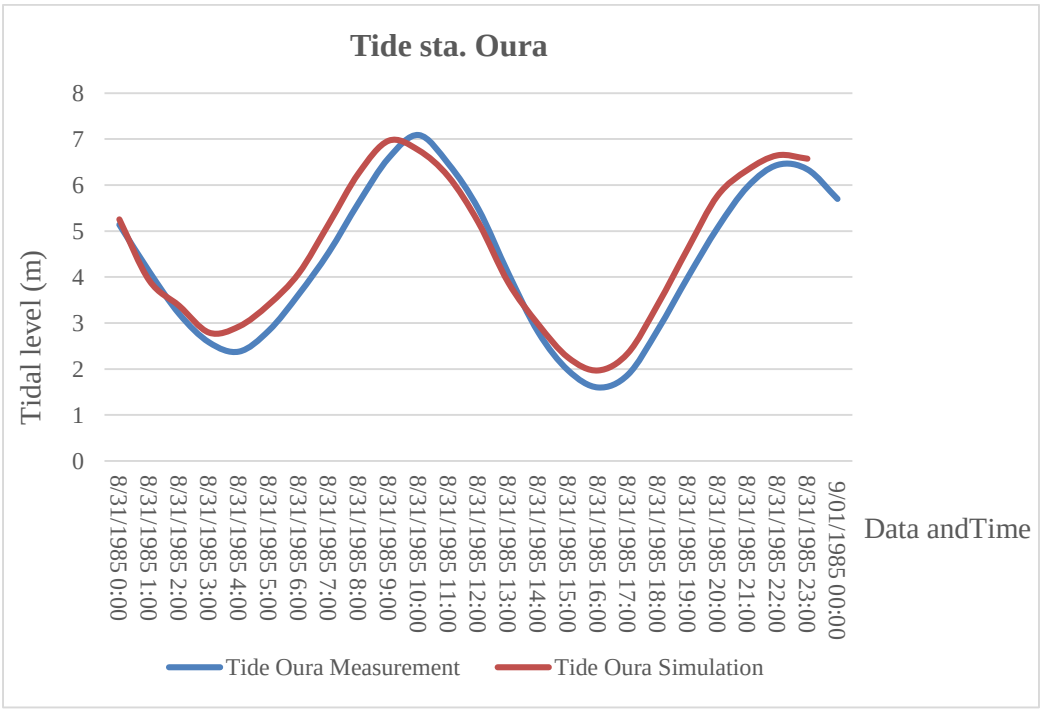

Figure 4.11: Calibration of tide at Oura station

Based on model calibration, tide condition at the Misumi station between simulation and measurement are same. Although there were some discrepancies between tide observation and simulations at the Oura station, but overall the simulation result of tide coordinated well with the observed data

4.4.2 Simulation Results

Table 4.3 shows the maximum water levels at each measurement line. The simulation's results on the seven specified location indicate that the maximum water levels elevation under 7 m. Figure 4.12 shows the water level simulated at each measurement lines is presented the water level does not exceed the height of the existing coastal dikes of 7.5 m high.

Table 4.3 Maximum water level

No	Lines Name	Maximum (m)	Time
1	Shiroishi (S)	6.956	10:00
2	Rokkaku Estuary (RE)	6.974	11:00
3	Kase Estuary (KE)	6.970	11:00
4	Higashiyoka (H)	6.961	10:00
5	Saga Airport (SA)	6.947	10:00
6	Chikugo Estuary (CE)	6.944	10:00
7	Ohamma (O)	6.932	10:00

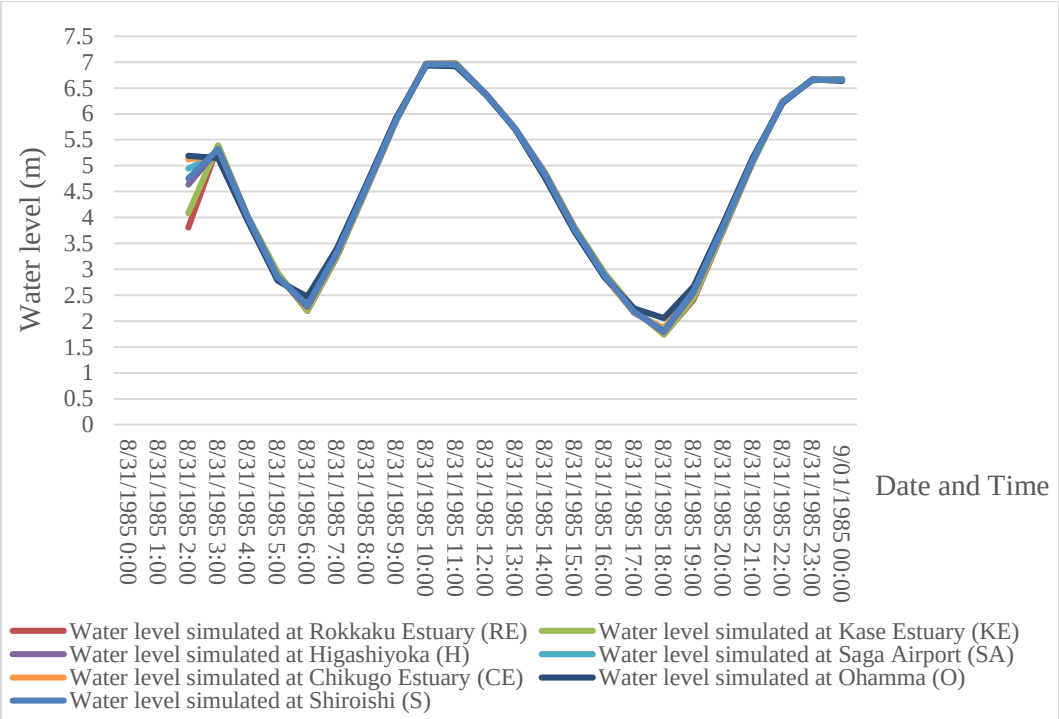

Figure 4.12: Water level simulated at each measurement lines

The following figures, Figure 4.13 to Figure 4.18 is simulation result of water level in the Ariake Sea when storm surge by Typhoon Pat occurred on August 31, 1985 to September 1, 1985 at each time 02:00, 06:00, 11:00, 15:00 and 19:00 on August 31, 1985 and at time 00:00 on September 1, 1985, respectively.

This research and previous research by Dundu (2012) and Thambas (2015) simulation results is relative same, there were no water level exceeded the existing coastal dyke. In the real condition when the Typhoon Pat occurred in this study area on August to September, 1985, there were no water level exceeded the existing coastal dyke was caused by high tide. Althought, at the some place was caused damage of fish port due to wave overtopping in the Ariake coast, Ashikari cho, Saga Prefecture as showed in the Figure 3.5 in Chapter 3.

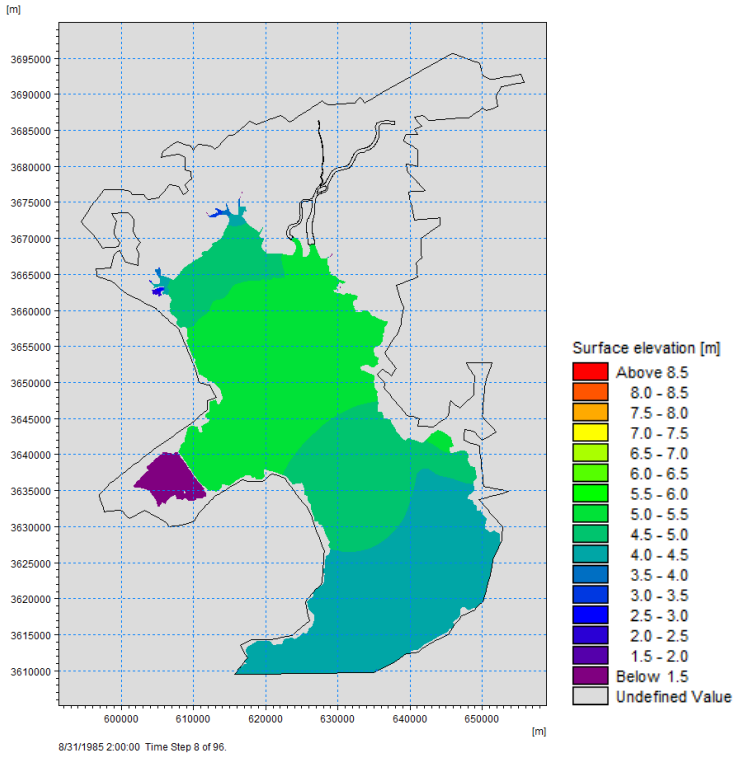

Figure 4.13: Water level on August 31, 1985, at the time 02:00

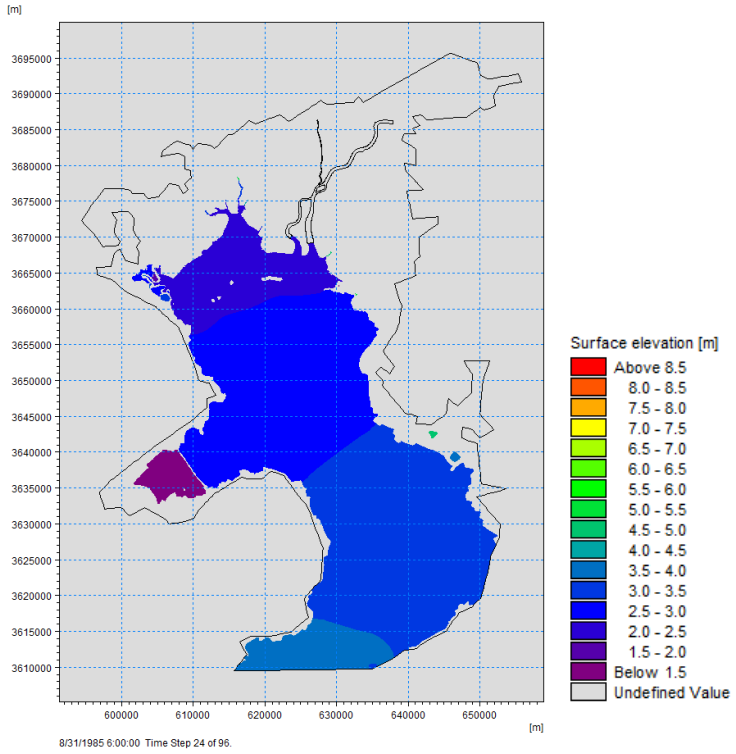

Figure 4.14: Water level on August 31, 1985, at the time 06:00

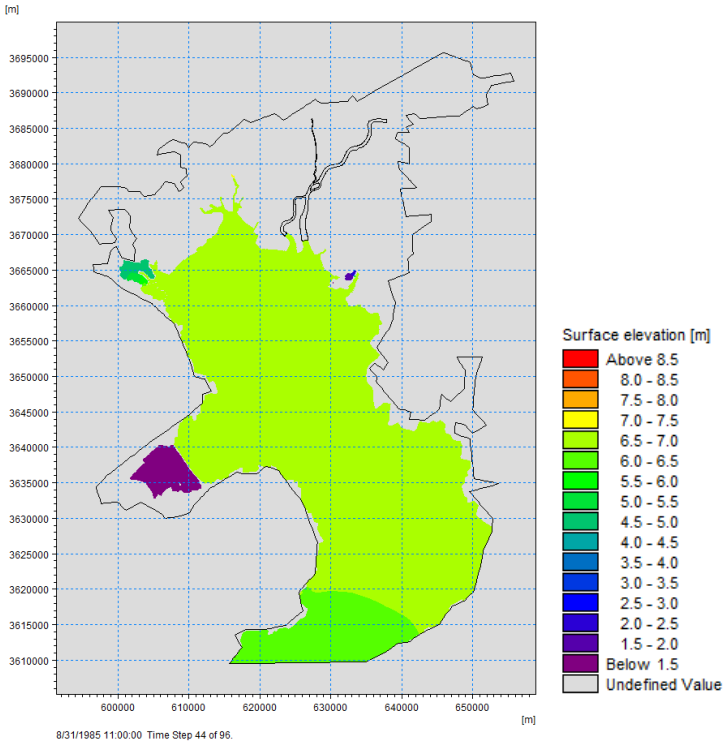

Figure 4.15: Water level on August 31, 1985, at the time 11:00

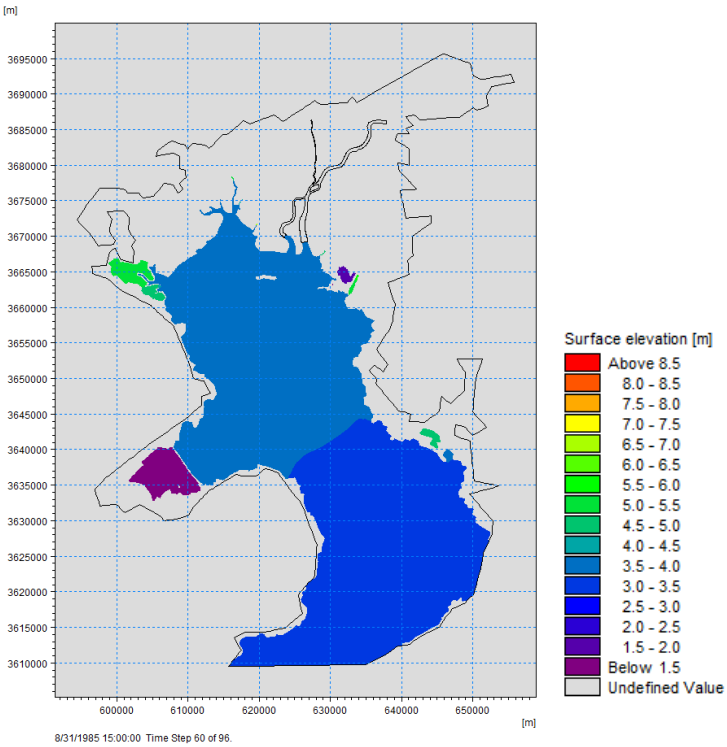

Figure 4.16: Water level on August 31, 1985, at the time 15:00

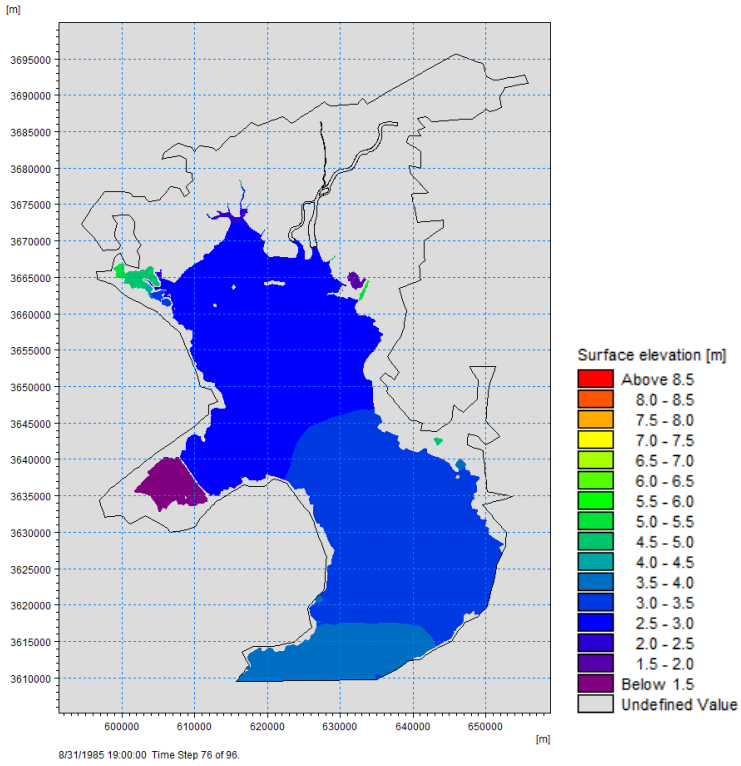

Figure 4.17: Water level on August 31, 1985, at the time 19:00

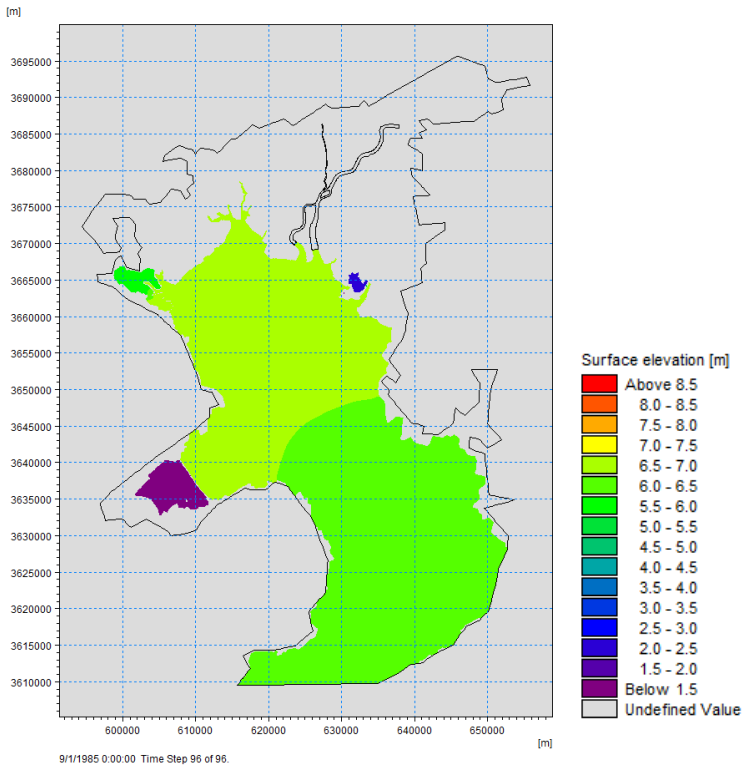

Figure 4.18: Water level on September 1, 1985 at the time 00:00

4.4.3 Comparison of the results with previous researches

Table 4.4 shown the comparison results of maximum water level at the same place (measurement line) with previous researches by Dundu, (2012) and Thambas, (2015). In their research used same data when the Typhoon Pat occurred in the Ariake Sea on August, 31 to September 1, 1985.

Table 4.4 Maximum water level (comparison)

No	Lines name	Maximum water level (m) and time					
		This research	Time	Dundu (2012)	Time	Thambas (2015)	Time
1	Shiroishi (S)	6.956	10:00	6.457	24:00	6.655	10:00
2	Rokkaku Estuary (RE)	6.974	11:00	6.459	24:00	6.687	10:00
3	Kase Estuary (KE)	6.970	11:00	6.459	24:00	6.685	10:00
4	Higashiyoka (H)	6.961	10:00	6.458	24:00	6.671	10:00
5	Saga Airport (SA)	6.947	10:00			6.644	11:00
6	Chikugo Estuary (CE)	6.944	10:00			6.646	11:00
7	Ohamma (O)	6.932	10:00			6.634	11:00

The maximum water level at the Shiroishi (S), Rokkaku Estuary (RE), Kase Estuary (KE) and Higashiyoka (H) was obtained at time 10:00 on August 31, 1985 by Thambas (2015), while Dundu (2012) was obtained at time 24:00 or at time 00:00 on September 1, 1985. The maximum water level in the Saga Airport (SA), Chikugo Estuary (CE) and Ohamma (O) was obtained at time 11:00 on August, 31 by Thambas (2015). In this research, the maximum water level at the Rokkaku Estuary (RE) and Kase Estuary (KE) was obtained at time 11:00 and the maximum water level at the Shiroishi (S), Higashiyoka (H), Saga Airport (SA), Chikuko Estuary (CE) and Ohamma (O) was obtained at time 10:00 on August 31, 1985.

Dundu (2012) used 3-D numerical model simulation to analyze the storm surge by Typhoon Pat and Thambas (2015) used 2-D model simulation and in the boundary condition make open boundary at the Kumamoto station observation with

using tide and wind data from Misumi station when the Typhoon Pat occurred on August 31 to September 1, 1985.

The difference of maximum water level simulated between this research and previous research by Dundu (2012) and Thambas (2015) is considered to occur due to determining the boundary condition's location and computational mesh such as shown in the Figure 4.19 and Figure 4.20. The difference time of the maximum water level simulated on each researches is caused the peak of water level have two times of period. The first time period between times 10:00 to 11:00 and the second time period between times 23:00 to 24:00 as showed in Figure 4.10 on previous page.

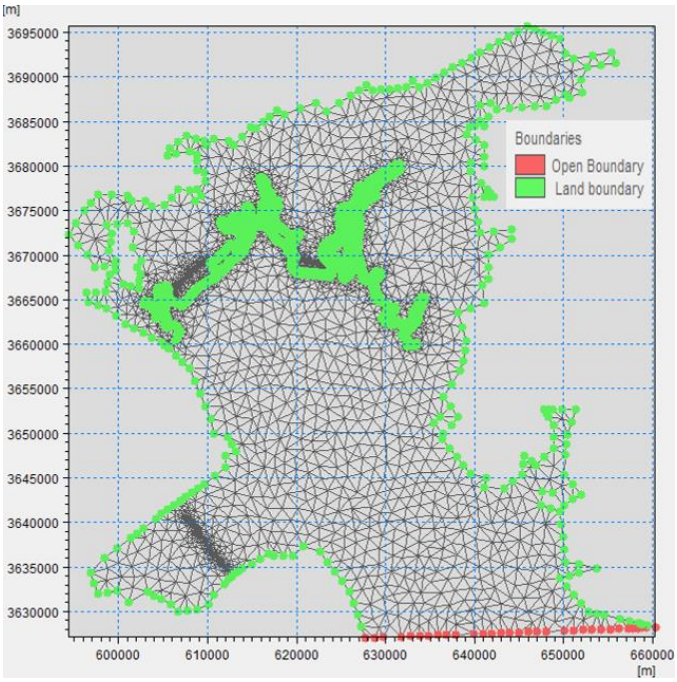

Figure 4.19: Boundary condition and mesh used by Dundu (2012)

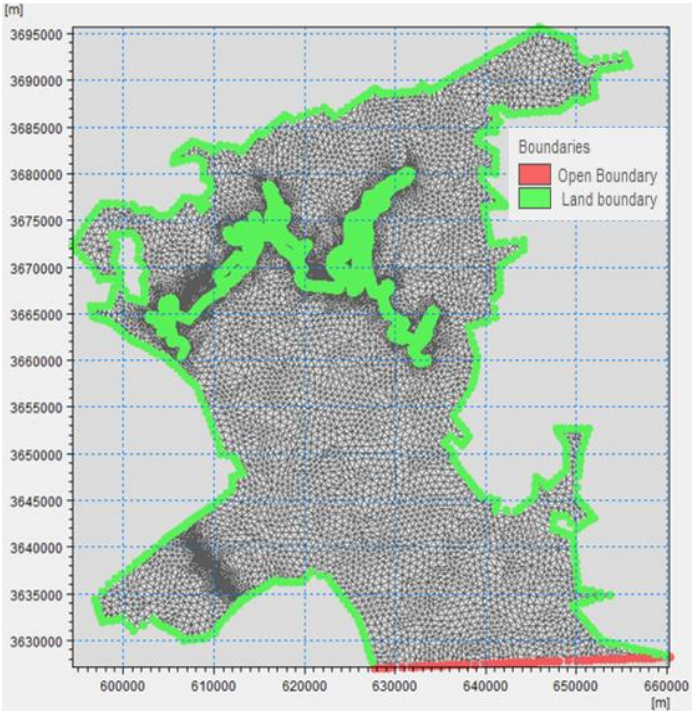

Figure 4.20: Boundary condition and mesh used by Thambas (2015)

4.5 CONCLUSIONS

Based on the simulation results, the water level does not exceed the height of the existing coastal dikes of 7.5 m high; it means no inundation in the coastal area of the Ariake Sea and Saga lowland when the storm surge occurred in this area. The maximum water level at each measurement line is relative same but the times are the difference.

Chapter 5

1-D HYDRODYNAMIC MODELING OF FLOODING IN THE CHIKUGO RIVER

5.1. INTRODUCTION

Chikugo River is located on Kyushu Island in Japan, belongs to Oita, Fukuoka, Kumamoto, and Saga prefectures. It is mainly covered with forest, wetlands, agriculture, and urban–built up areas. The total basin area is about 2,800 km^2. The Chikugo River rises under the Mount Aso and discharges into the Ariake Sea. With a total length of 143 kilometers, it is the longest river of Kyushu Island which empties into the Ariake Sea. The upper reaches of the river are important to forestry, whereas the middle and lower reaches are important for the local agriculture, providing irrigation to some 400 km^2 of rice fields on the Tsukushi Plain. The river is also important for the industry, with twenty electrical power plants are located along the banks of the Chikugo River, as well as the major city of Kurume in Fukuoka Prefecture.

In July 2012, torrential rain in the Kyushu island caused high discharge or river flood in the Chikugo River. Recorded from Senoshita station at Chikugo River, the maximum of high discharge was 5864.9 m^3/s on July 14, 2012 at 01:00 pm. To see how much influences of flood in this river, this study is conducted to analyze of river flooding by using 1-D simulation model.

5.2. STUDY AREA AND DISASTER

5.2.1 Study area

The Chikugo River empties into the Ariake Sea from km 0 at Estuary to km 23 at Senoshita station, including the river branch along of this route such as Hayatsue River, Jobaru River, Sagae River and Morodomi River as shown in Figure 5.1.

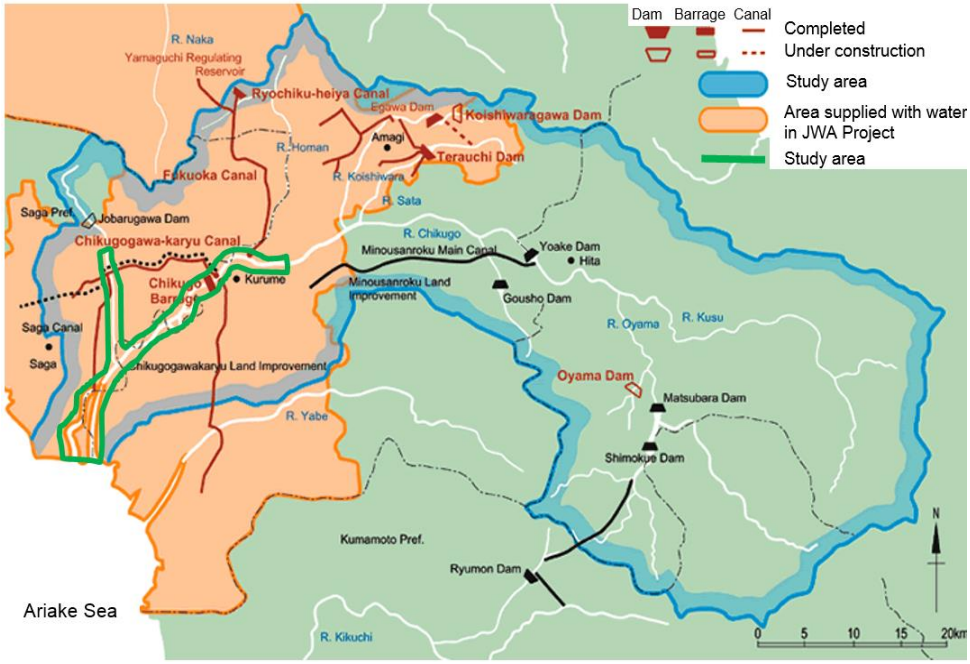

Figure 5.1: Study area of Chikugo River
(Source: Japan Water Agency, 2015)

5.2.2. Studied disaster

Studied disaster is the high discharge, or river flood has been occurred at the Chikugo River due to torrential rain on July 2012.

5.3. METHODOLOGY

This study utilizes a one-dimensional hydrodynamic model, MIKE 11 developed by DHI (Danish Hydraulic Institute). This software is used to analyze the water level in the high discharge condition at the Chikugo River including the river branch. The data required for this analysis such as: cross-section of the river, a network of river and boundary data. The geometry of cross-sections of Chikugo River and branch was obtained from MLIT Chikugo River Office, Japan.

5.3.1 Cross-section

Cross-section obtained from field measurement data. The original data was analyzed such as shown in Figure 5.2 and Figure 5.3.

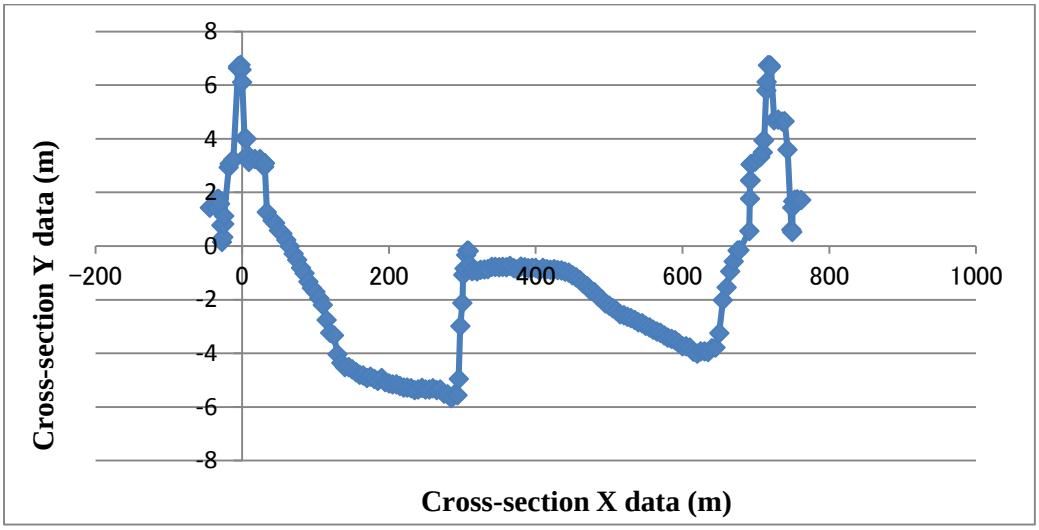

Figure 5.2 : Original data of cross-section
(source: MLIT Chikugo River office, Japan)

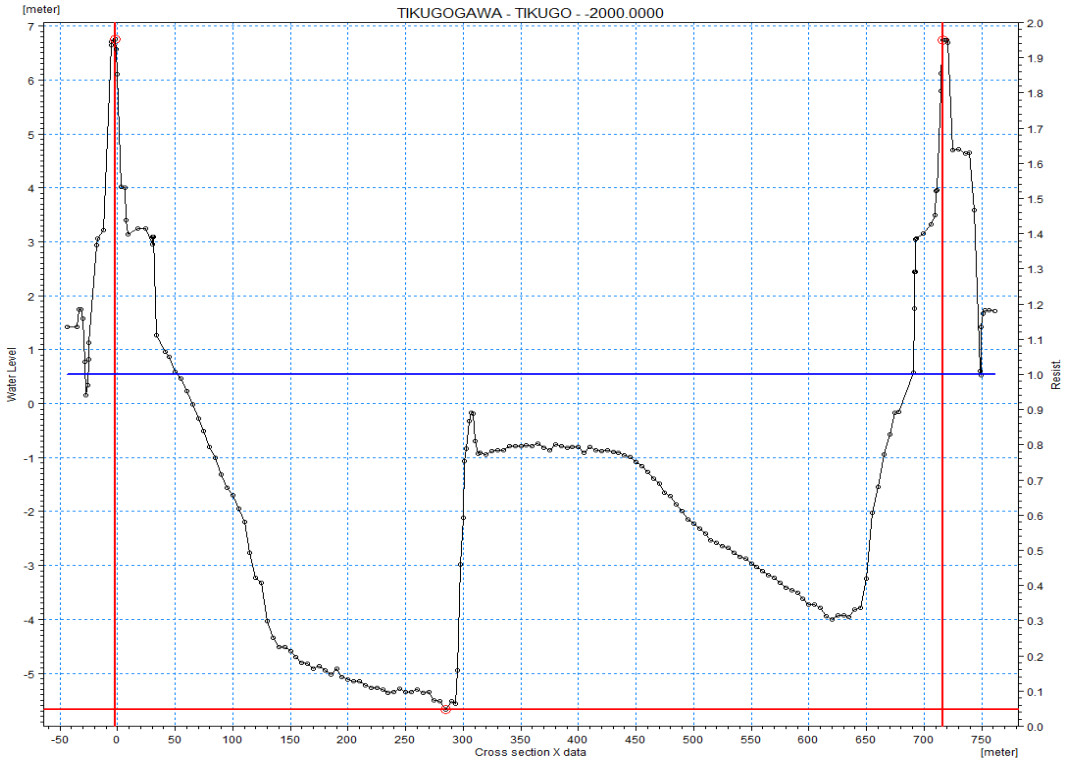

Figure 5.3 : Analysis of cross-section data

5.3.2 Network

The network was obtained based on the analysis of cross-section data. The lowest river bottom of each cross-section or the lowest point of each cross section data analysis become a points the network of river. Figure 5.4 shows the network of Chikugo River and its branch with cross-sections.

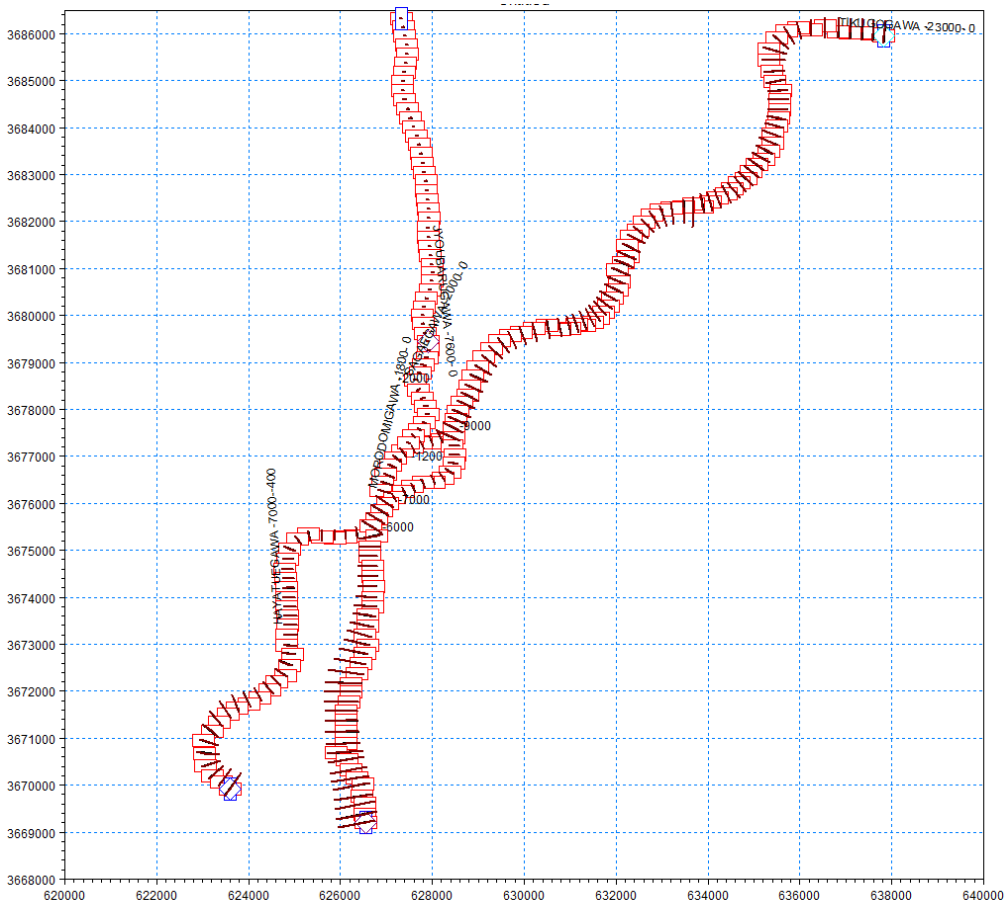

Figure 5.4: Network of Chikugo River and branch with cross-section

5.3.3 Boundary data

The input data in boundary is discharge at upstream and water level at downstream of the river. In this case the discharge data was taken from upstream of Chikugo River and Jyobaru River and the water level data was taken from downstream of Chikugo River and Hayatsue River. The discharge data of Chikugo River was obtained from Senoshita station and discharge data of Jyobaru river was obtained from Hidekibashi station by the time series format of discharge data. The

water level data was obtained from tide data at near estuary of each rivers Chikugo and Hayatsue as shown in Figure 5.5 to Figure 5.7.

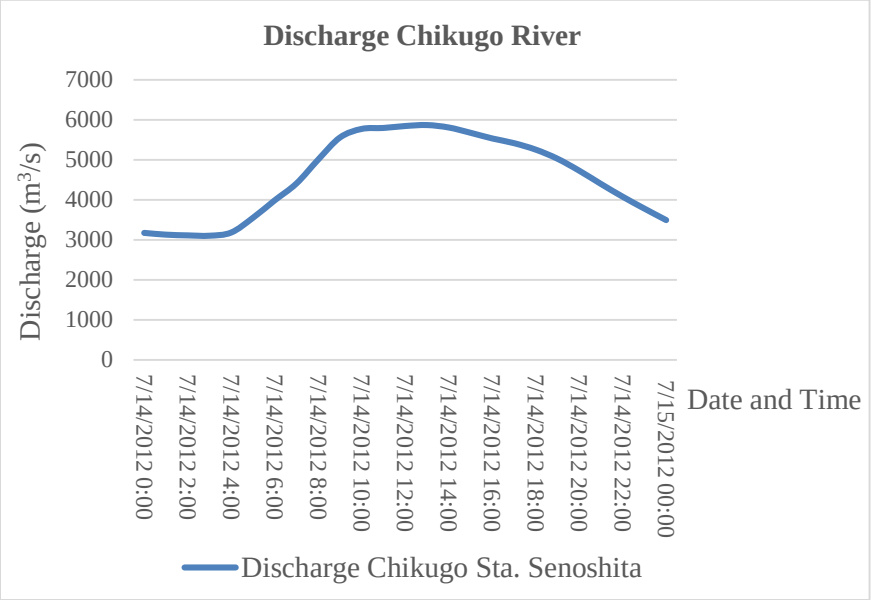

Figure 5.5: Discharge hydrograph of Chikugo River at Senoshita Station

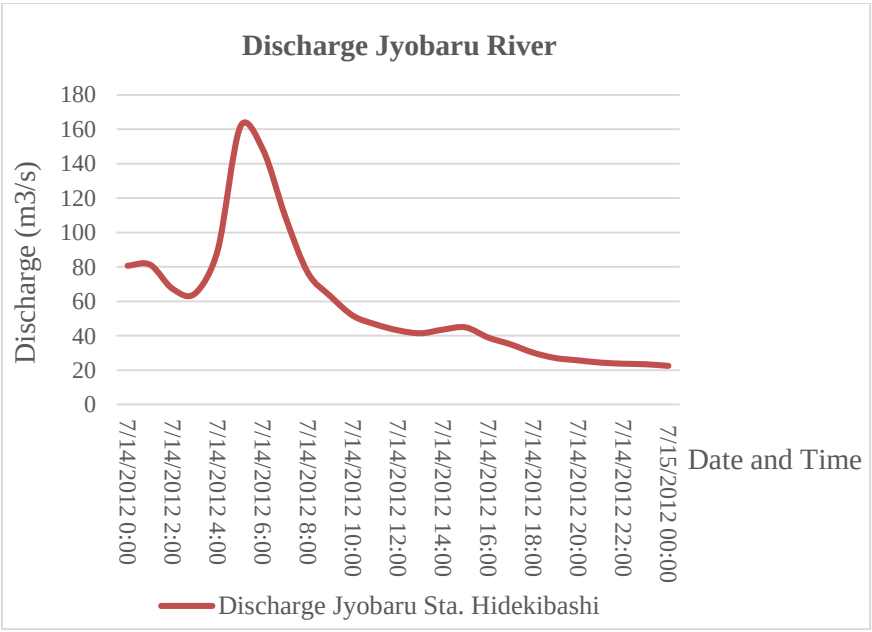

Figure 5.6: Discharge hydrograph of Jyobaru River at Hidekibashi Station

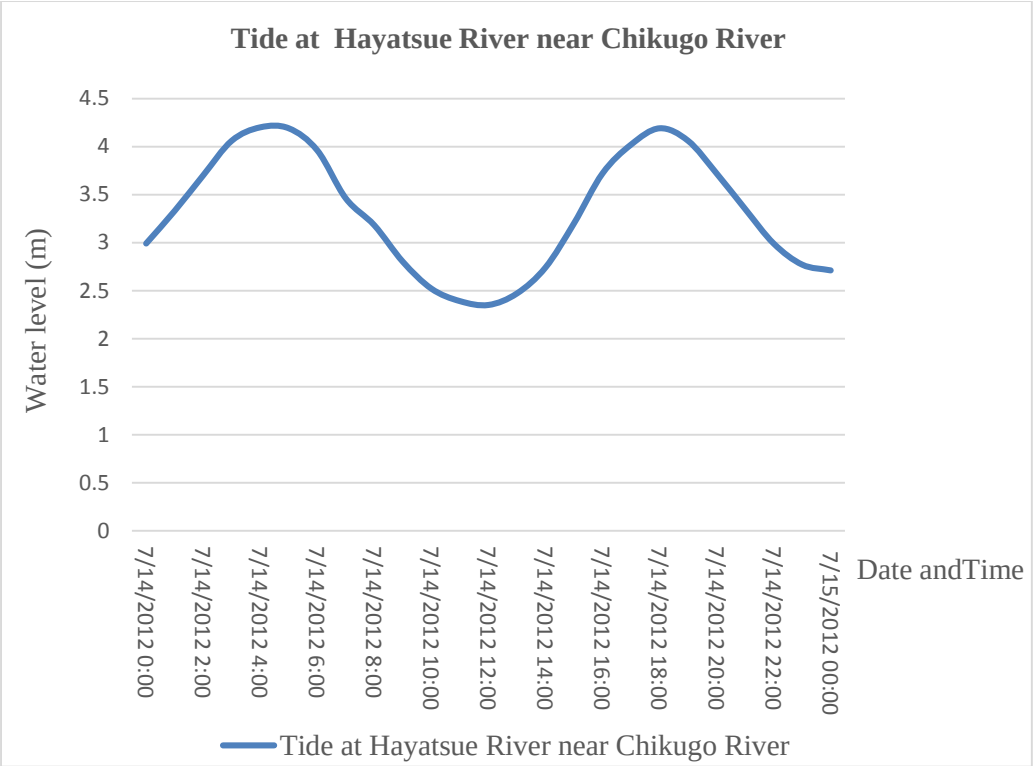

Figure 5.7: Tidal hydrograph of Hayatsue River near Chikugo River

5.4. RESULTS AND DISCUSSIONS

5.4.1 Model Calibration

5.4.1.1 Water level

Calibration of water level is performed based on the boundary condition of the water level data input at downstream of the Chikugo River and Hayatsue River. The water level condition based on simulation result at the downstream of the Chikugo River and Hayatsue River. The results of model calibration are shown in Figure 5.8 and 5.9

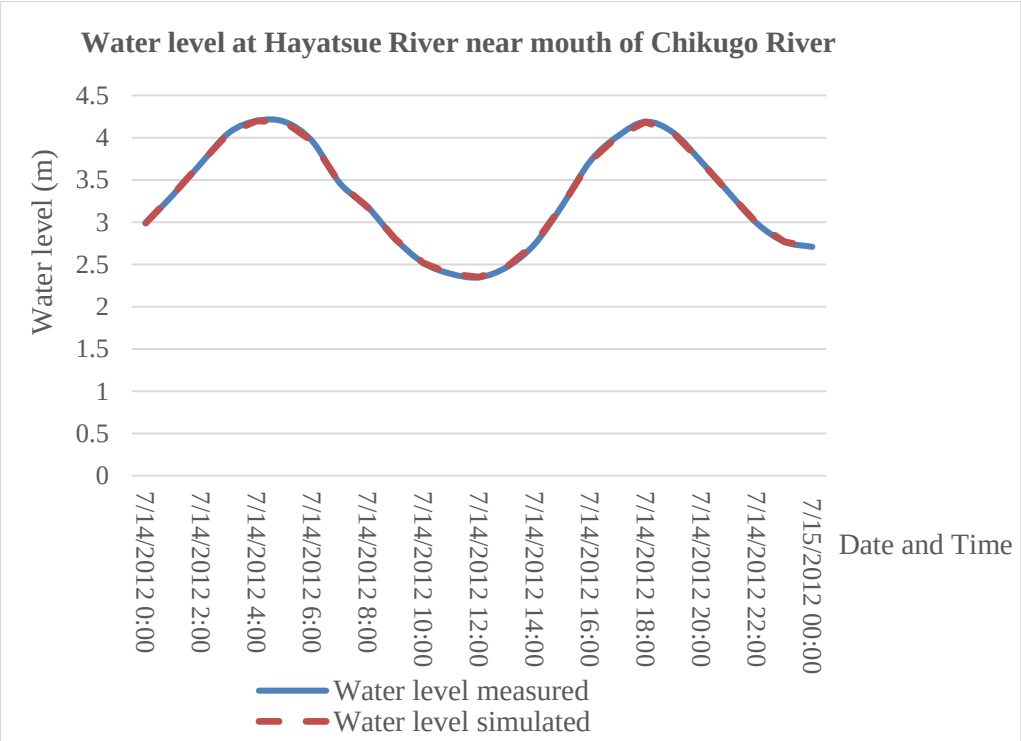

Figure 5.8: Calibration of water level at Hayatsue River near mouth of Chikugo River

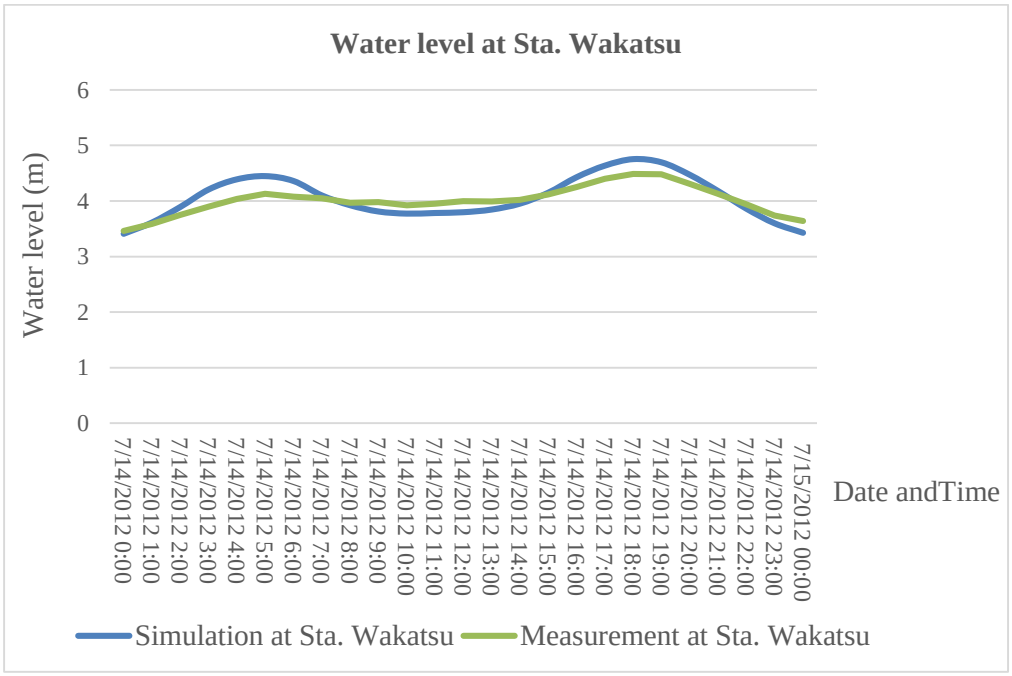

Figure 5.9: Calibration of water level at Wakatsu station

Based on model calibration of water level at Hayatsue River near mouth of Chikugo River was obtained the water level measured related same with water level simulated. Although there were some discrepancies between the measurement and simulation of the water level at the Wakatsu station, but overall the water level simulated were coordinated well with the measured data.

5.4.1.2 Discharge

Calibration of discharge is performed based on the boundary condition of the discharge data input at upstream of the Chikugo River and Jyobaru River. The discharge condition based on simulation result at the upstream of the Chikugo River and Jyobaru River. Discharge condition between measurement and simulation result are same. The model calibration of discharge is shown in Figure 5.10 and Figure 5.11.

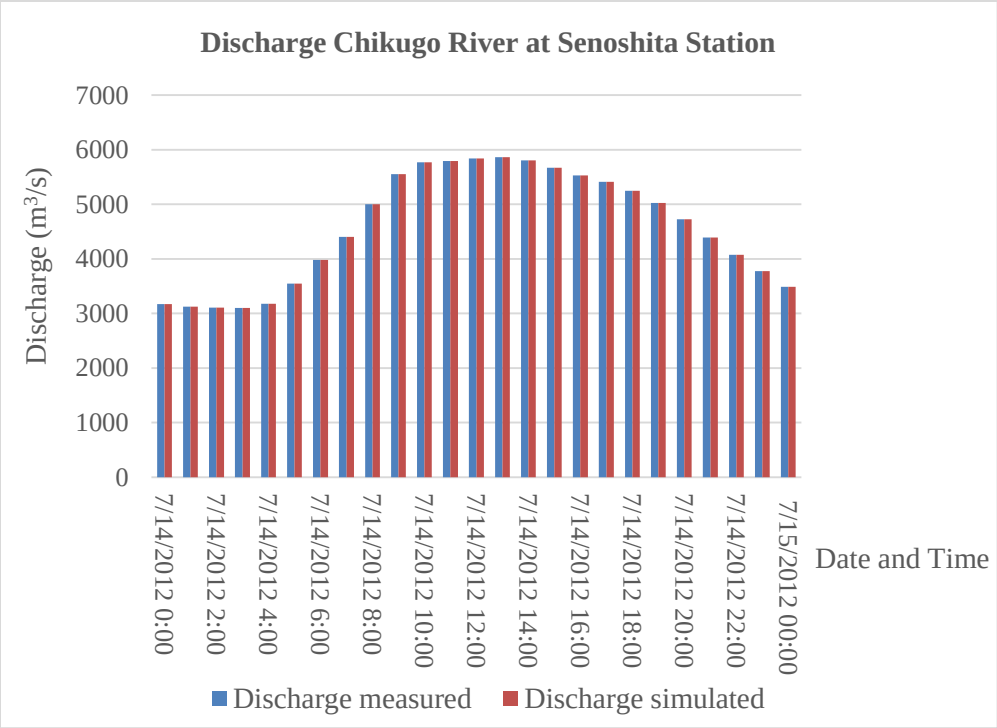

Figure 5.10: Calibration of discharge at Senoshita Station

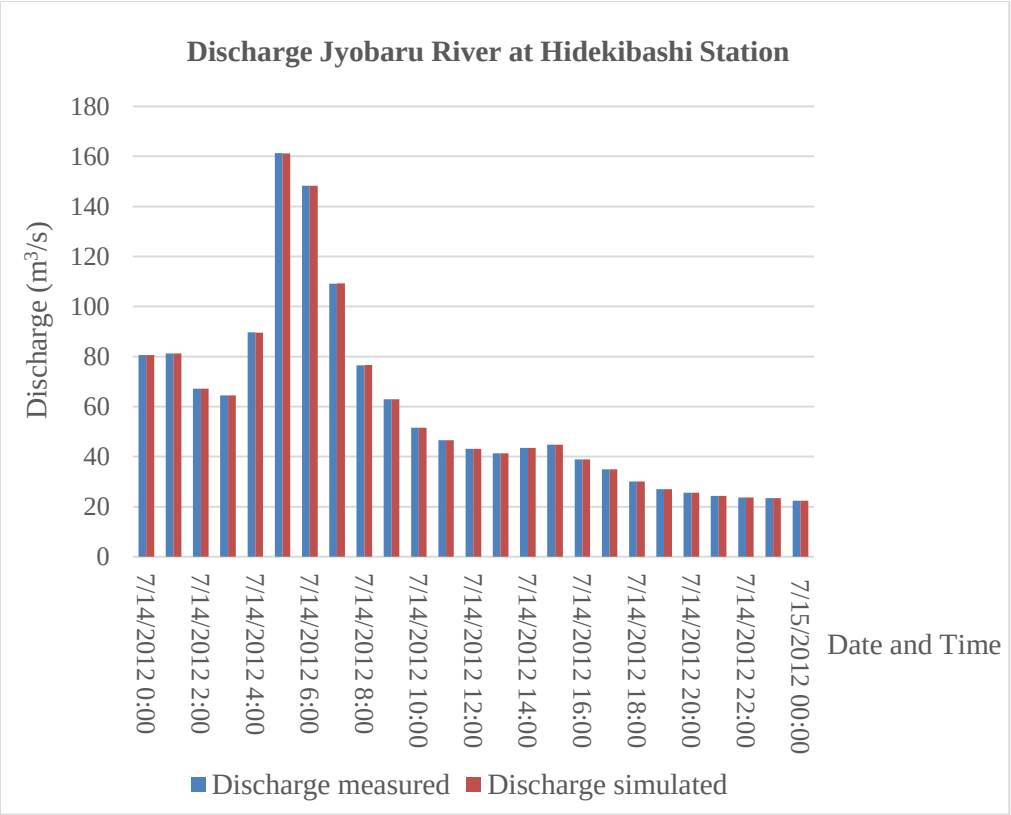

Figure 5.11: Calibration of discharge at Hidekibashi station

5.4.2 Simulation results

In the simulation result, the water level condition depended on the tide condition at the mouth of the river in the downstream and discharge condition in the upstream. Figure 5.12 showed the hydrograph of discharge and tide as the boundary condition in the upstream and downstream.

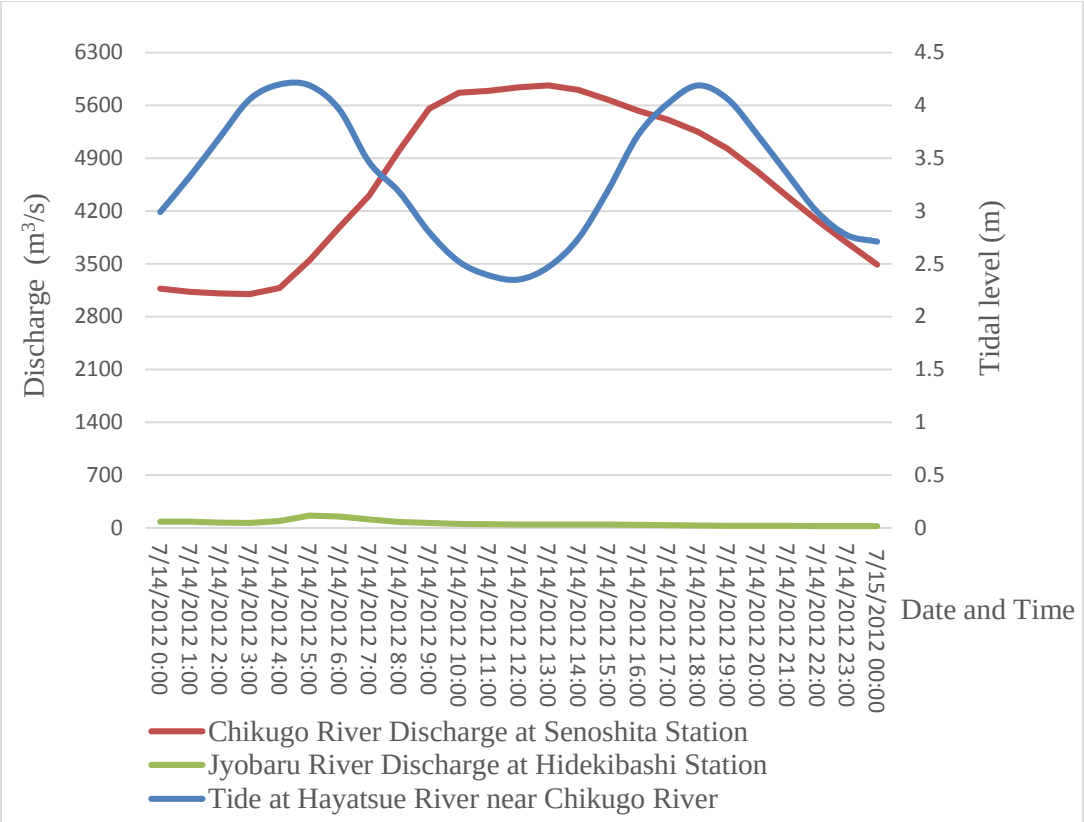

Figure 5.12: Hydrograph of discharge and tide

The simulation result of water level is based on the boundary condition on the upstream and downstream of the Chikugo River. The pattern of water level changes following the boundary condition at upstream and downstream. Figure 5.13 to Figure 5.15 shows the pattern of water level simulated changing following the pattern of water level measurement at the mouth of Chikugo River and Hayatsue River.

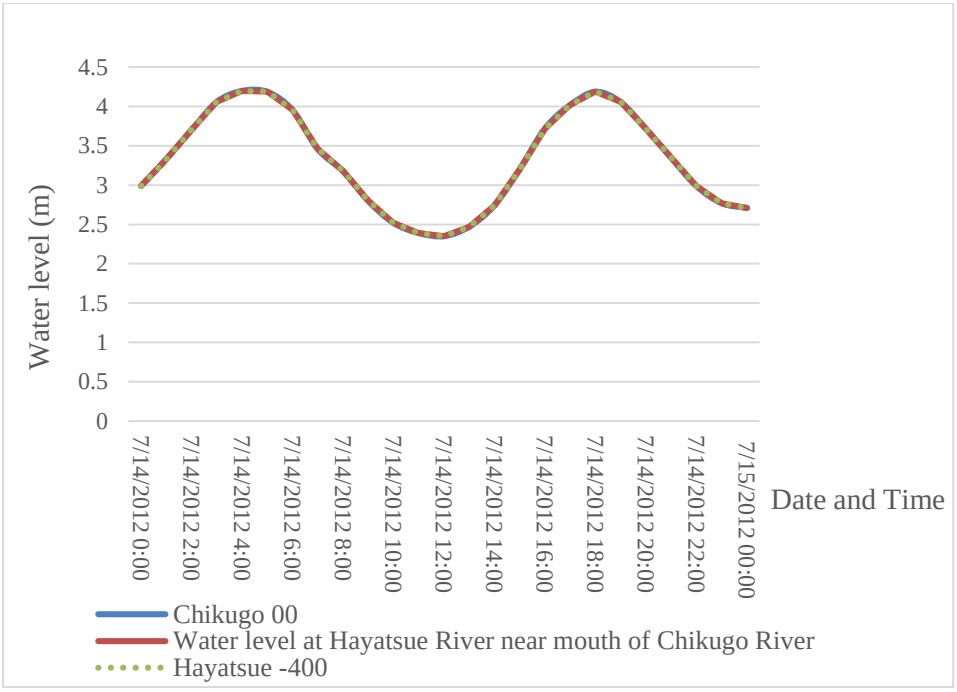

Figure 5.13: The pattern of water level simulated at Chikugo Km. 0 and Hayatsue Km. 0.4

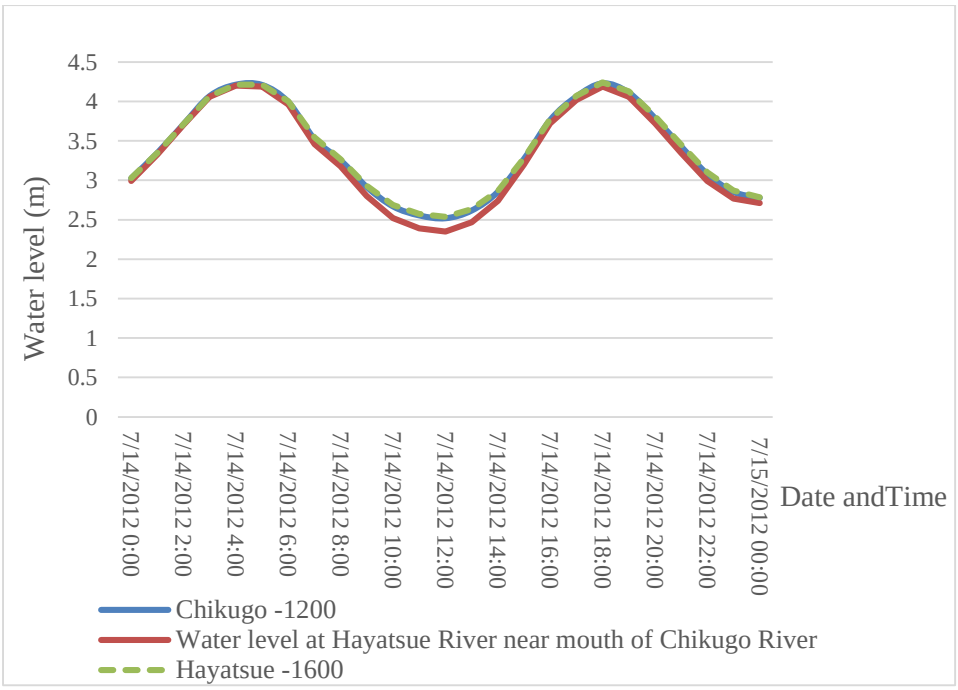

Figure 5.14: The pattern of water level simulated at Chikugo Km. 1.2 and Hayatsue Km. 1.6

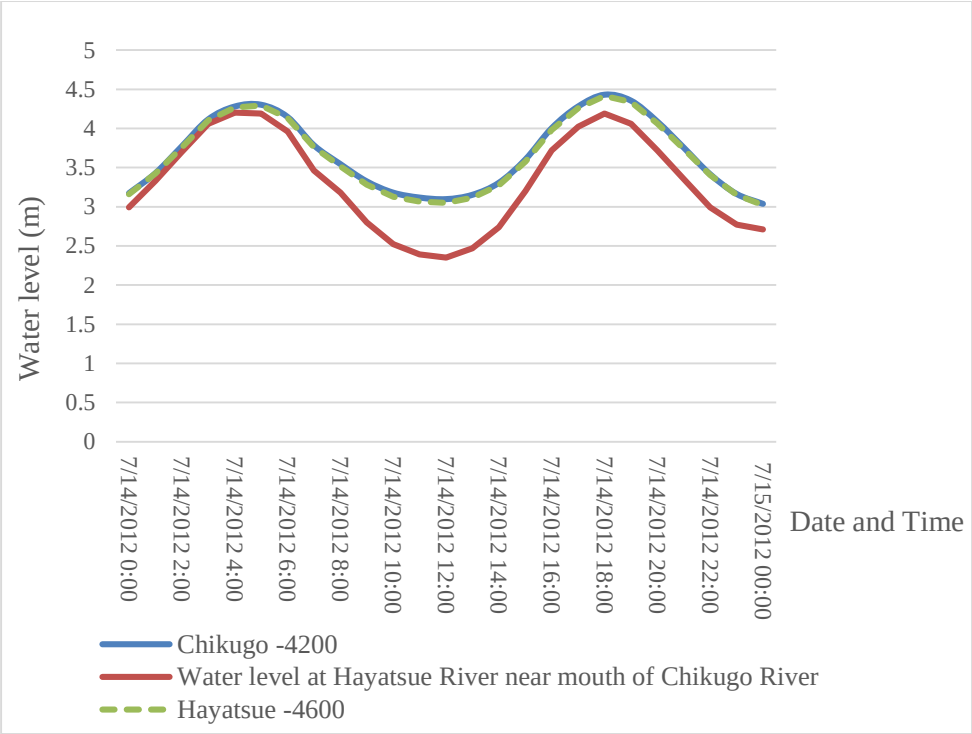

Figure 5.15: The pattern of water level simulated at Chikugo Km. 4.2 and Hayatsue KM. 4.6

Figure 5.16 showed that the pattern of water level changes at Chikugo Km. 5.4 and Hayatsue Km. 5.8 follows the water level pattern between mouth of Chikugo at Km 0 (measurement and boundary condition) and Sta. Wakatsu at Km 6.85 (measurement).

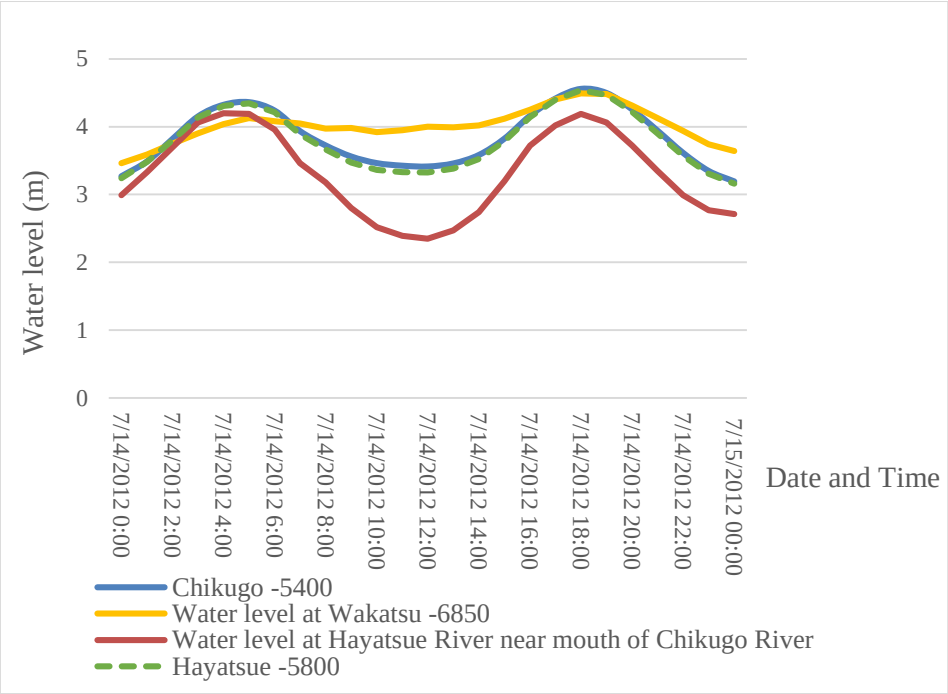

Figure 5.16: The pattern of water level simulated at Chikugo Km 5.4 and Hayatsue Km. 5.8

Based on the pattern of water level simulated, tide was influenced until Chikugo River at Km. 6.8 from the river mouth as shown in the Figure 5.17 and Figure 5.18. In Figure 5.17 is showed the pattern of water level change at Chikugo River Km 6.8 (-6800) still followed the pattern of water level or tide from downstream. As for, Figure 5.18 is showed the pattern of water level at Chikugo River Km 7.0 (-7000) is followed the pattern of water level at Wakatsu station or stronger to follows the flow from upstream condition.

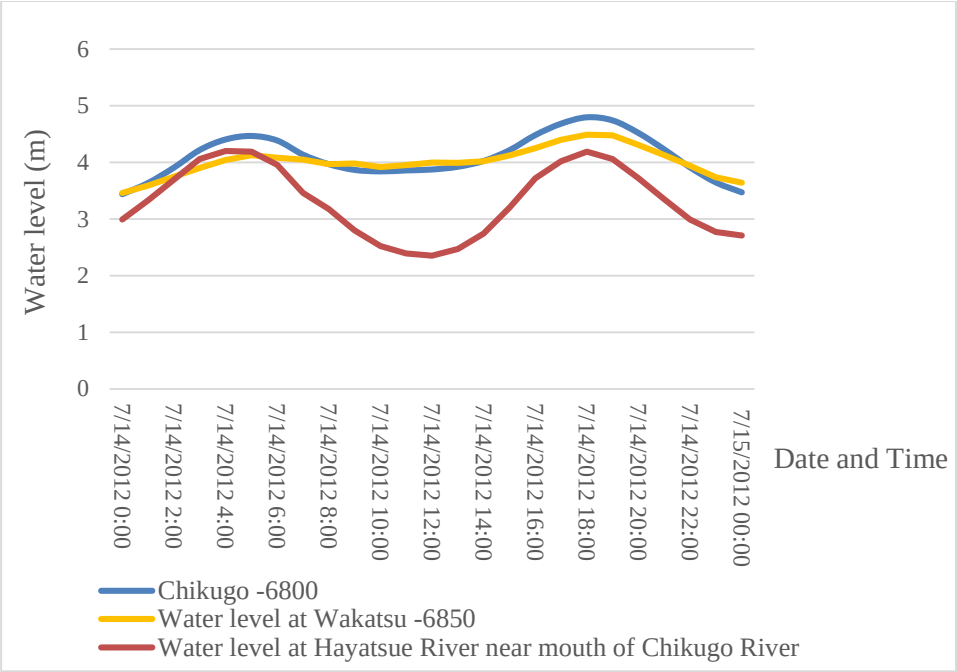

Figure 5.17: The pattern of water level simulated at Chikugo River Km 6.8

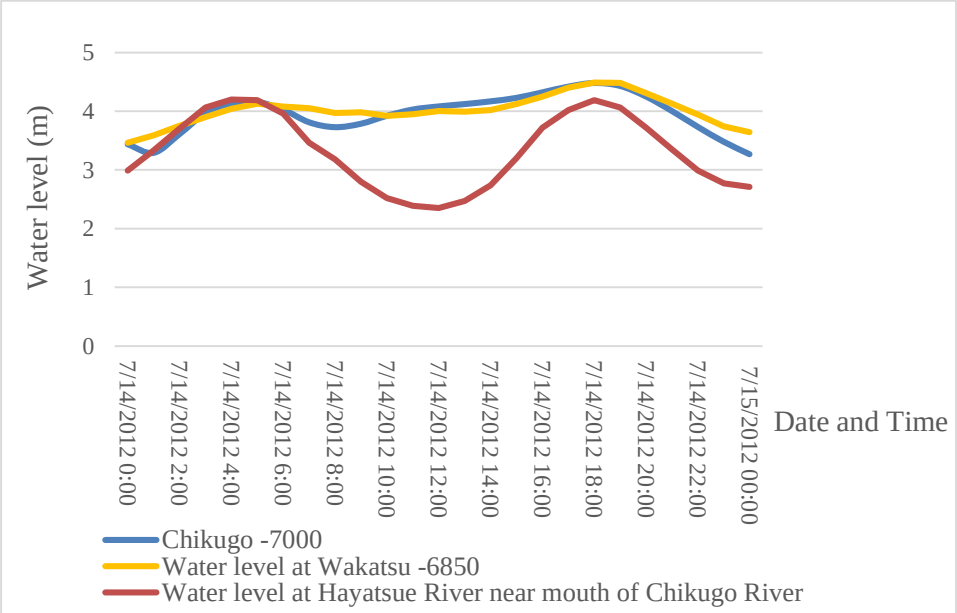

Figure 5.18: The pattern of water level simulated at Chikugo River Km 7.0

Figure 5.19 to Figure 5.22 show that the patterns of water level simulated changes following the discharge pattern at Sta. Senoshita Km 23.0 (measurement and boundary condition). It means, the influences of discharge pattern from upstream as boundary condition is stronger because the location of water level simulated nearly the boundary condition in upstream.

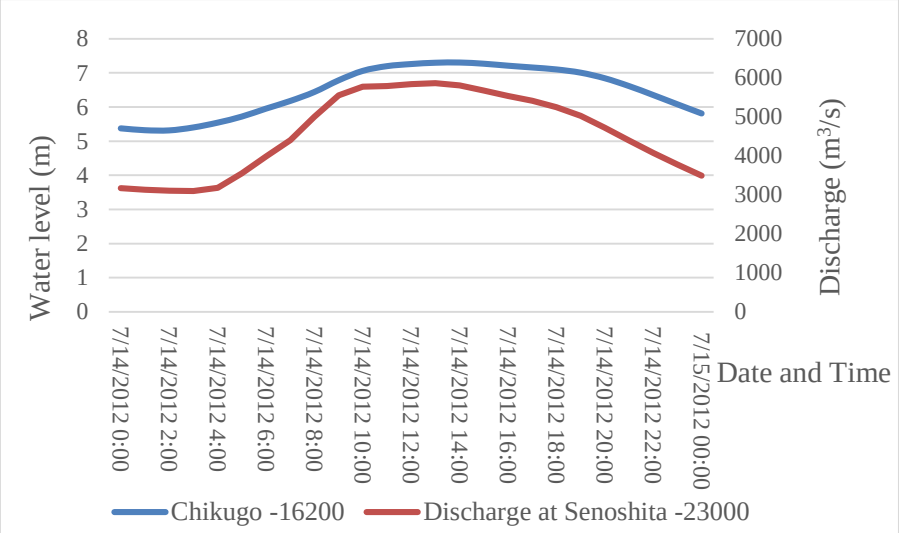

Figure 5.19: The pattern of water level simulated at Chikugo River Km 16.2

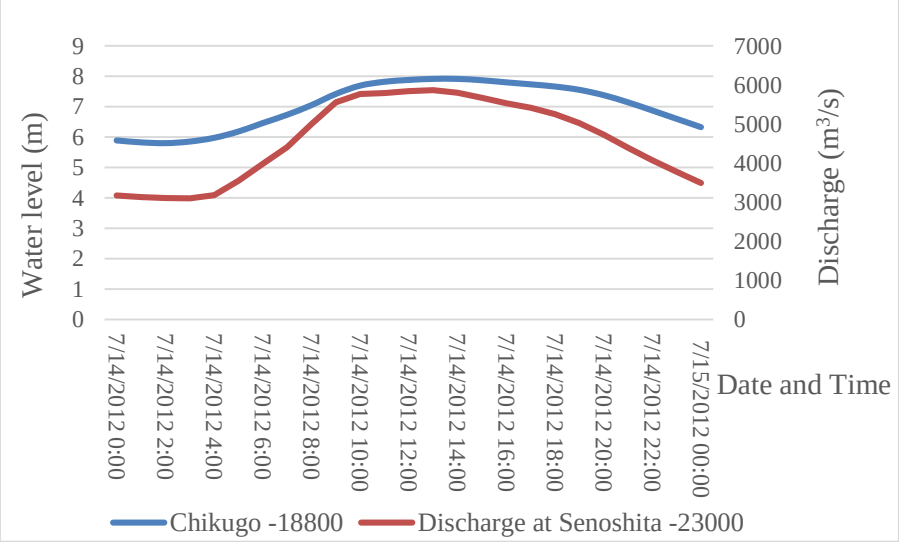

Figure 5.20: The pattern of water level simulated at Chikugo River Km 18.8

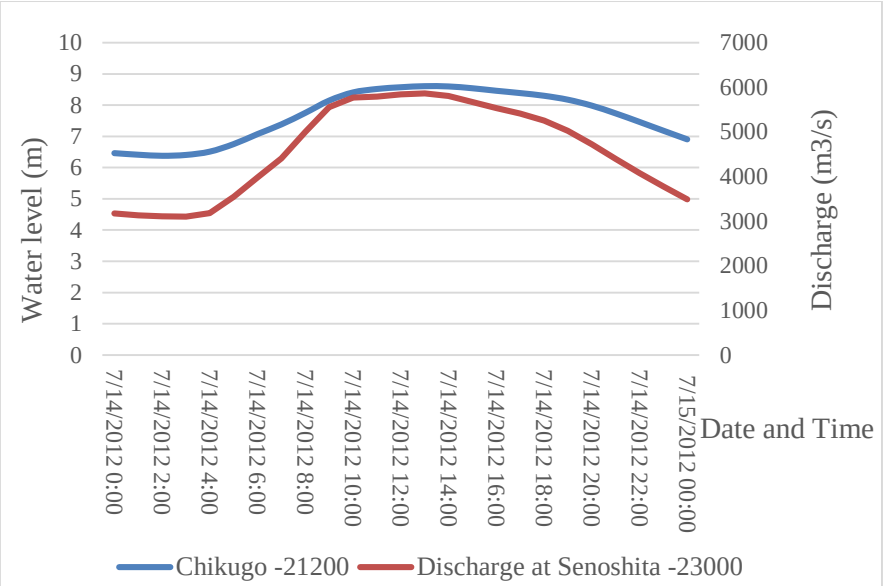

Figure 5.21: The pattern of water level simulated at Chikugo River Km 21.2

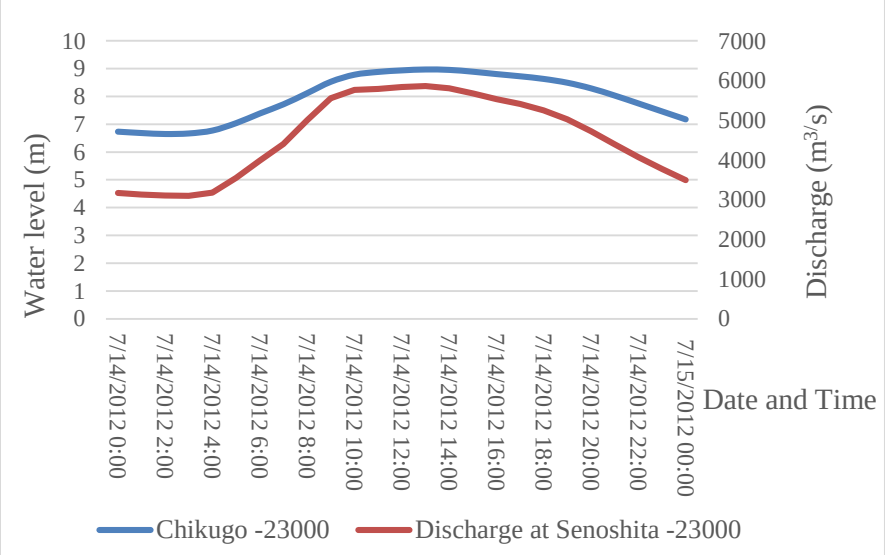

Figure 5.22: The pattern of water level simulated at Chikugo River Km 23.0

The longitudinal of water level conditions at Chikugo River section could be seen in Figure 5.23 and Hayatsue-Jyobaru River section is shown in Figure 5.24. The maximum water level at the Chikugo River section and Hayatsue-Jyobaru River section could be seen in the Figure 5.25 and Figure 5.26.

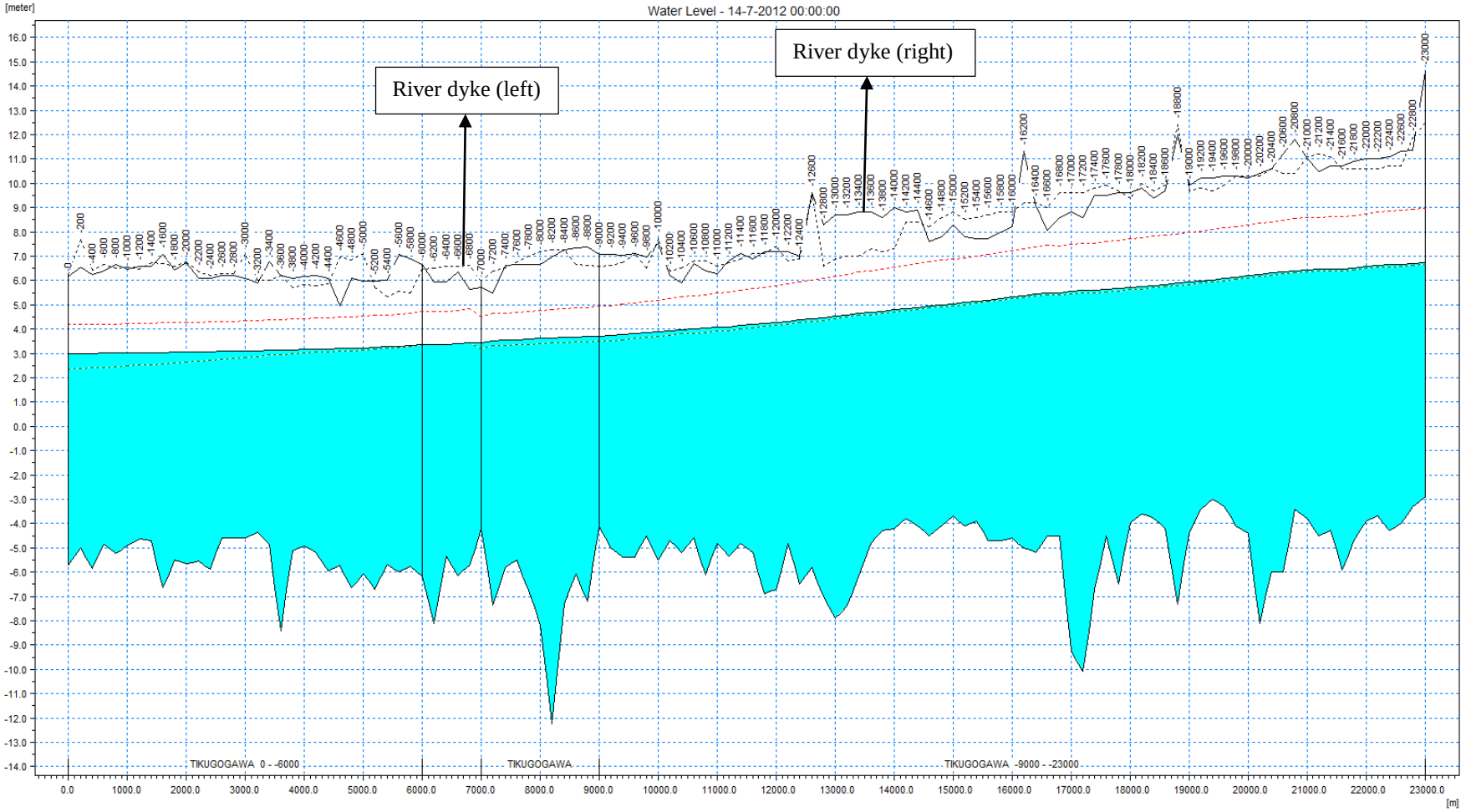

Figure 5.23: Water level condition at Chikugo River section (initial condition)

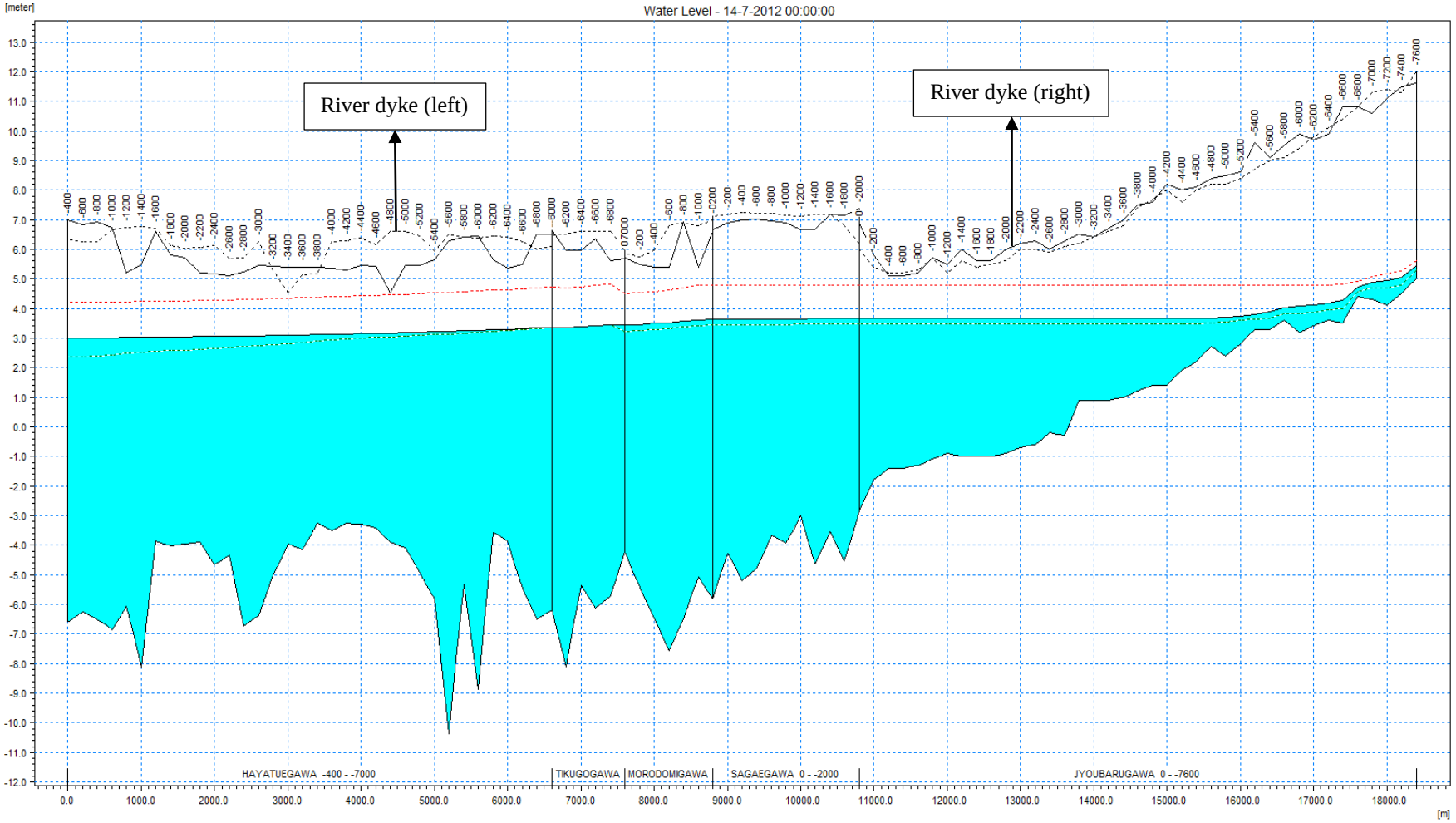

Figure 5.24: Water level condition at Hayatsue - Jyobaru Rivers section (initial condition)

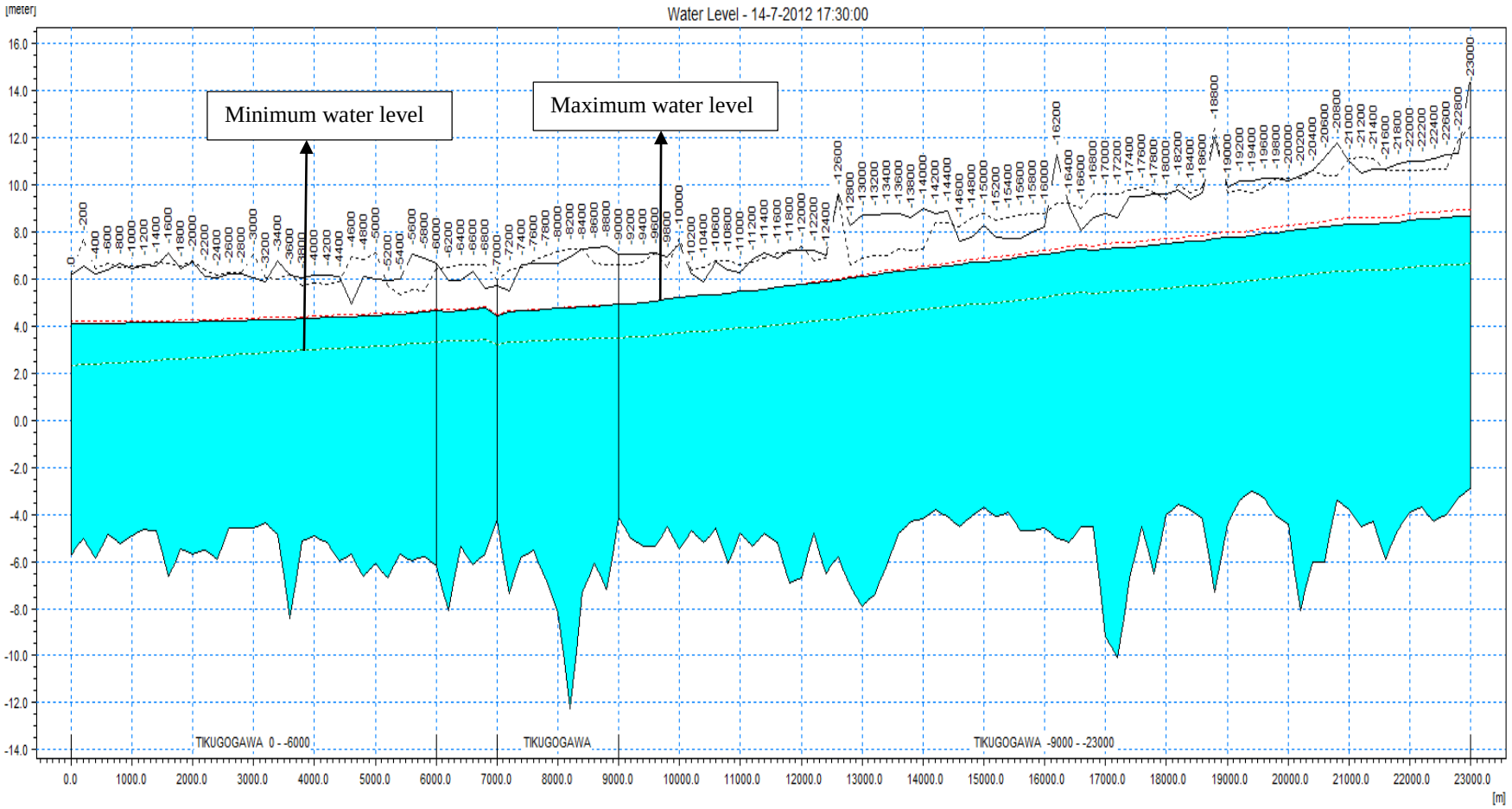

Figure 5.25: Maximum water level at Chikugo River section at the time 17:30 on July 14, 2012

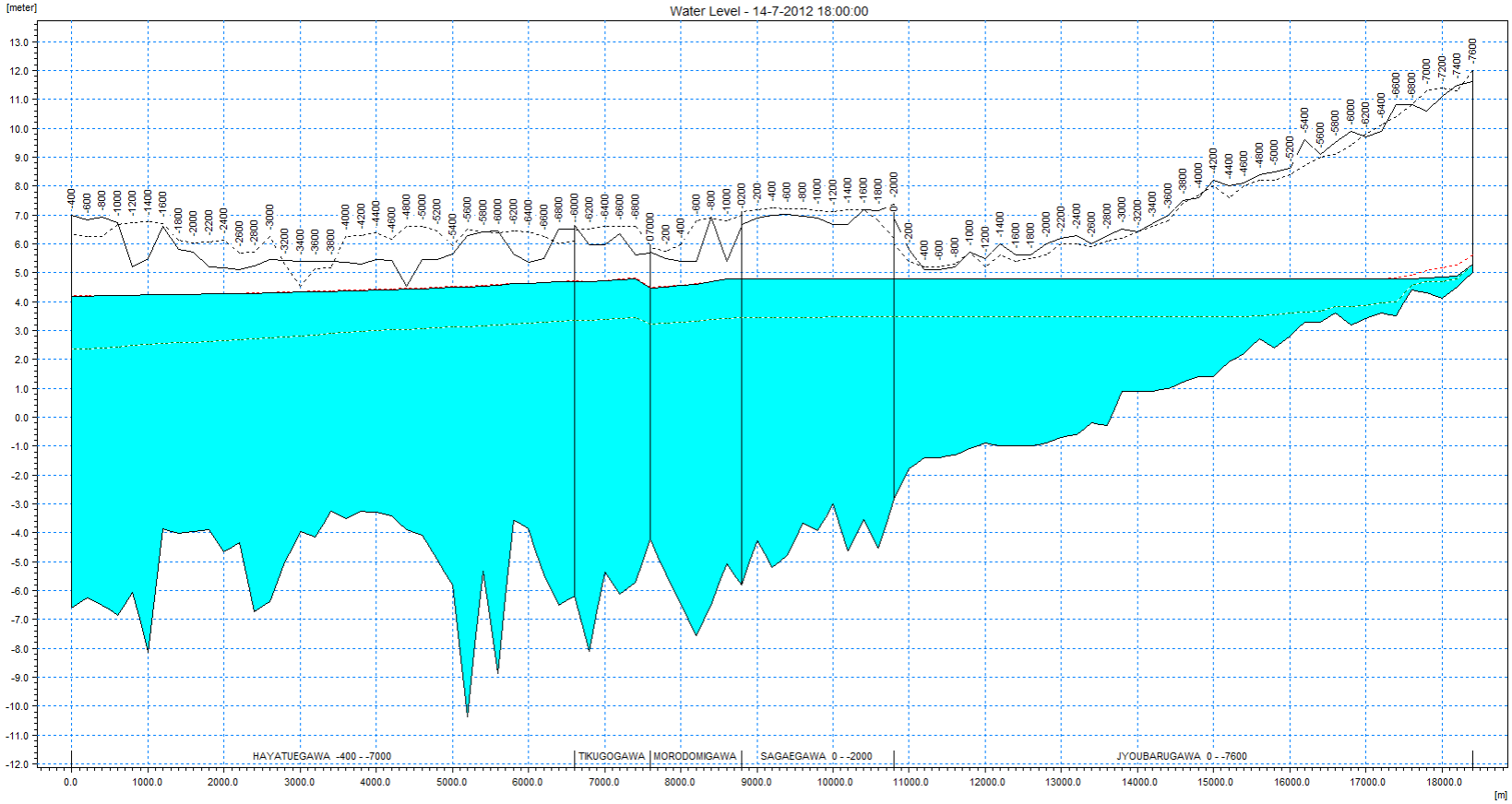

Figure 5.26: Maximum water level at Hayatsue-Jyobaru Rivers section at the time 18:00 on July 14, 2012

5.5 CONCLUSIONS

Based on the simulation results, the water level does not exceed the height of the existing coastal dykes of 7.5 m high, it means no inundation in the coastal area of the Ariake Sea and along of the Chikugo River and its branch when the high discharge or river flood by torrential rain occurred in this area on July 14 to 15, 2012.

The pattern of water level changes following the pattern of water level measurement at the mouth of Chikugo at Km. 0 and the pattern of discharge measurement at Senoshita Station at Km. 23.00 (-23000) from the river mouth of Chikugo.

The pattern of water level simulated near boundary condition in the downstream is followed the tide measurement at the mouth of Chikugo River as Km 1.2 (-1200), Km 4.2 (-4200), Km 5.4 (-5400) even to Km 6.8 (-6800) from the river mouth.

The pattern of water level simulated near boundary condition in the upstream is followed the discharge measurement at the Senoshita station as Km 21.2 (-21200), Km 18.2 (-18800) and Km 16.2 (-16200) from the mouth of Chikugo river.

The pattern of water level simulated near Wakatsu station Km 6.85 (-6850) from the mouth of Chikugo river is followed the water level measurement at Wakatsu station as Km 6.8 (-6800) and Km 7.0 (-7000).

Based on the pattern of water level simulated, the effect of boundary at the river mouth extents to Km 6.8 (-6800) at the Chikugo River. It means, the influences of tide extents to Km 6.8 near Wakatsu station.

Chapter 6

COUPLED MODEL ANALYSIS OF INUNDATION IN THE COASTAL AREA OF THE ARIAKE SEA DUE TO STORM SURGE AND FLOOD

6.1. INTRODUCTION

The coupled model of 1-D and 2-D hydrodynamic model linking the river channel flooding simulation and storm surge model simulation analysis was proposed for the numerical resolution in this study. The numerical models using one-dimensional (1-D) approximation were commonly based on the finite difference method (Chaudhry 2007; Cunge et al. 1980) and the finite element method (Nwaogazie and Tyagi 1984; Sen and Garg1998; Szymkiewicz 1991). Nevertheless, the finite difference method is still popular because of comparatively less computational effort. In this approach, the model flood simulation is conducted using the 1-D numerical model simulation and the storm surge model simulation is conducted using the 2-D numerical model simulation.

In chapter 4, the model simulation of the storm surge by Typhoon Pat that has occurred in the Ariake Sea on August to September 1985 using the 2-D numerical model was performed. This study utilized a two-dimensional hydrodynamic model, and considered transections are 7 measurement lines: Shiroishi, Higashiyoka, Rokkaku estuary, Kase estuary, Chikugo estuary, Saga airport and Ohamma. In the simulation results, the water levels did not exceed the elevation of existing coastal dyke, which means no seawater inundation happens in the coastal area of the Ariake Sea.

In chapter 5, flood or high discharge by torrential rain that has occurred on July 2012 is analyzed at Chikugo River and branch. This study utilized a one-dimensional numerical model. This study analyzes of the cross-section and the network of the Chikugo River and branch. The discharge data from upstream of Chikugo River and Jyobaru River and the water level data from downstream of Chikugo River and Hayatsue River are used for input data in the boundary. The discharge data of Chikugo River is obtained from Senoshita station and discharge data of Jobaru River obtained from Hidekibashi station with time series format data of discharge based on the time series of simulation. The water level data is obtained from water level data at near estuary of each rivers Chikugo and Hayatsue. In the simulation result shows there is no water level exceeded the existing dyke along Chikuko River in the study area.

The storm surge by typhoon sometimes occurred during the rainy season in Japan. In July 2015, a total 72 hours rainfall from typhoon Nangka occurred in Japan causing landfall and flooding (Erdman and Wiltgen, 2015). With the assumption that the flood in chapter 5 and the storm surge in chapter 4 simultaneously occurred at the same time in the study area, the coupled model analysis will be conducted.

6.2. STUDY AREA AND SUPPOSED DISASTERS

6.2.1 Study area

Study area is the coastal area of the Ariake Sea and Saga lowland where there is Chikugo River and its branch that empties into the Ariake Sea, such as shown in Figure 6.1

Figure 6.1: Study area

6.2.2 Supposed Disasters

Supposed disasters are a storm surge and a flood that have occurred in this area. The first disaster is the storm surge by typhoon Pat that occurred on August, 31 to September 1, 1985. The second disaster is the river flood in the Chikugo River and its branch by torrential rain from July 14 to 15, 2012.

6.3. COMPUTATIONAL TOOL AND METHODOLOGY

6.3.1. Computational tool

The numerical simulation model MIKE-FLOOD integrates the 1D model MIKE-11 and the 2D model MIKE-21 into a single, dynamically coupled modelling system. Using a coupled approach, MIKE-FLOOD enables to extract the best features of both MIKE-11 and MIKE-21 to simulate floods, while avoiding many of the limitations of resolution and accuracy encountered when using MIKE-11 or MIKE-21 separately. In the following sections, separate descriptions and usage of the component models MIKE-11 and MIKE-21, and the integrated model MIKE-FLOOD is briefly described.

6.3.2. Methodology

The simulation results of 1-D numerical model analysis of flood in chapter 5 and simulation results of 2-D numerical model analysis of storm surge in chapter 4 are used as data input in the dynamically coupled modeling system. For simulation, the time series data must be same, in this case with the assumption the storm surge and the flood simultaneously occurred on July 14-15, 2012.

2-D model setup

In chapter 4, 2-D model setup of storm surge simulation in the Ariake Sea has been done using MIKE 21 model setup. For using the coupled 1D-2D model

simulation, the setup data of the time series data must be changed based on the assumption as mentioned above.

1-D model setup

In chapter 5, 1-D model flood simulation in the Chikugo River and its branch has been carried out using MIKE 11, such as cross section, network, and boundary. For using the coupled 1D-2D model simulation, the setup data of the time series is same because the time simulation at July 14-15, 2012 is the same time or based on the time series were used in the 1-D model setup in chapter 5.

Coupling of 1D-2D model setup

The MIKE-11 river network was connected to the MIKE-21 bathymetry using the lateral link and standard link option available in the MIKE-FLOOD. Figure 6.2 shows the connected river network and bathymetry.

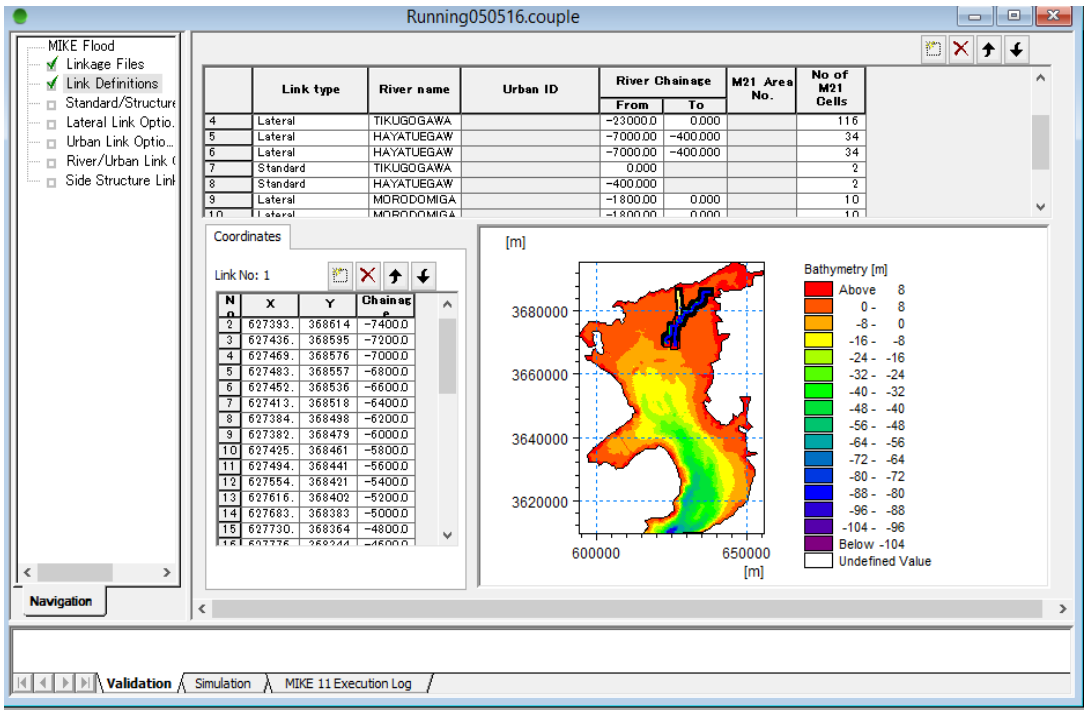

Figure 6.2: The connected network and bathymetry

6.4. SIMULATION RESULTS

For simulation both of flood and storm surge in the coupled model, the coordinate system must be same for making the river network and bathymetry connected, as shown in Figure 6.2. Also, time series data must be same. The simulation results could be presented using result viewer in the frame MIKE ZERO developed by DHI on the frame 1-D model and simulation result of inundation could be presented using MIKE 21 in the frame 2-D model. Figure 6.3 to Figure 6.11 shown the inundation processes.

The simulation showed that the exceeding of water level of the river dyke starting from 1:57 AM at the left bank of Hayatue River at the cross-section -3400 as

shown in Figure 6.3. In the Chikugo River, the water level exceeds the existing river dyke starting from 2:07 AM at the right bank of the cross-section -4600 as shown in Figure 6.4.

At the time 6:00 AM, the water level receded and there was no inundation area such as shown in Figure 6.5 and Figure 6.6.

The maximum water level of all cross sections in the Chikugo River section was occurred at the time 11:00 AM on July 14, 2012 and the maximum water level of all cross sections in the Hayatue-Jyobaru River section was occurred at the time 11:00 AM on July 14, 2012 and at the time 0:00 on July 15, 2012, as shown in Figure 6.7 to Figure 6.9.

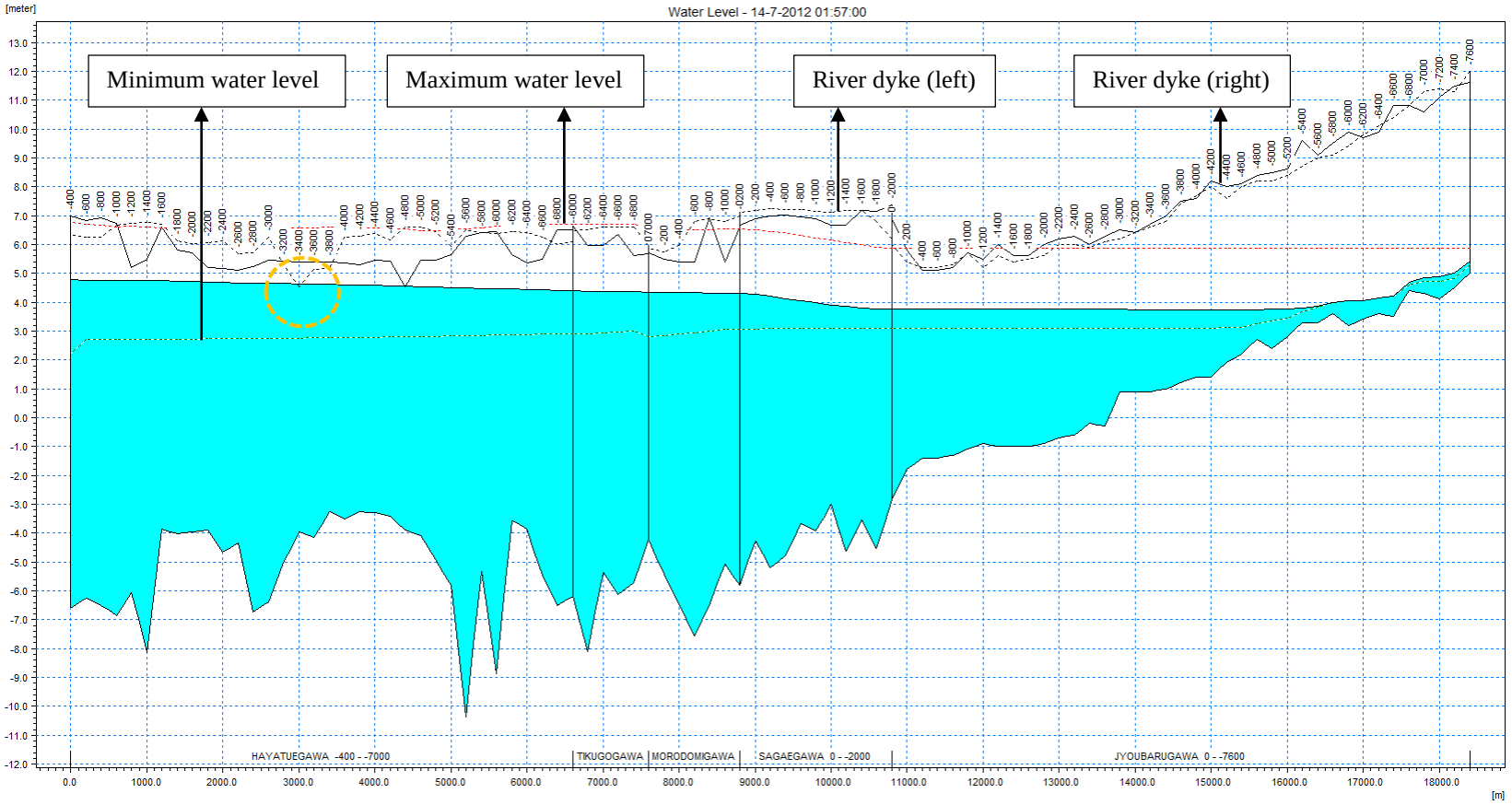

Figure 6.3: Water level in the Hayatsue-Jyobaru River section at time 01:57 on July 14, 2012

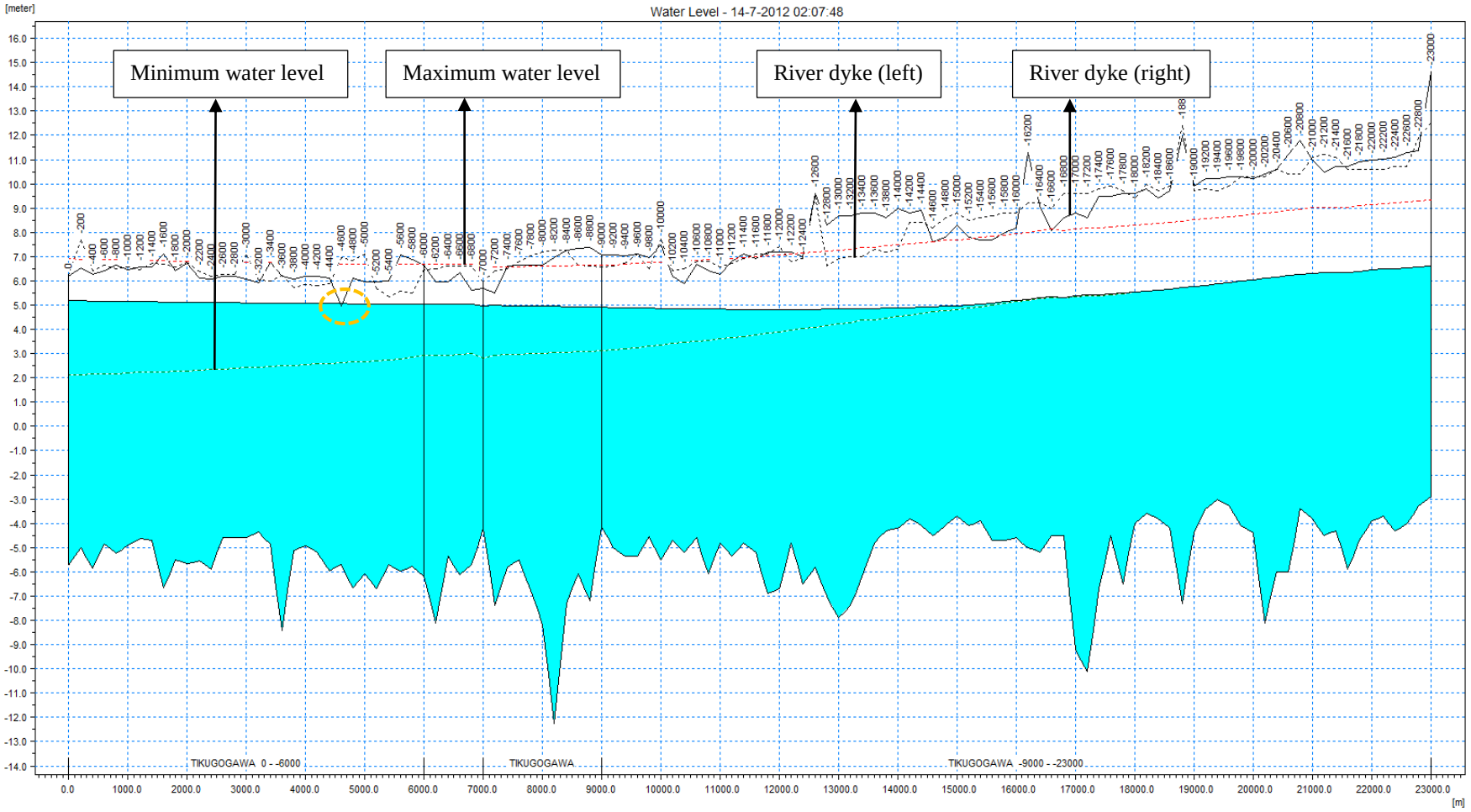

Figure 6.4: Water level in the Chikugo River section at time 02:07 on July 14, 2012

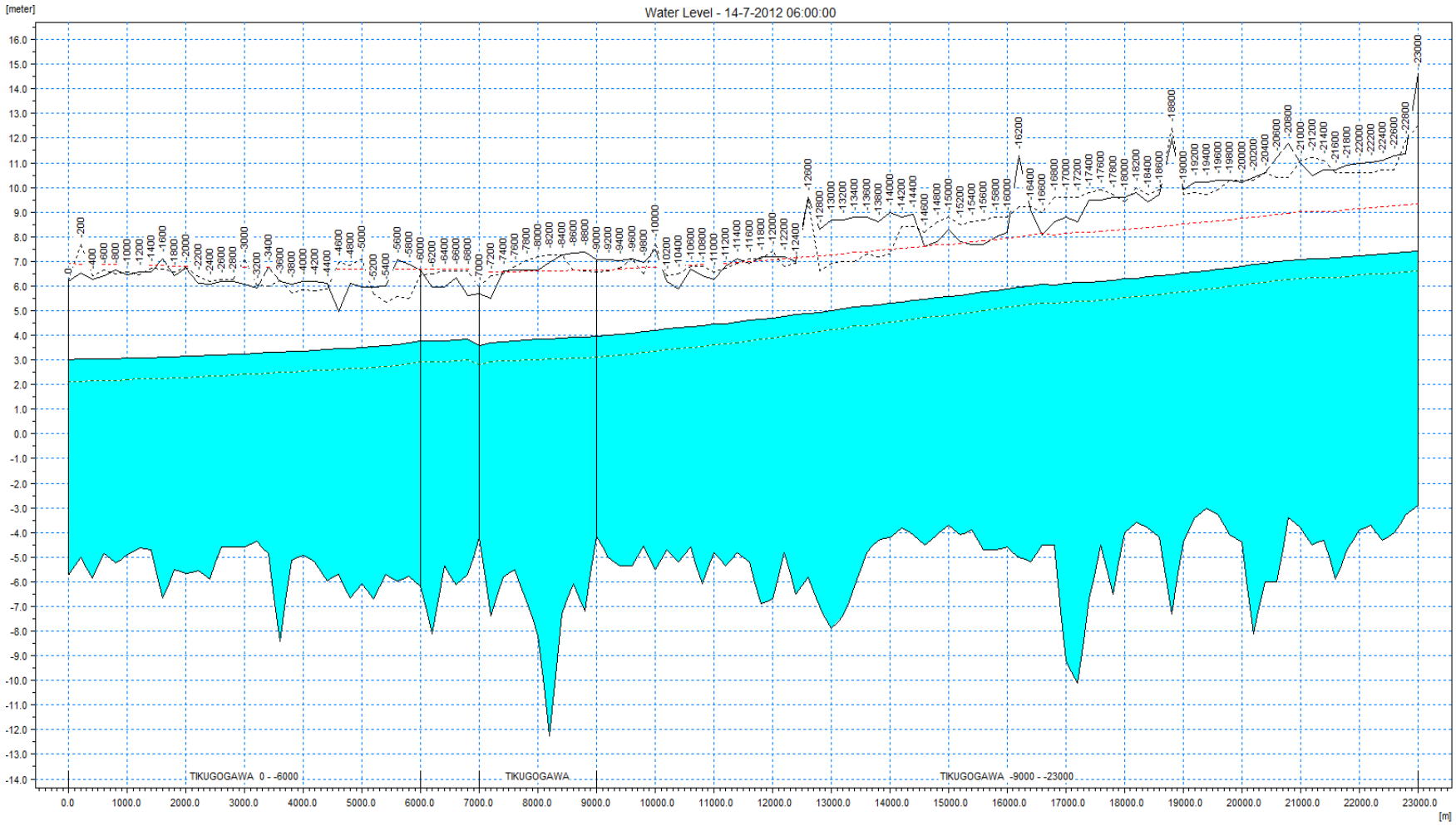

Figure 6.5: Water level in the Chikugo River section at time 06:00 on July 14, 2012

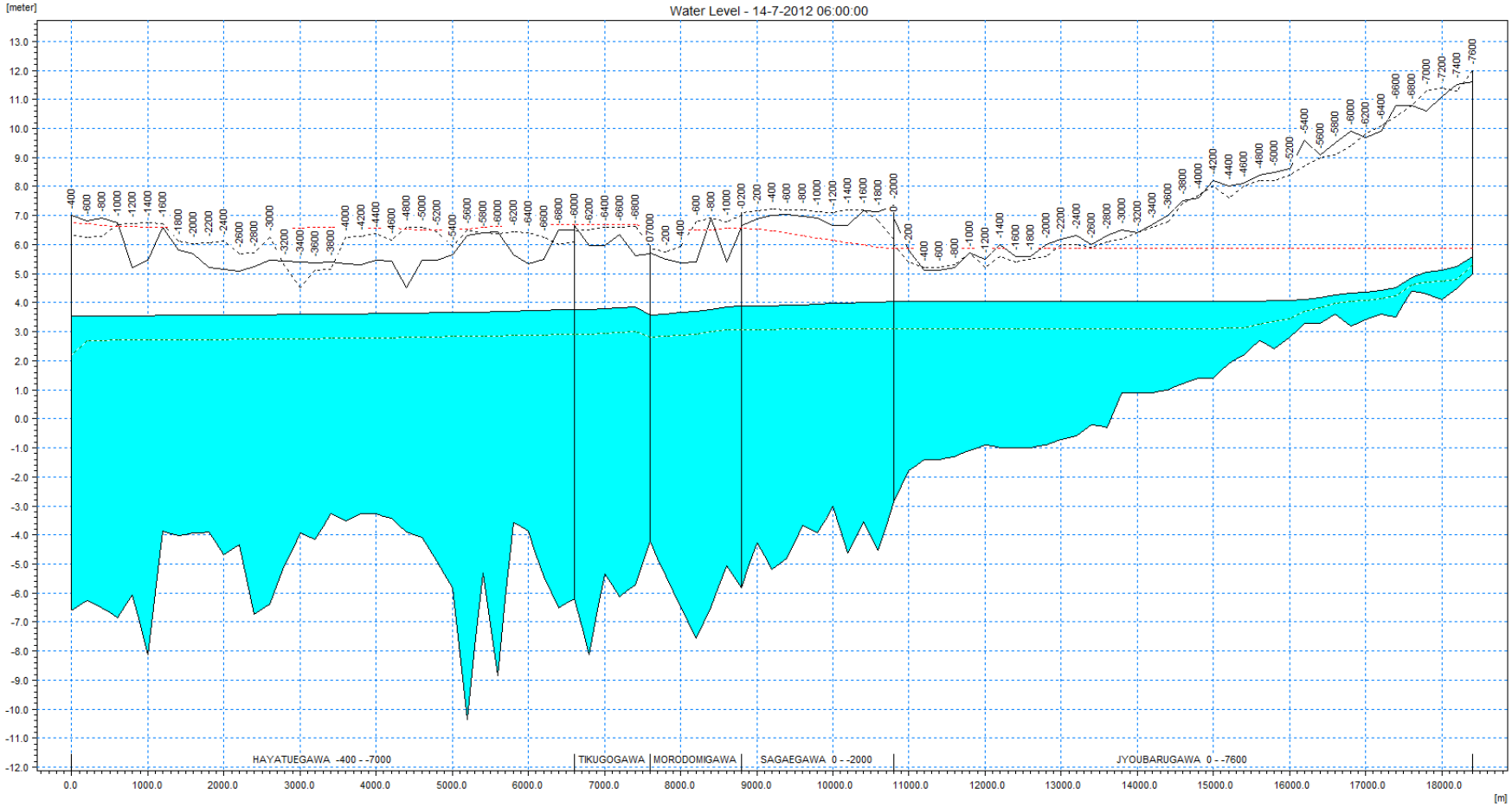

Figure 6.6: Water level in the Hayatsue-Jyobaru River section at time 06:00 on July 14, 2012

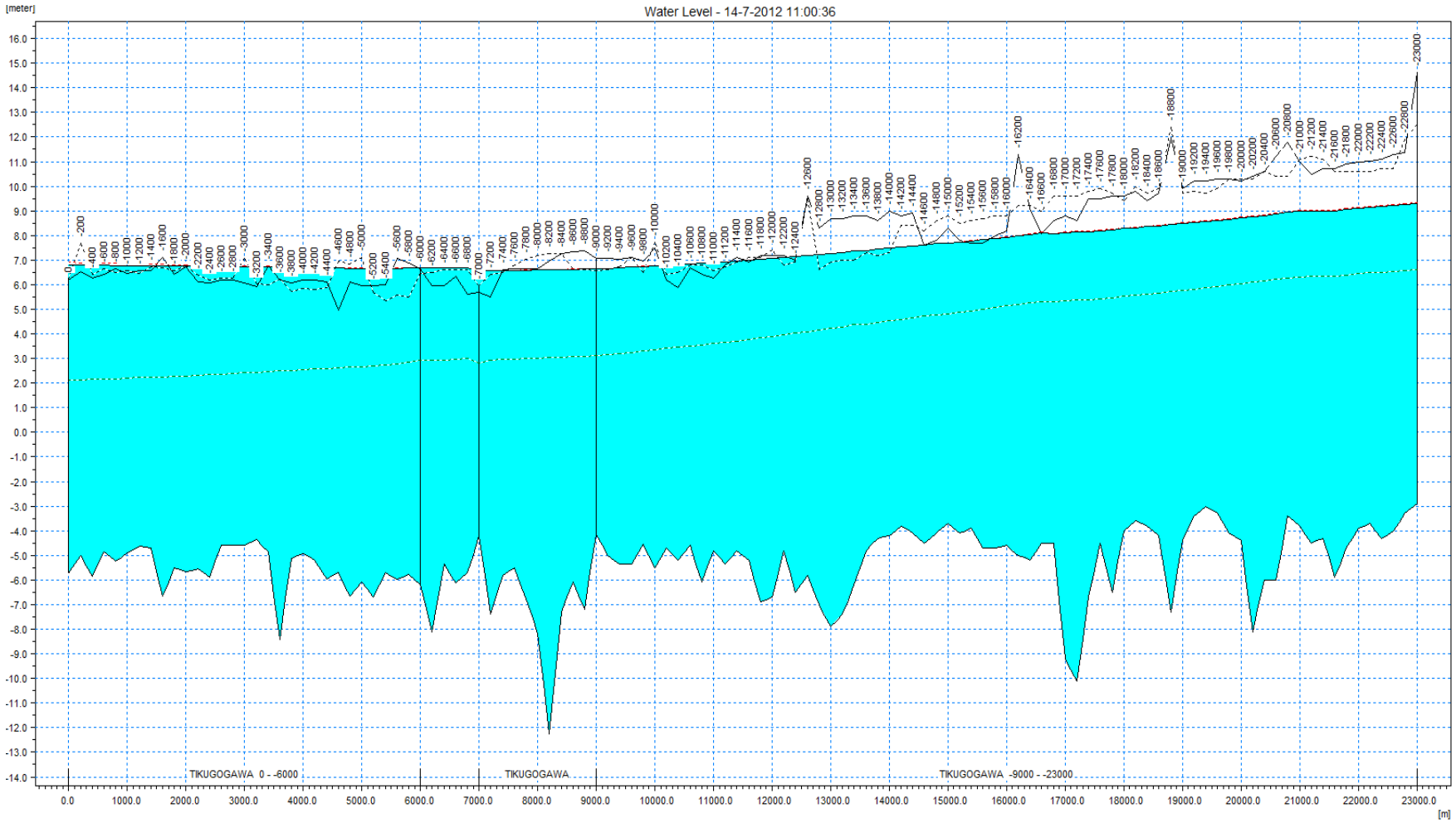

Figure 6.7: Maximum water level in the Chikugo River section at time 11:00 on July 14, 2012

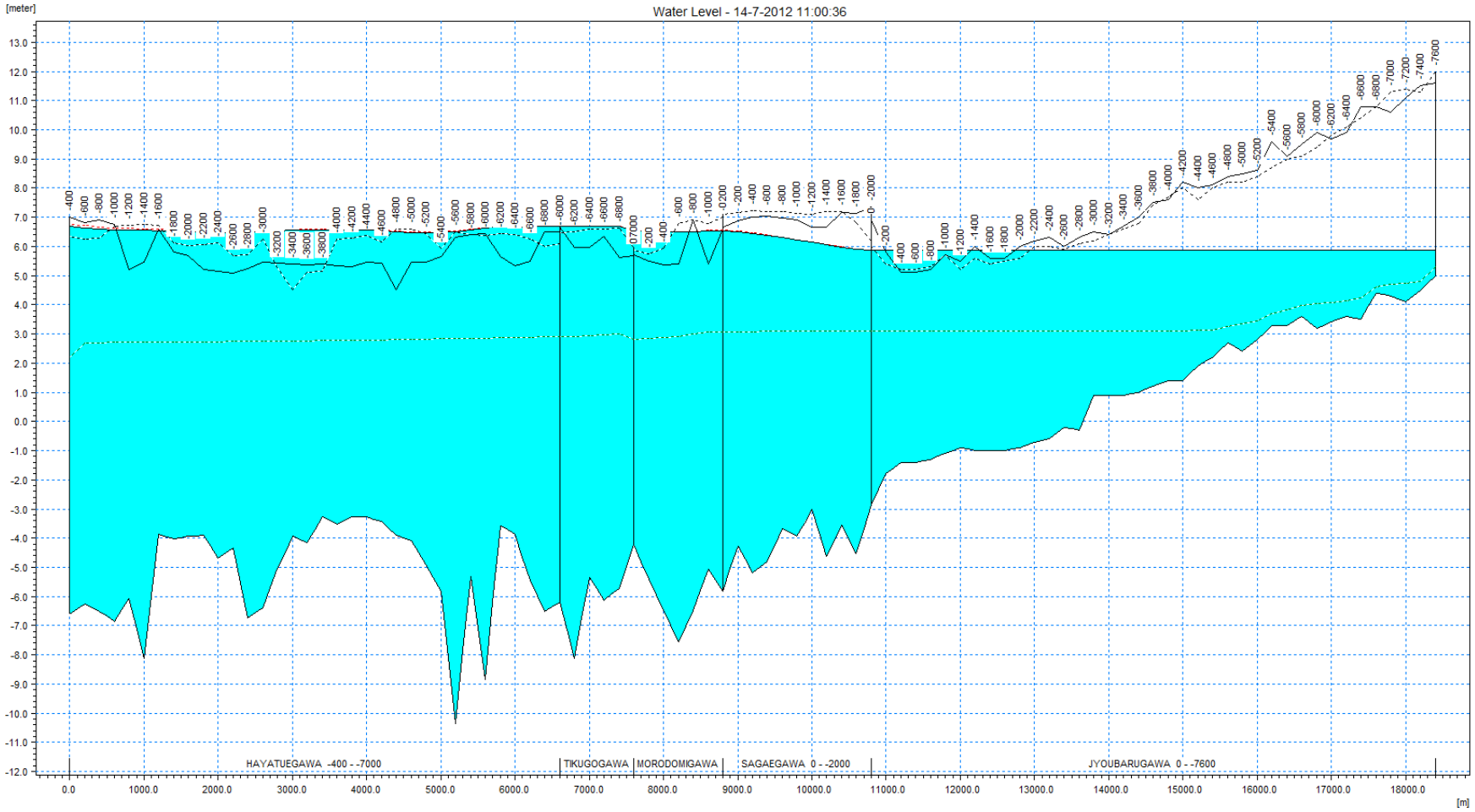

Figure 6.8: Maximum water level in the Hayatsue-Jyobaru River section at time 11:00 on July 14, 2012

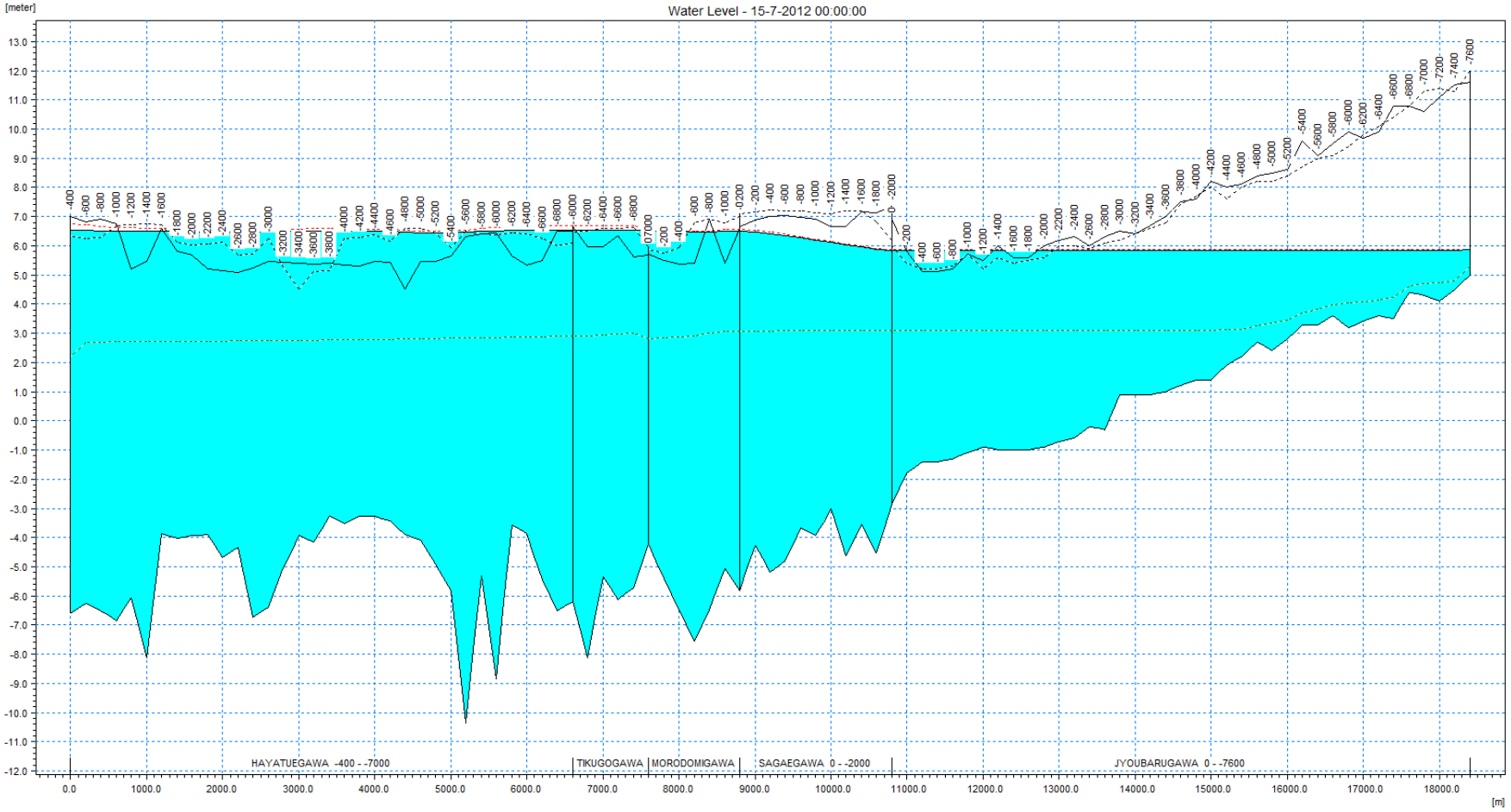

Figure 6.9: Maximum water level in the Hayatsue-Jyobaru River section at time 00:00 on July 15, 2012

Figure 6.10 to Figure 6.19 showed the water surface distribution when the storm surge and the river flood occurred in the coastal area of Ariake Sea and Saga lowland near of Chikugo estuary.

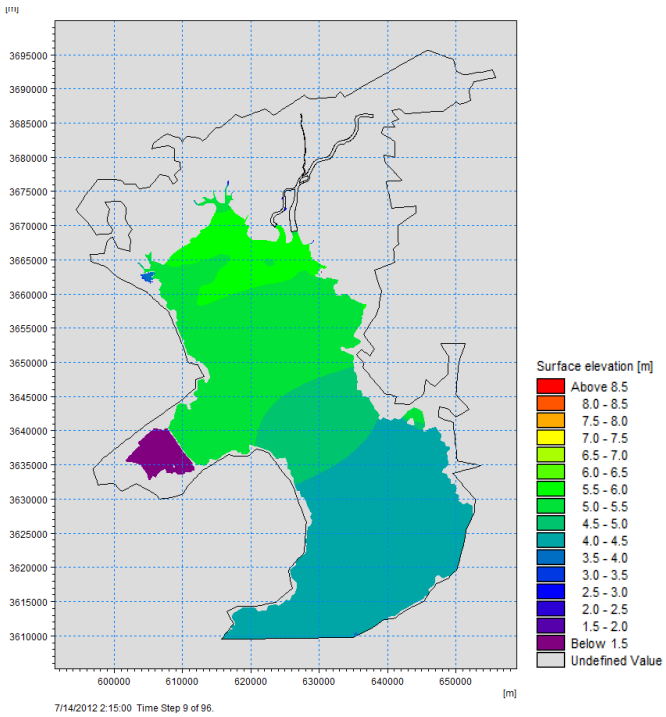

Figure 6.10: Water surface distribution in the coastal area of the Ariake Sea at time 02:15 on July 14, 2012

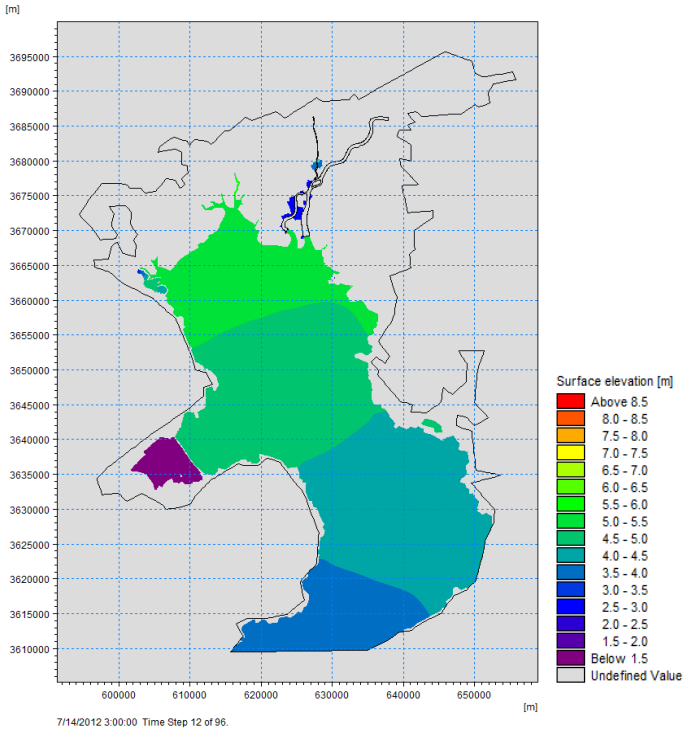

Figure 6.11: Water surface distribution in the coastal area of the Ariake Sea at time 03:00 on July 14, 2012

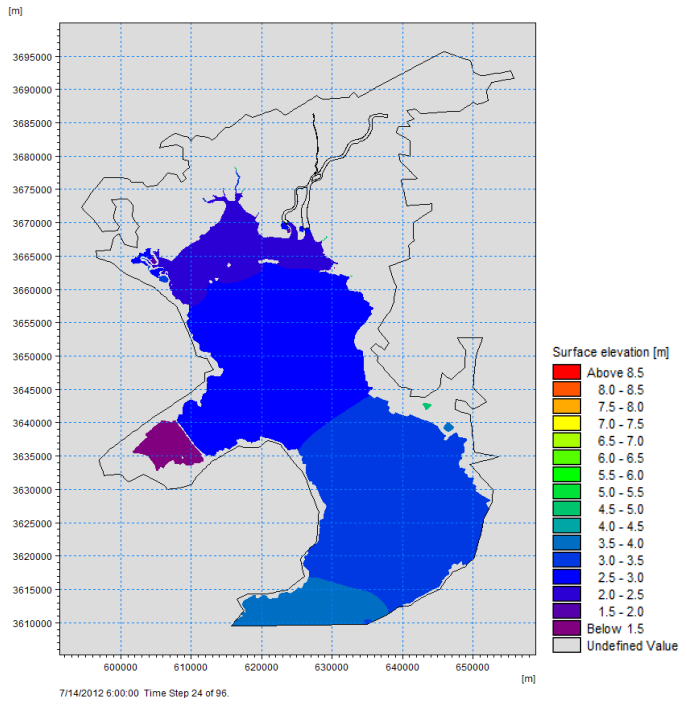

Figure 6.12: Water surface distribution in the coastal area of the Ariake Sae at time 06:00 on July 14, 2012

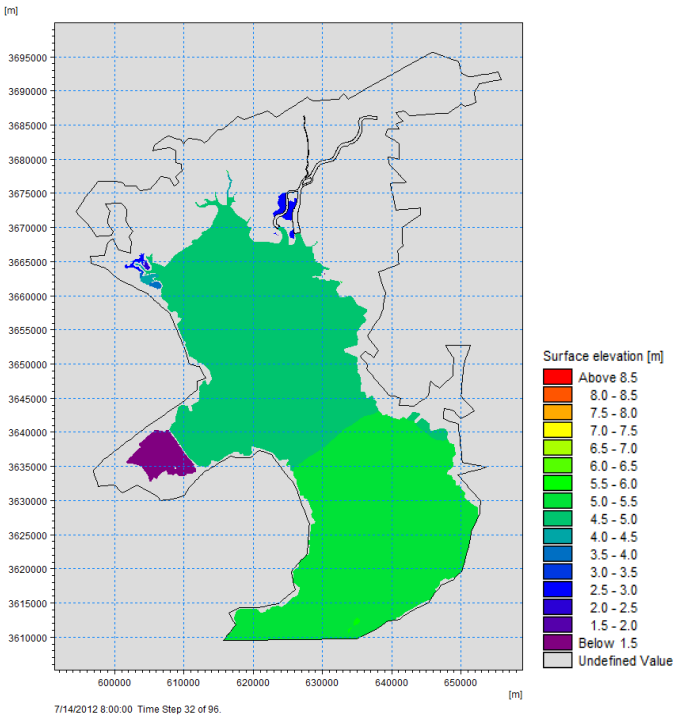

Figure 6.13: Water surface distribution in the coastal area of the Ariake Sea at time 08:00 on July 14, 2012

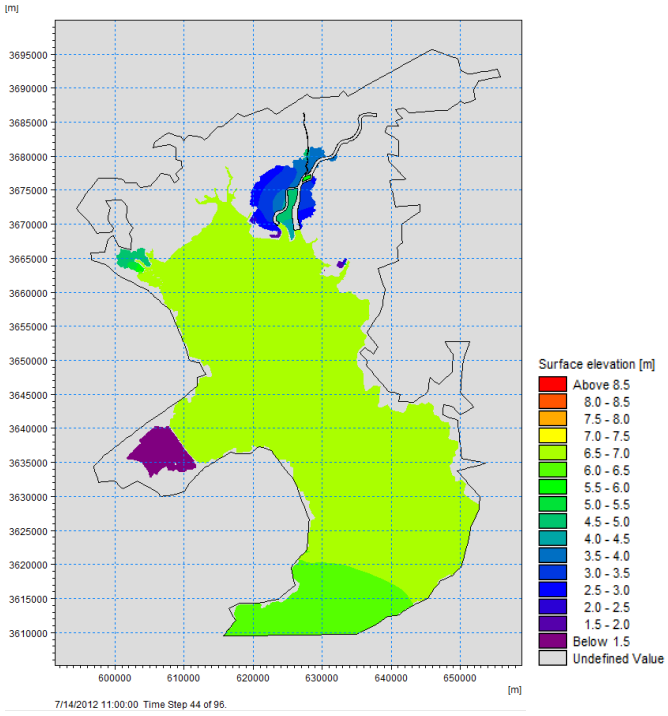

Figure 6.14: Water surface distribution in the coastal area of the Ariake Sea at time 11:00 on July 14, 2012

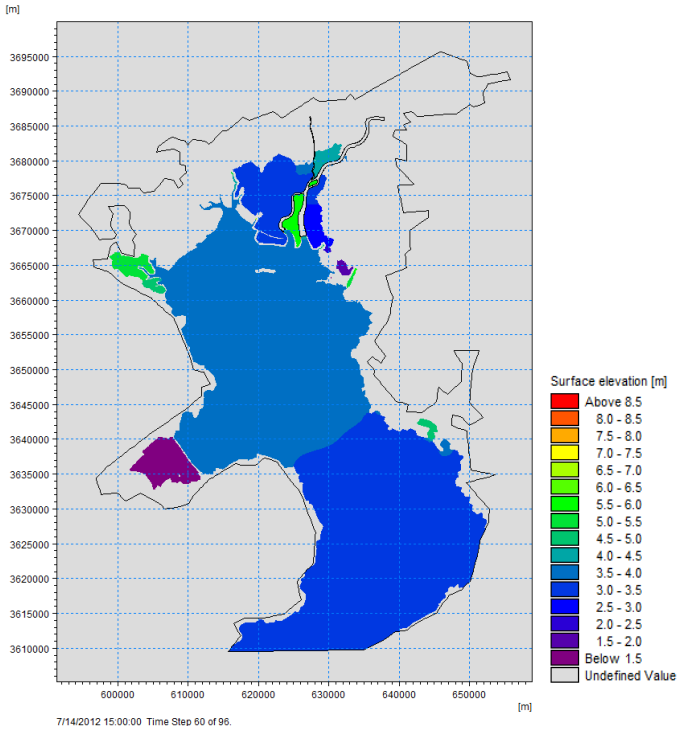

Figure 6.15: Water surface distribution in the coastal area of the Ariake Sea at time 15:00 on July 14, 2012

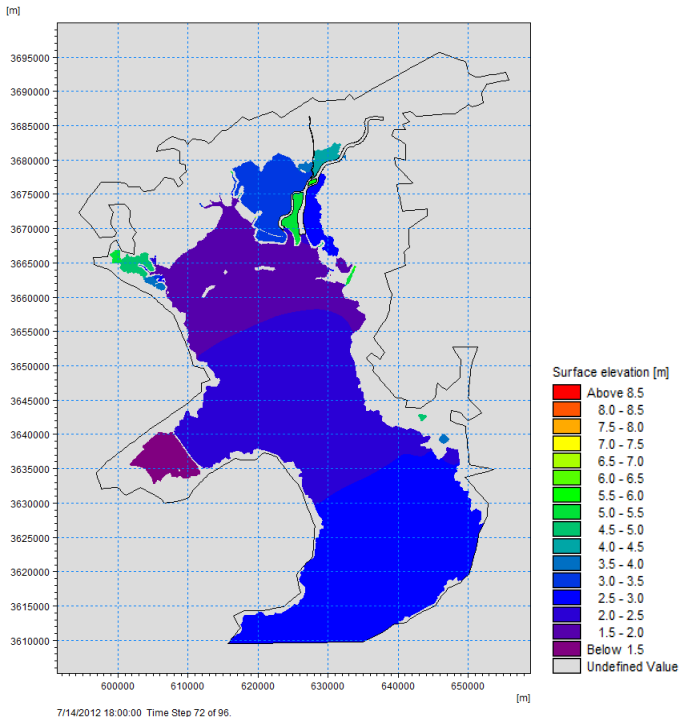

Figure 6.16: Water surface distribution in the coastal area of the Ariake Sea at time 18:00 on July 14, 2012

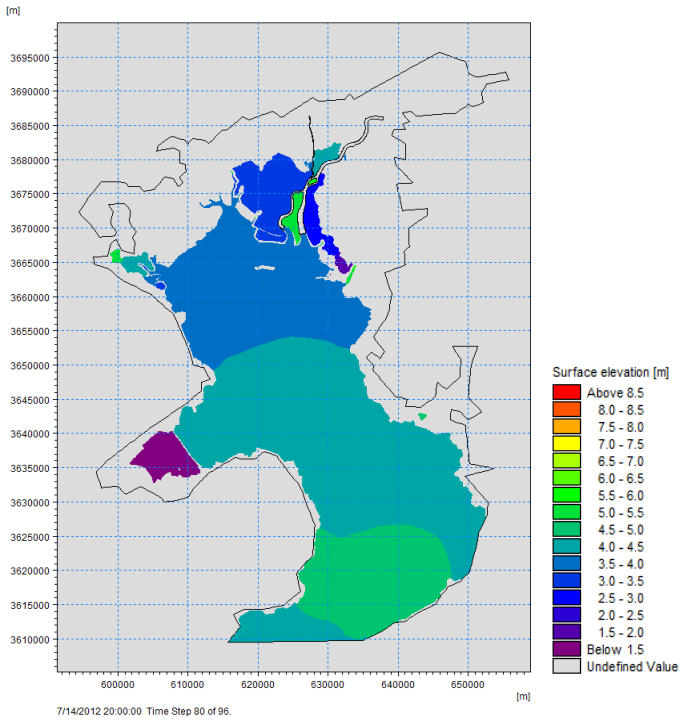

Figure 6.17: Water surface distribution in the coastal area of the Ariake Sea at time 20:00 on July 14, 2012

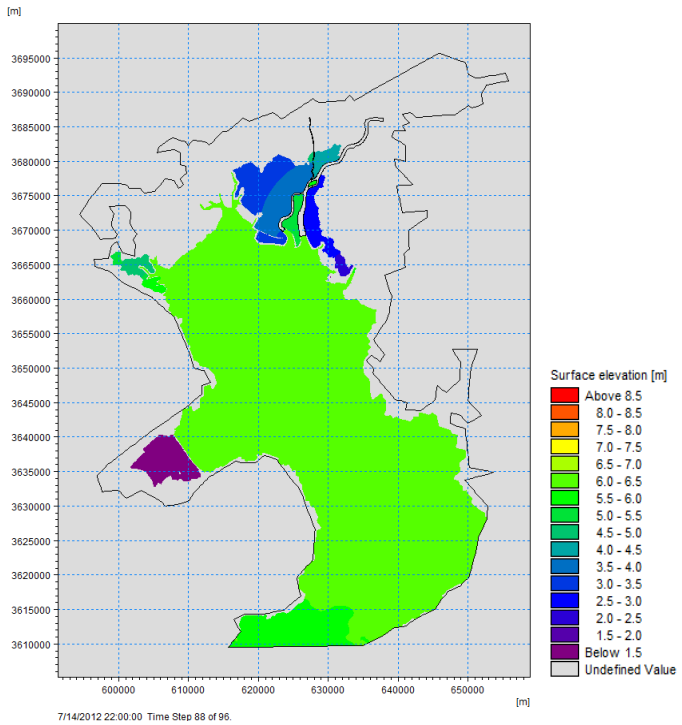

Figure 6.18: Water surface distribution in the coastal area of the Ariake Sea at time 22:00 on July 14, 2012

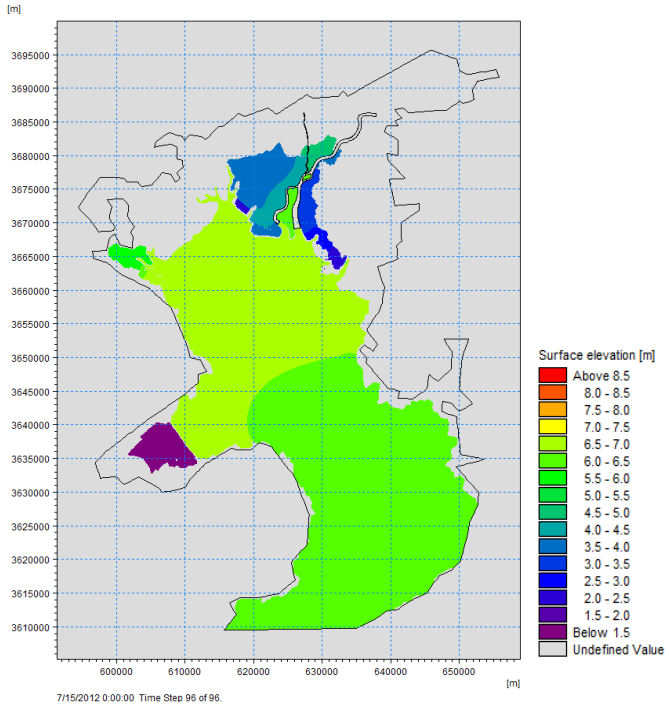

Figure 6.19: Water surface distribution in the coastal area of the Ariake Sea at time 00:00 on July 15, 2012

6.5. CONCLUSIONS

Based on the simulation result by the coupled model simulation, if the river flood in the Chikugo River and its branch and the storm surge in the Ariake Sea simultaneously occurred, the coastal area of the Ariake Sea and Saga lowland near of the Chikugo River estuary were inundated.

The water level rise during the storm surge occurs in the Ariake Sea can cause sea water inside in the Chikugo River and the same time the flood from Chikugo river occurs can cause water level in the Chikugo river exceed the existing river dyke. This situation resulted inundation in the coastal area of the Ariake Sea and Saga lowland near of the Chikugo river estuary.

In the simulation result, no sea water exceeds the existing coastal dyke with 7.5 m high. The inundation in the coastal area of the Ariake Sea and Saga lowland occurred due to water level exceeding the existing river dyke or water overflowing of the Chikugo River and its branch.

Chapter 7

DISASTER MANAGEMENT IN THE COASTAL AREA OF THE ARIAKE SEA AND SAGA LOWLAND

7.1 INTRODUCTION

Storm surge is a phenomenon in which ocean water surface elevations rise as a result of strong winds and decreases in atmospheric pressure during tropical storms and typhoon. Storm surge by the typhoon is the one of the frequent disasters in Japan, which can cause significant inundation in the coastal communities. Lives and properties located in the coastal area of typhoon-prone regions are significant risk during large storm events.

Many of the risks are given by the storm surge along the coastal areas including residential areas, industries, agriculture, etc., with exposure to inundation from the combination of storm surge and river flooding. However, storm surge combined with the flood in the coastal area is not well studied. Understanding of these risks of inundation as a result of storm surge and river flooding is quite necessary, especially for the coastal communities. River flooding by high discharge is also a disaster that could cause inundation in the coastal area.

This study aims to get an overview of inundation when the two disasters, storm surge, and river flood simultaneously occurred in the coastal area of Ariake Sea and Saga lowland. GIS analysis will be presented to obtained the inundation affective in the houses or buildings and the public facilities. Also, created an inundation risk map in the coastal area of Ariake sea and saga lowland for the future of coastal disaster management.

7.2 STUDY AREA AND SUPPOSED DISASTERS

The Ariake Sea, which is surrounded by Fukuoka, Saga, Nagasaki and Kumamoto Prefectures, is the biggest Bay in Kyushu island. This is an inner bay, where many rivers are flowing in such as Chikugo River, Kase River, Rokkaku River, Yabe River, etc. This bay includes muddy tidal flat. The Ariake Sea's tidal range is the largest in Japan, and the maximum tidal range is as much as 5 m to 6 m at the innermost part. Coastal areas of this bay are mainly lowland with an unusually small slope, so once the sea water enters these areas, they will be immediately inundated.

If the typhoon track coincides with the Ariake Sea's longitudinal axis, it can cause a significant storm surge. The large rivers such as Chikugo River, Kase River, and Rokkaku River empty into this bay. There are settlements, airport, agriculture, industrial and office buildings and other public facilities in this coastal area. Therefore, the Japanese government has built a coastal dyke along the shorelines and river within this region with the maximum elevation of 7.5 m based on the analysis of Isewan Typhoon in 1959.

In 1985, the typhoon Pat hit a track in this area. With highest winds of 80 mph (130 km/h) this typhoon resulted in the storm surge in the region of Kyushu island, 79 people were injured, 38 houses in Japan were demolished, 110 were damaged, and over 2,000 were flooded. More than 160,000 homes lost power, a total of 165 flights were cancelled (Wikipedia, https://en.wikipedia.org/wiki/Typhoon_Pat_(1985). In July 2012 torrential rains caused high discharge and widespread flooding in this area, causing at least 10 people deaths, 20 were missing and around 50,000 evacuations (http://www.hurriyetdailynews.com/50000-flee-as-record-rain-in-japan-kills-10-.aspx?pageID=238&nID=25346&NewsCatID=356).

7.3 INUNDATION RISK ANALYSIS

7.3.1 GIS Model Analysis

GIS model analysis are conducted to obtain the inundation risk affected based on the result of 2-D inundation numerical simulation. The data of 2-D simulation result are converted to shape file. Furthermore, inputted data of buildings or houses and public facilities are also converted to the shape files. According to the level of the inundation risk, the amount of buildings or houses and public facilities inundated is obtained. Figure 7.1 and Figure 7.2 show the inundation risk of buildings and public facilities in the coastal area of Ariake Sea in the case that the storm surge and the flood simultaneously occur in this area. More than 96,000 buildings or houses and 245 public facilities were inundated.

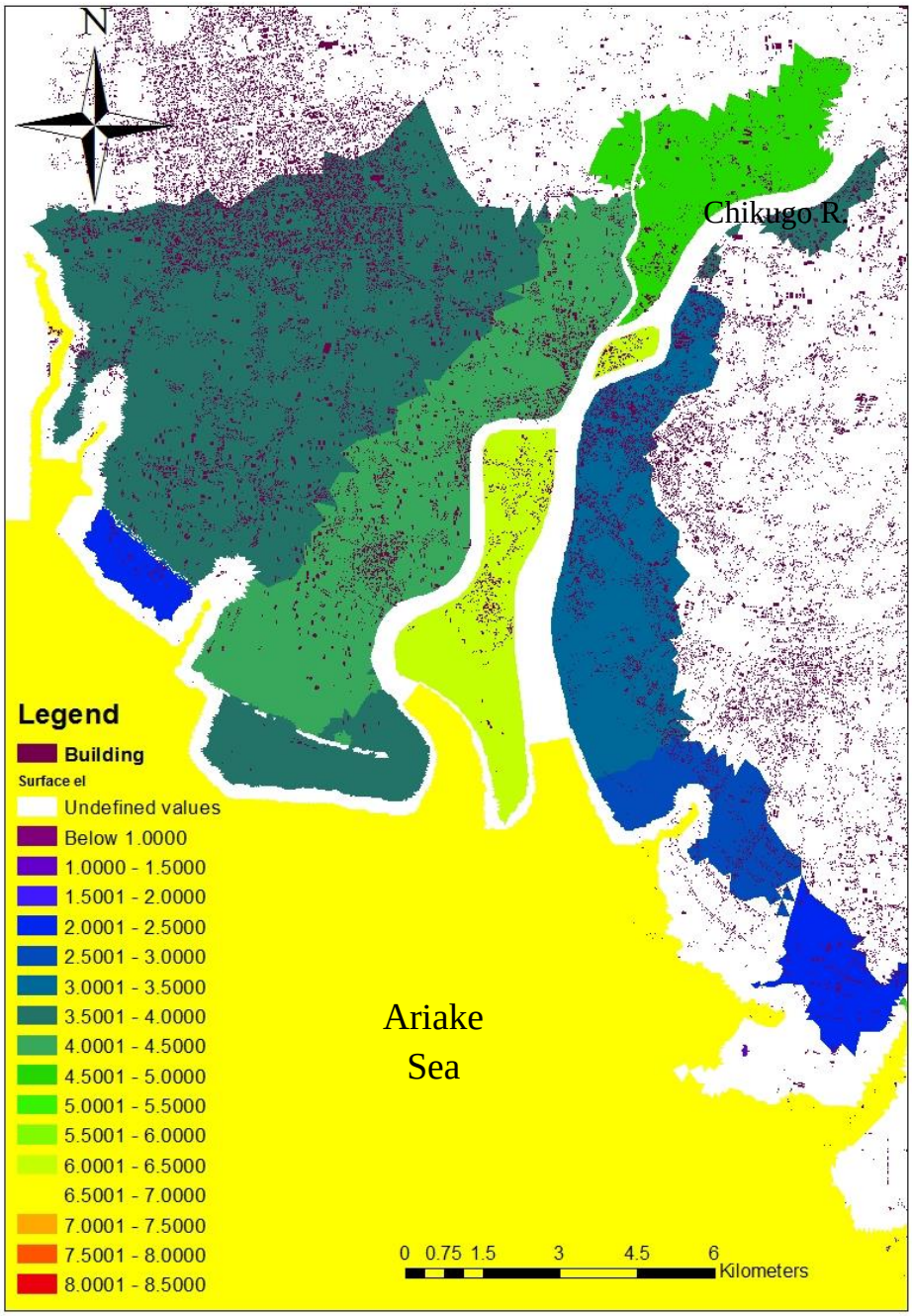

Figure 7.1: Inundation of the buildings or houses

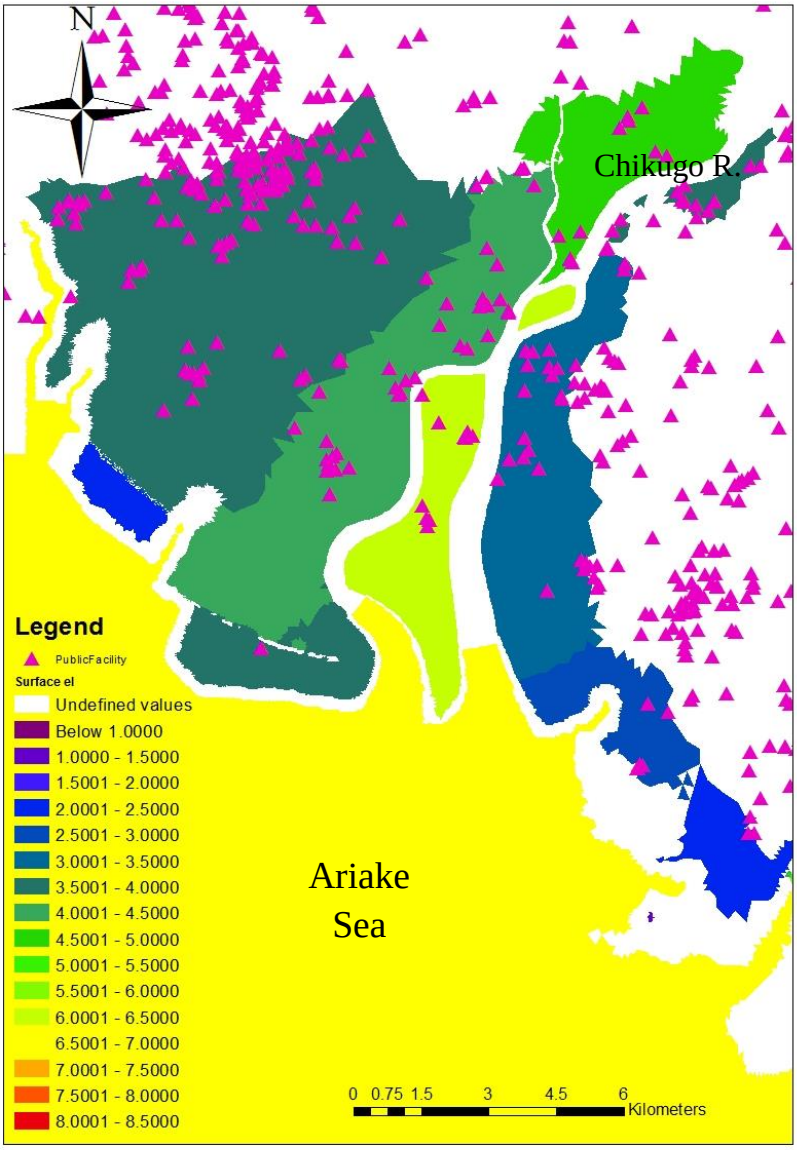

Figure 7.2: Inundation of the public facilities

7.3.2 Creation a risk map of Inundation

Based on the GIS analysis, the risk maps of inundation be created such as shown in Figure 7.3.

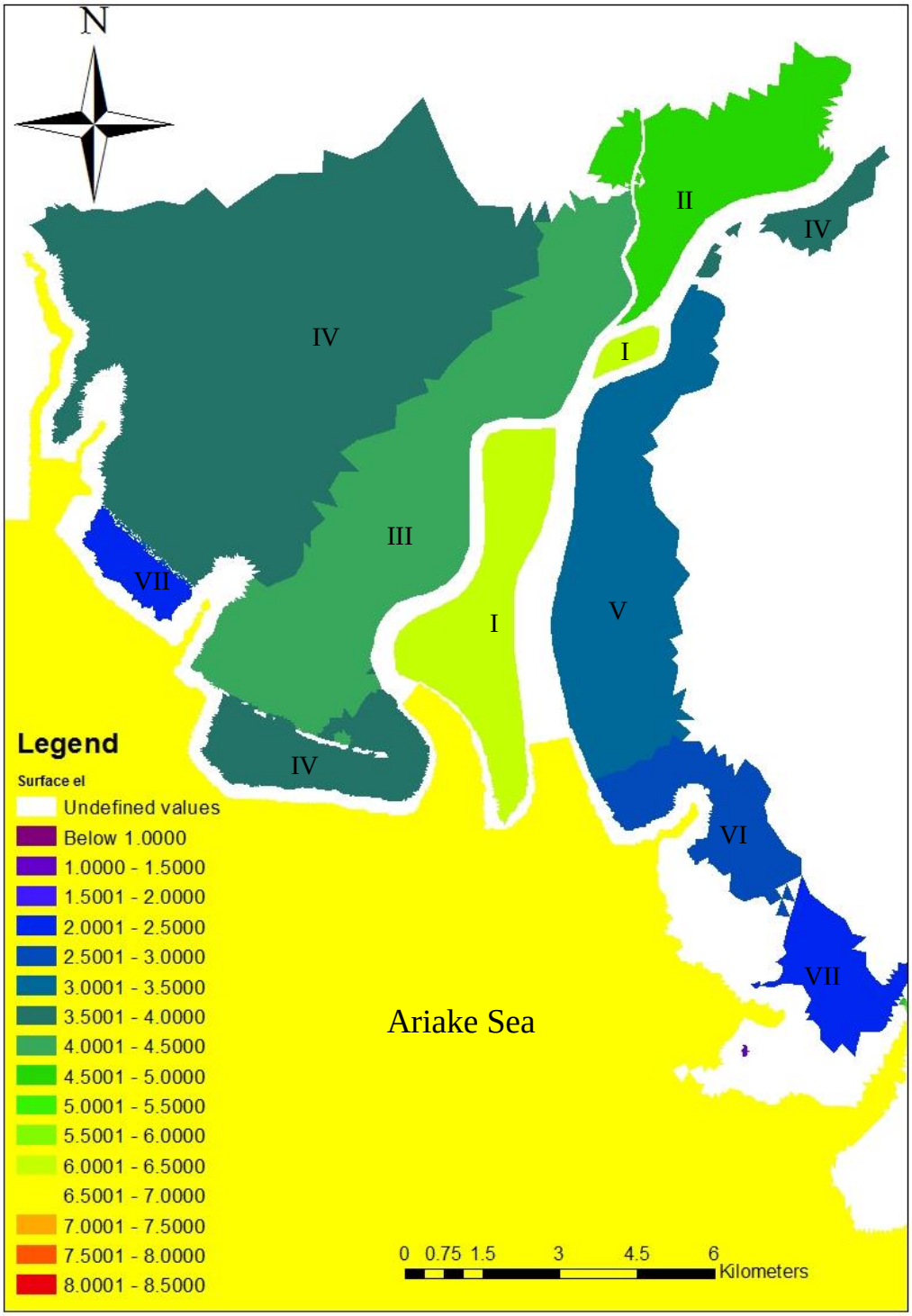

Figure 7.3: Risk maps of inundation

Based on GIS analysis in the risk map of inundation, table 7.1 below showed the criteria of inundation risk. The risk category was based on the inundation height and inundation affected to buildings or houses and public facilities.

Table 7.1: Inundation risk categories

Inundation area	Inundation height (m)	Buildings or houses affected (unit)	Public facilities affected (unit)	Risk category	Action
I	3.5 - 4.0	4484	11	High	Evacuation
II	3.0 – 3.5	2729	11	High	Evacuation
III	2.5 – 3.0	17425	32	High	Evacuation
IV	2.0 – 2.5	50889	156	High	Evacuation
V	1.5 – 2.0	14952	27	High	Evacuation
VI	1.0 – 1.5	3455	5	Middle	Evacuation
VII	0.5 – 1.0	2143	3	Middle	Evacuation

Figure 7.4 showed the evacuation route to places that are not affected by the inundation such as school, hospital, open spaces or garden and other public facilities.

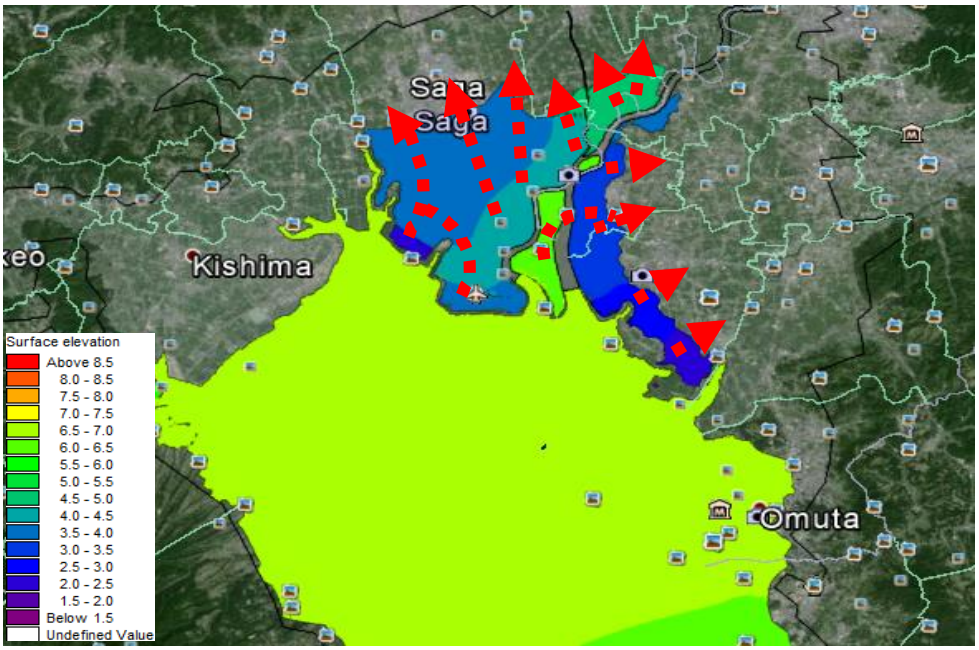

Figure 7.4: Possible evacuation route

7.4 FLOOD DISASTER MANAGEMENT IN THE COASTAL AREA

Clear policy, necessary laws, and legislation are an important mechanisms in Inundation or flood management. Also, the institutional arrangement with clear roles and does not create redundant work with other organizations can effectively support mitigation planning and implementation. The single agency that is fully responsible to overall flood management in every level such as national, region, province and local, will have efficient flood management and power in co-operation and implementation with other organizations. Inundation disaster management consists of four main activities which can be described by the cycle of activities as shown in Figure 7.5 as following:

Activity 1: Preparedness for flood prevention and mitigation

Preparedness for inundation prevention and mitigation is formed by both structural and non-structural measures (NSWG, 1986; ESCAP, 1991). Structural measures refer to physical construction work. Non-structural measures are those in agreement with sustainable development, well commonly acceptable, and environmental friendly. Among non-structural measures are watershed or landscape control, laws and regulations, socio-economics, an efficient flood forecast and warning system, inundation risk assessment, people awareness, inundation databases, etc. a site-specific mix of structural and non-structural measures seems to be a proper solution. Flood disaster mitigation includes the followings: updating of laws and legislation, community-base approaches to disaster mitigation, establishment of information system, capability building, public awareness and social marketing, establishment of database system, setting up safety standard in inundation control

project, inundation risk maps, inundation forecasting and warning system, land use control and land conservation and insurance.

Activity 2: Inundation readiness

Readiness enables governments, organizations, communities and individuals to respond rapidly and effectively to disaster situations. Readiness measures include the formulation of a viable disaster plan, maintenance of resources and training of personnel. The readiness can be divided into the following items: Warning: when a hazard has been identified but is not yet threatening a particular area. Threat: when a hazard has been identified and assessed as threatening a particular area. Precaution: Action was taken after receipt of warning to offset effects of disaster impact.

Activity 3: Emergency response

Response measures are those which are taken immediately prior to and following disaster. Such measures are directed towards saving life and protecting property and to dealing with the immediate damage caused by the disaster. Disaster response should be comprehensive and meets a broad range of urgent needs and problems arising in the community.

Activity 4: Flood recovery and rehabilitation

Recovery is the process by which communities and the nation are assisted in returning to their proper functioning following a disaster. Post-flood recovery is often less spectacular than actions during the flood, as national leaders and the media who have left the natural catastrophe are become disinterested (Kundzewicz, 2002). The recovery process can be very protracted, taking 5-10 years or even more. Three main

categories of activity are normally regarded as: restoration, rehabilitation, reconstruction

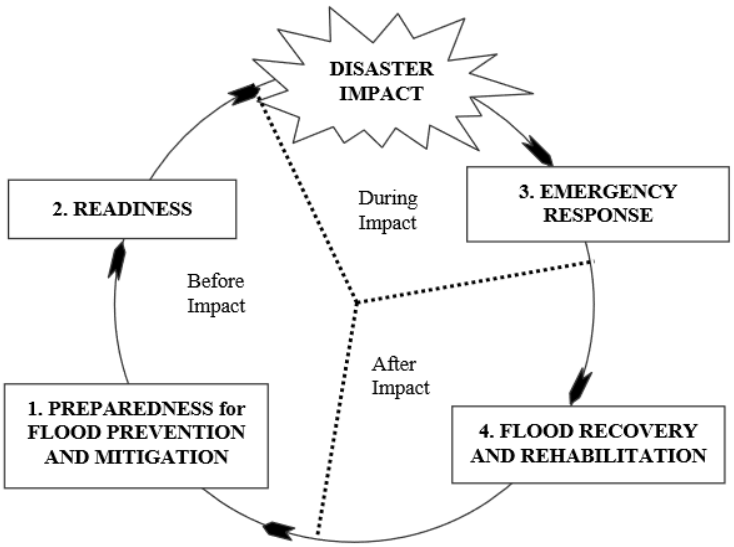

Figure 7.5: Flood disaster management cycle (Tingsanchali, 2012)

7.5 APPLICATION OF FLOOD DISASTER MANAGEMENT CYCLE

Based on the inundation simulation results and inundation risk affected in the coastal area of the Ariake Sea and the Saga lowland area due to storm surge and flood, this area is a high risk of inundation where buildings or houses and public facilities were affected. Also very influential to human and communities life in the surrounding of this area. Required an action or efforts to reduce the risk of inundation by implementing of disaster management systems based on flood disaster management cycle following as:

1. *Mitigation*: Measures put in place to minimize the results from a disaster. Examples: building codes and zoning; vulnerability analysis; public education.
2. *Awareness*: Planning how to respond. Examples: preparedness plans; emergency exercises/training; warning systems.
3. *Response*: Initial actions taken as the event takes place. It involves efforts to minimize the hazards created by a disaster. Examples: evacuation; search and rescue; emergency relief.
4. *Recovery*: Returning the community to normal. Ideally, the affected area should be put in a condition equal to or better than it was before the disaster took place. Examples: a temporary housing; grants; medical care.

Figure 7.6 shown the suggestion for required an action or efforts to reduce the risk of inundation by implementing of disaster management systems based on flood disaster management cycle for the coastal disaster management in this area.

Figure 7.6: Inundation disaster management cycle
(Photograph source from MLIT Takeo office, 2011)

The existing system for flood disaster management in the study area was conducted as shown in Figure 7.7:

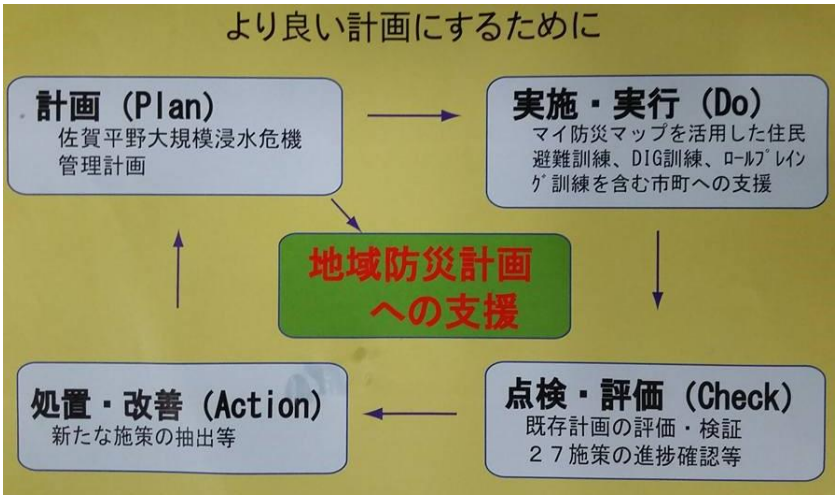

Figure 7.7: Flood disaster management existing in study area
(Source: MLIT Takeo office, 2011)

1. *Plan :* Planning for flood disaster management in Saga Plain
2. *Do :* Implementation and execution such as residents evacuation drill, training or emergency exercise with utilizing the disaster prevention map.
3. *Check :* Inspection and evaluation of the progress confirmation, etc. in the field (Saga Plain) to evaluation and verification 27 measures of the existing plan, consists of; information collection and transmission, wide area support and emergency transportation network, and strengthening cooperation.
4. *Action :* Treatment and improvement

Inundation disaster management cycle proposed to be implemented, as shown in Figure 7.6 is a simplification from the existing flood disaster management in the study area (Figure 7.7) to be more easily understood and applied both before, while and after the disaster.

7.6 CONCLUSIONS

Based on the 2-D inundation numerical modeling, the storm surge and the flood by torrential rain at the same time can cause inundation disaster near the river mouth, the inundation risk in the coastal area is high. The buildings or houses and public facilities are supposed to have a serious disaster. More than 96,000 buildings or houses and 245 public facilities were inundated.

The simulation result was presented the area of inundation is high risk with inundation height 0.5 m -3.5 m. Evacuation must be carried out for action to reduce the risk of inundation.

Required an action or efforts to mitigate the risk of inundation by implementing of disaster management systems based on flood disaster management cycle for the coastal disaster management in this area be recommended.

Chapter 8

CONCLUSIONS AND RECOMMENDATION

The overarching aim of this research is to modeling of the inundation in the coastal area of the Ariake Sea head based on the disasters has occurred in the coastal area of the Ariake Sea in the past, such as storm surge by typhoon and river flood or high discharge by torrential rain. The previous chapter in this dissertation has been presented of the objective of this research.

In the numerical simulation of river flood by torrential rain on 14 to 15 July 2012 at the Chikugo River and branch using 1-D model simulation, no water level overflow. It means no inundation in the coastal area of the area of the Ariake Sea and Saga lowland around of the Chikugo River.

The pattern of water level change in the Chikugo River and branch based on or following the boundary condition in the upstream and downstream of the Chikugo River and branch. The pattern of water level simulated near boundary condition in the downstream is followed the tide measurement at the mouth of Chikugo River until Km 6.8 (-6800) from the river mouth. The pattern of water level simulated near boundary condition in the upstream is followed the discharge measurement at the Senoshita station until Km 16.2 (-16200) from the mouth of Chikugo river. It means, the pattern of water level change is followed the discharge condition extents to 6.2 kilometer from Senoshita station at Km 23.0 (-23000).

The pattern of water level simulated near Wakatsu station Km 6.85 (-6850) from the mouth of Chikugo river is followed the water level measurement at Wakatsu station as Km 6.8 (-6800) and Km 7.0 (-7000).

Based on the pattern of water level simulated, the effect of boundary at the river mouth extents to Km 6.8 (-6800) at the Chikugo River. It means, the influences of tide extents to Km 6.8 near Wakatsu station.

In the numerical simulation of storm surge by typhoon Pat on August 31 to September 1, 1985, at the Ariake Sea using 2-D model simulation, no water level exceed of the existing coastal dyke. It means no inundation in the coastal area of the Ariake Sea and Saga lowland. Inundation occurred in the coastal area of the Ariake Sea, and Saga lowland near Chikugo River estuary due to water level exceed of existing river dyke at Chikugo River and branch during the storm surge and river flood simultaneously occurred. No sea water exceed of the existing coastal dyke.

The coastal area of Ariake Sea and Saga lowland are vulnerable against the inundation due to the simultaneous occurrence of the storm surge and river flood. Required an action or efforts to reduce the risk of inundation by implementing of disaster management systems based on flood disaster management cycle for the coastal disaster management in this area.

For the further analysis of the storm surge, the effects of wind speed distribution and the waves should be considered additionally.

REFERENCES

1. A. D. Mc Cowan, et al., (2001), Improving the Performance of a Two-dimensional Hydraulic Model for Floodplain Applications, Conference on Hydraulics in Civil Engineering, The Institution of Engineers, Australia.
2. A.E. K. Vozinaki, N. N. Kourgialas and G. P. Karatzas, (2012), Estimation of agricultural flood loss in the Koiliaris river basin in Crete, Greece, European Water, 39, pp. 53-63.
3. Agency France-Presse, (2013), Cyclone, hurricane, typhoon: difference names, same phenomenon. (http://www.rappler.com/science-nature/43386-meteorology-tropical-cyclones-naming).
4. A.K.T. Dundu and K. Ohgushi, (2012), A Study on Impact of Storm Surge by Typhoon in Saga Lowland and Surroundings using Hydrodynamic Numerical Modeling, International Journal of Civil & Environmental Engineering IJCEE-IJENS Vol: 12 No: 01.
5. Aljazeera News, (2015), (http://www.aljazeera.com/news/2015/09/ japanese-city-submerged-river-bursts-banks-150910061924837.html.).
6. B. Lin, J.M. Wicks, R.A. Falconer and K. Adams, (2006), Integrating 1D and 2D hydrodynamic models for flood simulation, Proceedings of the Institution of Civil Engineers, Water Management, 159, pp.19-25.
7. Bates, P.D., M.S. Horritt, and T.J. Fewtrell, (2010), A simple inertial formulation of the shallow water equations for efficient two-dimensional flood inundation modelling. Journal of Hydrology, pp. 33-45.

8. Cardone, V.J., Cox, A.T. Greenwood, J.A. and Thompson, E.F., (1992), Upgrade of tropical cyclone surface wind field model. CERC-94-14, U.S. Army Corps of Engineers.
9. Cunge, J.A., F.M. Holly, and A. Verwey, (1980), Practical Aspects of Computational River Hydraulics. London: Pitman Publishing Limited.
10. DHI, (2006), MIKE 21, Short introduction and tutorial, Danish Hydraulic Institute, Denmark.
11. DHI, (2007), MIKE FLOOD, 1D-2D modelling user manual, (http://tnmckc.org/upload/document/wup/1/1.3/Manuals/MIKE%2011/MIKE_FLOOD_User_Manual.pdf)
12. DHI, (2009), MIKE 21 Flow Model: Hydrodynamic Module Scientific Documentation, Danish Hydraulic Institute, Denmark.
13. DHI, (2011), MIKE 21 FLOW MODEL FM, Hydrodynamic module, user guide, Danish Hydraulic Institute, Denmark.
14. Daniel Gilles and Matthew Moore, (2010), Review of Hydraulic Flood Modeling Software used in Belgium, The Netherlands, and The United Kingdom, International Perspectives in Water Resource Management IIHR – Hydroscience & Engineering University of Iowa, College of Engineering
15. Debashree Sen, What is river flood? (http://www.ehow.com/about_ 6310709_ river-flood_.html)
16. E.D. Fernandez-Nieto, J. Marin and J. Monnier, (2010), Coupling superposed 1D and 2D shallow-water models: Source terms in finite volume schemes, Computers and Fluids, 39, pp.1070-1082

17. Erich, J. P.,(2002), Flood risk and flood management, Journal of Hydrology 267, pp. 2-11
18. ESCAP (Economic and Social Commission for Asia and the Pacific), (1991), Manual and Guidelines for Comprehensive Flood Loss Prevention and Management. ST/ESCAP/933, ESCAP, Bangkok, Thailand.
19. Frank, E., A. Ostan, M. Coccato, and G.S. Stelling, (2001), Use of an integrated one-dimensional/two-dimensional hydraulic modelling approach for flood hazard and risk mapping. In River Basin Management, by R.A. Falconer and W.R Blain, 99-108. Southhampton, UK: WIT Press.
20. Fumio Kato, (2007), Saga Ariake sea coastal area. (http://www.mext.go.jp/component/a_menu/science/micro_detail/__icsFiles/afieldfile/2015/04/17/1253274_019.pdf)
21. Gambolati, G., (2002), GIS simulation of the inundation risk in the coastal lowlands of the northern Adriatic sea. Mathematical and Computer Modelling. 35, pp. 963-972
22. Geenaert, G.L., and Plan, W.J., (1990), Surface waves and fluxes, Dordrecht: Kluwer Academic Publisher, 2, pp. 339-368
23. H. Araki, et al., (2001), Study on environmental change and peculiarity of the Ariake Sea, Japan, Transaction on Ecology and the Environment, vol 48, WIT Press.
24. H. Kanayama and H. Dan, (2006), A Finite Element Scheme for Two-Layer Viscous Shallow-Water Equations, Japan J. Indust. Appl. Math., 23, pp. 163–191

25. Hashimoto, N., et al., (2015), Bias correction in typhoon and storm surge projection considering characteristics of global climate model MRI-AGCM3.2S, Journal of Disaster Research, vol.10 No. 3, pp. 448-455.
26. Hideaki Oda, Typhoon Isewan (Vera) and its lessons, Japan Water Forum. (http://www.waterforum.jp/jpn/katrina/Typhoon_Isewan.pdf)
27. Hiroshi, K., Hiroshi, D., A Finite Element Scheme for Two-Layer Viscous Shallow-Water Equations, Faculty of Engineering, Kyushu University.
28. Horritt, M.S., and P.D. Bates, (2002), Evaluation of 1D and 2D numerical models for predicting river flood inundation. Journal of Hydrology, pp. 87-99.
29. Hydroeurope, Remote software, DHI water resources software. (http://www.hydroeurope.org/jahia/webdav/site/hydroeurope/shared/pics/remotedesktop/RemoteSoftware.pdf)
30. J. F. Dhondia and G. S. Stelling , (2002), Application of one dimensional-two dimensional integrated hydraulic model for flood simulation and damage. Proceedings of the 5th International Conference on Hydroinformatics, Cardiff, pp. 265-276.
31. Japan Water Agency, (2015), Chikugo water system, http://www.water.go.jp/honsya/honsya/english/jwa_ta/map6.html
32. Japan Meteorological Agency, (2008), Annual Report on Activities of the RSMC Tokyo - Typhoon Center. Available online (http://www.jma.go.jp/jma/jma-eng/jma-center/rsmc-hp-pub-eg/AnnualReport/2007/Text/Text2007.pdf)
33. Jeffrey Masters, Storm surge basic, weather underground. (https://www.wunderground.com/hurricane/surge.asp)

34. Jon Erdman and Nick Wiltgen, (2015), Typhoon Nangka recap: 29 inches of rain reported. (https://weather.com/storms/typhoon/news/typhoon-nangka-west-pacific-japan-july2015)
35. K. Torii and F. Kato, (2003), Risk assessment on storm surge flood. (https://www.pwri.go.jp/eng/ujnr/joint/34/paper/83kato.pdf)
36. Kamel, A., H., (2008), Application of a hydrodynamic MIKE 11 model for the Euphrates river in Iraq, Slovak journal of civil engineering, pp. 1-7
37. Kitamoto, A., Digital typhoon: The intensity and size of typhoon-Unit of pressure and wind. (http://agora.ex.nii.ac.jp/digital-typhoon/help/unit.html.en).
38. Koichiro Ohgushi, et al., (2002), Applications of Remote Sensing And GIS for Estimating Water Quality in The Ariake Sea, Advances In Hydraulics And Water Engineering, Volumes II, Proceedings of the 13th IAHR-APD Congress, Singapore.
39. Konishi, T., (1997), A cause of storm surges generated at the ports facing open oceans effect of wave setup, Umi to Sora (Sea and Sky), 73, pp. 35-44.
40. Konishi, T., (1995), An experimental storm surge prediction for the western part of the Inland Sea with application to Typhoon 9119. Pap. Meteor. Geophys., 46, pp. 9-17.
41. Kwon J.I., J.C. Lee, K.S. Park, and K.C. Jun, (2008), Comparison of Typhoon Wind Models Based on Storm Surge Heights Induced by Typhoon Maemi. Asia-Pacific Journal of Atmospheric Sciences, 44, pp. 443-454.
42. Kyeong O. Kim and Takao Yamashita, (2008), Storm surge simulation using wind wave-surge coupling model, Journal of Oceanography, Vol. 64, pp. 621- 630.

43. Le Van CHINH, et al., (2010), A GIS–based Distributed Parameter Model for Rainfall Runoff Calculation using Arc Hydro Tool and Curve Number Method for Chikugo River Basin in Japan, J. Fac. Agr., Kyushu University, 55, pp. 313-319
44. MLIT Takeo office, (2011), New contingency plan, JICA Training. (http://www.qsr.mlit.go.jp/takeo/site_files/file/english/eng_03/2_8-1-1New_Contingency_Plan.pdf)
45. M. Abualtayef, et al., (2007), A numerical simulation of wind-induced flows in Ariake Sea, Journal of Applied Sciences 7 (10), pp. 1446-1451.
46. M. Abualtayef, et al., (2008), A three dimensional hydrostatic modeling of a bay coastal area. Journal of Marine and Science and Technology, 13, pp. 40-49
47. M. Abualtayef, et al., (2010), Development of a three dimensional circulation model based on fractional step method, Inter J Nav Archit Oc Engng, 2, pp. 14-23
48. M. Morales-Hernandez , et al., (2014), A conservative strategy to couple 1D and 2D models for shallow water flow simulation, proceedings of the International Conference on Fluvial Hydraulics (River Flow 2014), Lausanne, Switzerland.
49. M. Takezawa, et al., (2014), Assessment of the flood disaster management plans for the medical services in Tokyo and Fukuoka, WIT Transactions on Information and Communication Technologies, Vol 47, pp. 345-356.
50. Masahiko Murase, (2011), Risk sharing in practice towards integrated flood management, ICFM5, Tokyo.

51. Masakazu Higaki, et al., Outline of the storm surge prediction model at the Japan Meteorological Agency, (http://www.jma.go.jp/jma/jma-eng/jma-center/rsmc-hppub-eg/techrev/text11-3.pdf)
52. Mason, D.C., D.M. Cobby, M.S. Horritt, and P.D. Bates, (2003), Floodplain friction parameterization in two-dimensional river flood models using vegetation heights derived from airborne scanning laser altimetry. Hydrological Processes, pp. 1711-1732.
53. Maugeri, A., (2012), Capabilities of a coupled 1D/2D model for flood inundation simulation, Columbia Water Center – ENGEES.
54. Mc Cowan, A., Rasmussen, E. and Berg, P., (2001), Improving the performance of a two-dimensional hydraulic model for floodplain applications. Conference on Hydraulics in Civil Engineering, Hobart.
55. National Weather Service, Storm surge, (http://www.srh.noaa.gov/jetstream/ /tropics/tc_hazards.html)
56. National Weather Service-Weather Forecast Office, Definition of flood and flash flood. (http://www.srh.noaa.gov/mrx/hydro/flooddef.php)
57. NSWG (New South Wales Government), (1986), Flood plain development manual. PWD 86010, NSWG, Australia.
58. Parto, S., et al., (2009), Hydrodynamic modeling of a large flood-prone river system in India with limited data, Hydrological Processes, 23, pp. 2774-2791.
59. Patro, S., et al., (2009). Flood Inundation Modeling using MIKE FLOOD and Remote Sensing Data, Journal of the Indian Society of Remote Sensing, 2009: pp. 107-118.
60. Phillip Harwood, (2012), What is a storm surge?, eSurge, (http://www.storm-

surge.info/what-is-a-storm-surge)

61. Prashant Kadam, (2012), Flood inundation simulation in Ajoy River using MIKE-FLOOD, ISH Journal of Hydraulic Engineering, Vol. 18, No. 2, pp. 129-141.
62. S. Huang, S. Vorogushyn, and K. E. Lindenschmidt, (2007), Quasi 2D hydrodynamic modelling of the flooded hinterland due to dyke breaching on the Elbe River, Adv. Geosci., 11, pp. 21-29.
63. T. Tabata, et al., (2013), Numerical analysis of convective dispersion of pen sel Atrina pectinate larvae to support seabed restoration and resource recovery in the Ariake Sea, Japan, Elsevier, Ecological engineering 57, pp: 154-161.
64. T. Tabata, et al., (2015), Assessment of the water quality in the Ariake Sea using principal component analysis, Journal of Water Resource and Protection, 7, pp. 41-49
65. T. Tingsanchali and M. F. Karim, (2005) Flood hazard and risk analysis in the southwest region of Bangladesh. Hydrol. Processes 19(10), pp. 2055–2069.
66. T. Tingsanchali, (2012), Urban flood disaster management, SciVerse ScienceDirect, Elsevier, Procedia Engineering 32, pp. 25-37
67. Thambas, A., H., Ohgushi, K., (2015), Inundation risk analysis of the storm surge and flood in the coastal area of the Ariake Sea using GIS and 2D flooding simulation, IJSR vol. 4, December, pp. 327-331.
68. Tomohiro Yasuda, et al., (2009), Evaluation of Typhoons due to Global Warming and Storm Surge Simulations by Using the General

Circulation Model Outputs, 33rd IAHR Congress, Vancouver, British Columbia, Canada.

69. Qiang L., Yi Qin, Yang Zhang, Ziwen Li, (2015), A coupled 1D–2D hydrodynamic model for flood simulation in flood detention basin, Nat Hazards Springer Journal vol. 75, p:1303-1325
70. Vanderkimpen, P. and Peeters, P., (2008), Flood Modeling for risk evaluation-a MIKE FLOOD sensitivity analysis. Accepted for River Flow 2008, Cesme-Izmir.
71. Vanderkimpen, P., Merger, E., and Peeters, P., (2009), Flood modeling for risk evaluation – a MIKE FLOOD vs. SOBEK 1D2D benchmark study, Flood Risk Management: Research and Practice, Taylor & Francis Group, London.
72. W. F. Li, Q W Chen and J Q Mao, (2009), Development of 1D and 2D coupled 666 model to simulate urban inundation: An application to Beijing Olympic 667 Village, Chinese Sci Bull, 54(9), pp. 1613-1621
73. Wei-Po Huang, et al., (2007), Numerical studies on typhoon surges in the Northern Taiwan, Coastal Engineering vol. 54
74. Wheather Underground, https://www.wunderground.com/prepare/storm-surge
75. Wikipedia, Chikugo River, (https://en.wikipedia.org/wiki/Chikugo_River).
76. Wikipedia, MIKE 11, (https://en.wikipedia.org/wiki/MIKE_11).
77. Wikipedia, MIKE 21, (https://en.wikipedia.org/wiki/MIKE_21)
78. X., Wang, et al., (2008), Simulation of flood inundation of Guiyang City using remote sensing, GIS and hydrologic model, The International Archives

of the Photogrammetry, Remote Sensing and Spatial Information Sciences. Vol. XXXVII. Part B8. Beijing

79. Xihua Yang and Bengt Rystedt, (2002), Predicting Flood Inundation and Risk Using GIS and Hydrodynamic, Indian Cartographer.
80. Yamashiro, M., et al., (2014), A study on possible critical storm surge under present climate condition in the ariake sea, Japan, Coastal Engineering.
81. Yano, S., Winterwerp, J.C., Tai, A. and Saita, T. (2010) Numerical experiments on features of nonlinear tide and its influences on sediment transport in the Ariake Sea and the Yatsushiro Sea, Journal of JSCE, Ser.B2 (Coastal Engineering), 66(1), pp.341-345. (In Japanese with English abstract)
82. Yoon, J.J., Shim, J.S., (2013). Estimation of storm surge inundation and hazard mapping for the southern coast of Korea. Journal of Coastal Research, Special Issue No. 65, pp. 856-861